國 立 交 通 大 學

機械工程學系

碩士論文

藉部分區域穩定理論之乾-兌八卦多重交織導數同步

Qian-Dui Hexagram Multiple Symplectic Derivative Synchronization by Partial Region Stability Theory

研 究 生：李健華

指導教授：戈正銘　教授

中華民國一零一年六月

Qian Trigram Symplectic Derivative Chaos Synchronization by Partial Region Stability Theory

研究生：李健華　　student：Chien-Hua Li
指導教授：戈正銘　　Advisor：Zheng-Ming Ge

國立交通大學

機械工程研究所

碩士論文

A Thesis of the Thesis
Submitted to Institute of Mechanical Engineering
College of Engineering
National Chiao Tung University
In partial Fulfillment of the Requirement
For the Degree of Master of Science
In Mechanical Engineering
June 2012
Hsinchu, Taiwan, Republic of China

中華民國一零一年六月

藉部分區域穩定理論之乾-兌八卦多重交織導數同步

學生： 李健華　　指導教授：戈正銘

國立交通大學

機械工程研究所

碩士論文

摘要

廣義同步是存在著主僕狀態之間的一個函數關係。一個新型的混沌同步，藉由部分區域穩定理論之多重交織導數同步，得到與原系統狀態變量和其他不同系統構成的“夥伴”關係。利用數值模擬來驗證部分區域穩定理論之多重交織導數同步的有效性。

在中國哲學中，陰代表是負或陰柔，而陽是代表正或陽剛。陰跟陽在中國哲學中兩個是互相對立的，然而太極結合陰陽，這可能意味著宇宙的起源。八卦是中國哲學的一部分，他們擁有各自的方位、數字、以及代表性。作為例證，本論文主要研究乾卦與兌卦，結合了在上面的乾卦與在下面兌卦得到六十四卦的乾-兌卦。乾-兌卦代表不同的混沌系統，並藉由部分區域穩定理論達成多重交織導數同步。

Qian Trigram Symplectic Derivative Chaos Synchronization by Partial Region Stability Theory

student：Chien-Hua Li Advisor：Zheng-Ming Ge

Department of Mechanical Engineering
National Chiao Tung University

Abstract

The generalized synchronization is that there exists a functional relationship between the states of the master and those of the slave. A new type of chaotic synchronization, multiple chaotic symplectic derivative synchronization, is obtained with the state variables of the original system and of another different order system as constituents of the functional relation of “partners”. Numerical simulations are provided to verify the effectiveness of the proposed scheme.

In Chinese philosophy, Yin means negative, historical, or feminine principle while Yang is positive, contemporary, or masculine principle. Yin and Yang are two fundamental opposites in Chinese philosophy, and “Tai Ji”, the great one, is the combination of Yin and Yang, which maybe the origin of Cosmos. The eight trigrams is a part of Chinese philosophy, and they have their own direction, figure, and representation. In this thesis, as examples, Qian trigram and Dui trigram are studied, combining Qian trigram in upper place and Dui trigram in lower place can get Qian-Dui hexagram. Qian-Dui hexagram can be annotated by chaos and its synchronization..

致謝

此篇論文及碩士學業之完成，首先必須感謝指導教授　戈正銘教授的耐心指導與教誨。老師在專業領域上的成就及對於文學和史學上的熱情，都令學生印象深刻且受益匪淺。這兩年的相處，在學術研究之餘也體會到古典文學的美，開拓了學生未知的視野。研究過程中，戈教授給了許多寶貴的意見指引學生正確的研究方向以及發現問題時解決問題的能力；聊天過程中，戈教授亦分享許多豐富的人生經驗，令學生受益無窮。

這段研究的日子中，承蒙李仕宇、何俊諺學長的熱心指導與照顧，同時也感謝張登順、紀亭宇、黃啟任同學的相互勉勵及幫忙，使得本篇論文能夠順利完成，再來感謝陳界誠、王聖唯、李志鴻、陳冠宏這群好友的瘋狂行為，讓我在課業繁忙中還能享受額外的生活樂趣。

最後感謝我的家人，讓我可以不必擔心課業以外的事物，無後顧之憂的完成學業。最後，僅以此文獻給你們。

Content

圖目錄

表目錄

Chapter 1

Introduction

Nonlinear dynamics has been extensively used in physics, mathematics, engineers, economics and philosophy studying in the past few decades. Chaos theory as a part of nonlinear dynamics has been widely used in various fields such as power converters, weather prediction, information processing, population dynamics, chemical reactions, biological systems, secure communications, etc [1-8]. Accepted chaos theory pioneer is Lorenz [9]. He discovered chaos in a simple system of three autonomous ordinary differential equations to describe the simplified Rayleigh-Benard problem.

In Chinese philosophy, Yin means negative, feminine or past, while Yang means positive, masculine or present. Yin and Yang are two fundamental opposites in Chinese philosophy [10]. Lü system [11-12] is studied in this paper. There are many articles in studying contemporary Lü system for time $0 \to +\infty$ which is called Yang Lü system, of which the chaos is called Yang chaos. Indeed we can also study the historical Lü system for time $0 \to -\infty$ which is called Yin Lü system of which the chaos is called Yin chaos. Furthermore, by Chinese philosophy, Tai Ji chaos, i.e. Great One chaos, which consists of Yin chaos and Yang chaos, of Lü system is studied firstly.

Chaos synchronization is proposed first in 1983 by Fujisaka and Yamada [13] but it is not received great attention. Until 1990, synchronization of two chaotic systems was introduced by Pecora and Corroll and has been widely used in science and engineering [14]. In recent years, synchronization in chaotic system is a very interesting problem and many control techniques to synchronize chaotic systems has

been widely researched [15-22].

Symplectic synchronization is defined as $y = H(x, y, t)$, where x, y are the state vectors of the "Partner A" and of the "Partner B", respectively [23]. The final desired state y of the "Partner B" not only depends upon the state of Partner A x but also depends upon the state of Partner B y itself. Therefore the " Partner B" is not a traditional pure slave obeying the "master" completely but plays a role to determine the final desired state of the "slave" system.

When the symplectic functions is extended to a more general form, $G(x, y, z, \cdots, \dot{x}, \dot{y}, \dot{z}, \cdots, \ddot{x}, \ddot{y}, \ddot{z}, \cdots, t) = F(x, y, z, \cdots, \dot{x}, \dot{y}, \dot{z}, \cdots, \ddot{x}, \ddot{y}, \ddot{z}, \cdots, t)$, the synchronization is called "multiple derivative symplectic synchronization". $G(x, y, z, \cdots, \dot{x}, \dot{y}, \dot{z}, \cdots, \ddot{x}, \ddot{y}, \ddot{z}, \cdots, t)$ and $F(x, y, z, \cdots, \dot{x}, \dot{y}, \dot{z}, \cdots, \ddot{x}, \ddot{y}, \ddot{z}, \cdots, t)$ are given vector functions of $x, y, z, \cdots, \dot{x}, \dot{y}, \dot{z}, \cdots, \ddot{x}, \ddot{y}, \ddot{z}, \cdots$,and time.

And the symplectic functions is extended to a more general form, $G(x, y, \cdots, \dot{x}, \dot{y}, \cdots, \ddot{x}, \ddot{y}, \cdots, t, \tau) + K = F(x, y, \cdots, \dot{x}, \dot{y}, \dot{x}_\tau, \dot{y}_\tau \cdots, \ddot{x}, \ddot{y}, \ddot{x}_\tau, \ddot{y}_\tau \cdots, t, \tau)$, τ is the function of time $t, \tau = \tau(t)$, where $\dot{x}_\tau = \frac{dx}{d\tau}$, $\dot{y}_\tau = \frac{dy}{d\tau}$, $\ddot{x}_\tau = \frac{d^2x}{d\tau^2}$, $\ddot{y}_\tau = \frac{d^2y}{d\tau^2}$, . The synchronization is called "multiple derivative symplectic synchronization with variable scales". $G(x, y, \cdots, \dot{x}, \dot{y}, \cdots, \ddot{x}, \ddot{y}, \cdots, t, \tau)$ and $F(x, y, \cdots, \dot{x}, \dot{y}, \cdots, \ddot{x}, \ddot{y}, \cdots, t, \tau)$ are given vector functions of $x, y, \cdots, \dot{x}, \dot{y}, \cdots, \ddot{x}, \ddot{y}, \cdots$,t and τ. y is no longer a function of x, y and t but a function of x, y, t and τ. Variable time scale τ and variable quadrant can be used. The derivative terms and variable time scales make the synchronization method more difficult.

In this thesis, a new chaos control strategy by GYC (Ge-Yao-Chen) partial region stability theory is proposed [24–26]. And the comparison of the new strategy with traditional method is given [27].

By "The Book of Changes", there are eight possible trigrams that could be

applied for multiple symplectic derivative chaos synchronization. Trigram has three parts, upper, central, and low. The three parts of Qian trigram and Dui trigram, a part of the eight trigrams, both represent three different chaos systems separately, and they are used to complete a two times multiple symplectic derivative synchronization by partial region stability theory. Then choose two trigrams to research. One is named "Qian". Its trigram figure is represented "☰". And another is "Dui". Its trigram figure is represented "☱". The unbroken line represents Yang, the creative principle. The broken line represents Yin, the receptive principle.

Finally, two trigrams can be combined into one hexagram. Hexagram has two parts, upper, and low. The Qian-Dui Hexagram is used for multiple symplectic derivative synchronization by partial region stability theory. $G(x, y, z, \cdots, \dot{x}, \dot{y}, \dot{z}, \cdots, t) = F(x, y, z, \cdots, \dot{x}, \dot{y}, \dot{z}, \cdots, t)$, is a more general form of symplectic synchronization. A new chaos control strategy by GYC (Ge-Yao-Chen) partial region stability theory [28-30] is used in this paper.

Chapter 2

Chaos of Yin, Yang and Tai Ji Lü Systems

2.1 Preliminary

Chaos of contemporary Lü system, i.e. Yang chaos of Lü system, has been investigated completely. In this thesis, chaos of historical Lü system, i.e. Yin chaos of Lü system, is studied with comparison to that of Yang chaos by time histories of states, phase portraits, bifurcation diagrams and Lyapunov exponents.

2.2 Yang Lü system and Yin Lü system

Lü system for time interval $0 \to +\infty$ is called Yang Lü system:

$$\begin{cases} \dfrac{dx_1}{dt} = a(x_2(t) - x_1(t)) \\ \dfrac{dx_2}{dt} = -x_1(t)x_3(t) + cx_2(t) \\ \dfrac{dx_3}{dt} = x_1(t)x_2(t) - bx_3(t) \end{cases} \tag{2.1}$$

Chaos of Yang Lü system appears when initial condition(x_{10}, x_{20}, x_{30}) = (0.2, 0.35, 0.2) and Yang parameters a=36, b=3 and c=20. The behaviors of corresponding Yang chaos are shown in Figs 2.1~2.3 by time histories, 2D and 3D phase portraits.

By replacing variable$(x_1(t), x_2(t), x_3(t), t)$ with$(x_1(-t), x_2(-t), x_3(-t), -t)$ in Eq. (1-1) to study the past $(-t: 0 \to -\infty)$ of the system, Yin Lü system is described as follows:

$$\begin{cases} \dfrac{dy_1(-t)}{d(-t)} = a(y_2(-t) - y_1(-t)) \\ \dfrac{dy_2(-t)}{d(-t)} = -y_1(-t)y_3(-t) + cy_2(-t) \\ \dfrac{dy_3(-t)}{d(-t)} = y_1(-t)y_2(-t) - by_3(-t) \end{cases} \tag{2.2}$$

The simulation results are tabulated in Table 1.

Table 2. 1. Dynamic behaviors of Yin Lü system for different signs of parameters

a	b	c	states
-	+	+	Approach to infinity
-	-	+	Approach to infinity
+	-	+	Approach to infinity
+	+	-	Approach to infinity
+	-	-	Approach to infinity
-	+	-	Approach to infinity
-	-	-	Chaotic and periodic

Table 2.1 shows dynamic behaviors of Yin Lü system for different signs of parameters. It shows that chaos of Yin Lü system appears for initial condition(x_{10}, x_{20}, x_{30}) = (0.2, 0.35, 0.2) and parameters a=-36, b=-3 and c=-20. The chaotic behaviors are shown in Figs 2.4~2.6 by time histories, 2D and 3D phase portraits.

2.3 Further Simulation results

In order to learn the difference and similarity between Yang and Yin Lü system, the bifurcation diagrams and Lyapunov exponents are also used. The simulation results are shown in three cases:

Case 1: Parameter a is varied and b, c are fixed. Bifurcation diagrams and Lyapunov exponents are shown in Figs 2.7~2.10. The simulation results are compared from Table 2.2 and Table 2.3.

Table 2. 2. Dynamic behaviors of Yang chaos for parameter a

Range of parameter a	Behaviors of chaos
30.000 ~ 36.930	Chaos
36.930 ~ 38.555	Periodic trajectory
38.555 ~ 47.265	Chaos
47.265 ~ 50.000	Periodic trajectory

Table 2. 3. Dynamic behaviors of Yin chaos for parameter a

Range of parameter a	Behaviors of chaos
-30.0 ~ -36.915	Chaos
-36.915 ~ -38.560	Periodic trajectory
-38.560 ~ -47.250	Chaos
-47.250 ~ -50.000	Periodic trajectory

Table 2.2 and Table 2.3 show the dynamic behaviors of chaos and periodic motion in varied ranges of parameter a and fixed parameters b, c of Yang and Yin Lü system. From these results, the Yin chaos and Yang chaos are different in many details. For example, when $-36.915 \leq a \leq -38.560$, periodic trajectories appear in Yin system but chaos appear in Yang system when $36.930 \leq a \leq 38.555$. Other differences can be discovered in the Tables. These phenomena match with the jargon of Chinese philosophy: Yin chaos and Yang chaos are "difference in same and same in difference".

Case 2: Parameter b is varied and a, c are fixed. Bifurcation diagrams and Lyapunov exponents are shown in Figs 2.11~2.14. From these results, the Yin chaos and Yang chaos are similar as a whole. The simulation results are listed in Table 2.4 and Table 2.5.

Table 2. 4. Dynamic behaviors of Yang chaos for parameter b

Range of parameter b	Behaviors of chaos
1.00 ~ 1.39	Chaos
1.39 ~ 2.77	Periodic trajectory
2.77 ~ 13.97	Chaos
13.97 ~ 20.00	Periodic trajectory

Table 2. 5. Dynamic behaviors of Yin chaos for parameter b

Range of parameter b	Behaviors of chaos
-1.00 ~ -1.40	Chaos
-1.40 ~ -2.77	Periodic trajectory
-2.77 ~ -13.94	Chaos
-13.94 ~ -20.00	Periodic trajectory

Table 2.4 and Table 2.5 show the dynamic behaviors of chaos and periodic motion in varied ranges of parameter b and fixed parameters a, c of Yang and Yin Lü system. From them, the Yin chaos and Yang chaos are different in many details. For example, when $1.39 \leq b \leq 2.77$ and $13.97 \leq b \leq 20.00$, periodic trajectories appear in Yang system while periodic trajectories appear in Yin system when $-1.40 \geq b \geq -2.77$ and $-13.94 \geq b \geq -20.000$. They are not the same when parameter b is 1.39~13.97. Other differences can be discovered in the Tables.

Case 3: Parameter c is varied and a, b are fixed. Bifurcation diagrams and Lyapunov exponents are shown in Fig. 2.15~2.18. The simulation results are listed in Table 2.6 and Table 2.7.

Table 2. 6. Dynamic behaviors of Yang chaos for parameter c

Range of parameter c	Behaviors of chaos
15.00 ~ 25.75	Chaos
25.75 ~ 25.80	Periodic trajectory
25.80 ~ 29.05	Chaos
29.05 ~ 32.00	Periodic trajectory

Table 2. 7. Dynamic behaviors of Yin chaos for parameter c

Range of parameter c	Behaviors of chaos
-15.00 ~ -25.77	Chaos
-25.77 ~ -25.80	Periodic trajectory
-25.80 ~ -29.05	Chaos
-29.05 ~ -32.00	Periodic trajectory

Table 2.6 and Table 2.7 show the dynamic behaviors of chaos and periodic motion in varied ranges of parameter c and fixed parameters a, b of Yang and Yin Lü system. Case 3 has different characteristics from that of Case 1 and Case 2 in that the Yin and Yang systems are more similar. Carefully observing the corresponding ranges, detailed differences can be found for Yin and Yang systems.

2.4 Tai Ji Lü system

"Tai Ji" Chen system, i.e. "Great One" Lü system, consists of Yin and Yang Lü system for time $-\infty$ to ∞. The jargon "Tai Ji" in Chinese philosophy, i.e. Yi classic, means the original chaotic substance which is the origin of the cosmos. The chaotic behaviors for time $-\infty$ to ∞ are shown in Figs 2.19~2.22 by time histories, 2D and 3D phase portraits.

Bifurcation diagrams of chaotic Yang and Yin Lü system in Figs 2.7, 2.9, Figs 2.11, 2.13 and Figs 2.15, 2.17 respectively, are almost symmetrical as a whole. Put

them together, and reverse the time order of Yin chaos, the time histories and phase portraits of Tai Ji Lü system are shown in Figs 2.19~2.22.

In order to study the difference between Yin and Yang chaos, the error values e_1, e_2 and e_3 are defined by

$$\begin{cases} e_1(t) = x_1(-t)_{\text{Yin}} - x_1(t)_{\text{Yang}} \\ e_2(t) = x_2(-t)_{\text{Yin}} - x_2(t)_{\text{Yang}} \\ e_3(t) = x_3(-t)_{\text{Yin}} - x_3(t)_{\text{Yang}} \end{cases} \tag{2.3}$$

The simulation results are shown in Fig. 2.23. Obviously, they are not the same. The bifurcation diagrams of Yang, Yin and Tai Ji Lü systems are shown in Figs 2.24~2.32.

2.5 Summary

In this research, Lü system is divided into Yang, Yin and "Tai Ji" systems and the "Tai Ji" Lü system is introduced firstly. Chaos of Yang system is studied by time histories, phase portraits, bifurcation diagrams and Lyapunov exponents. Next, the past of the system, Yin system, is studied. Finally, "Tai Ji" system is studied for past and future chaos and is compared with Yang and Yin systems via numerical simulations.

It is firstly discovered that the exact scientific chaos phenomena marvelously match with the ancient Chinese philosophy, "The Yin Classic" with English translation "The book of Change" which states that the original chaotic substance, Tai Ji, begets two fundamental opposites, Yin and Yang. Correspondingly, Tai Ji chaos consists of two opposites, Yin chaos and Yang chaos.

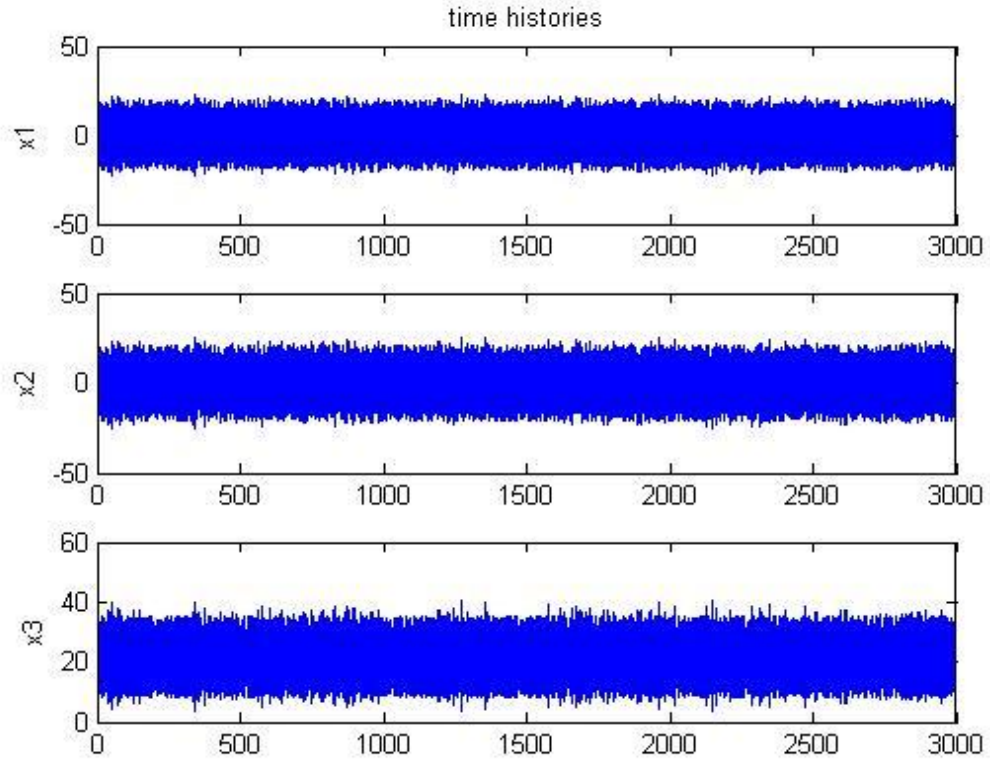

Fig.2 - 1 Time histories of Yang Lü chaos for Yang Lü system with a=36, b=3 and c=20.

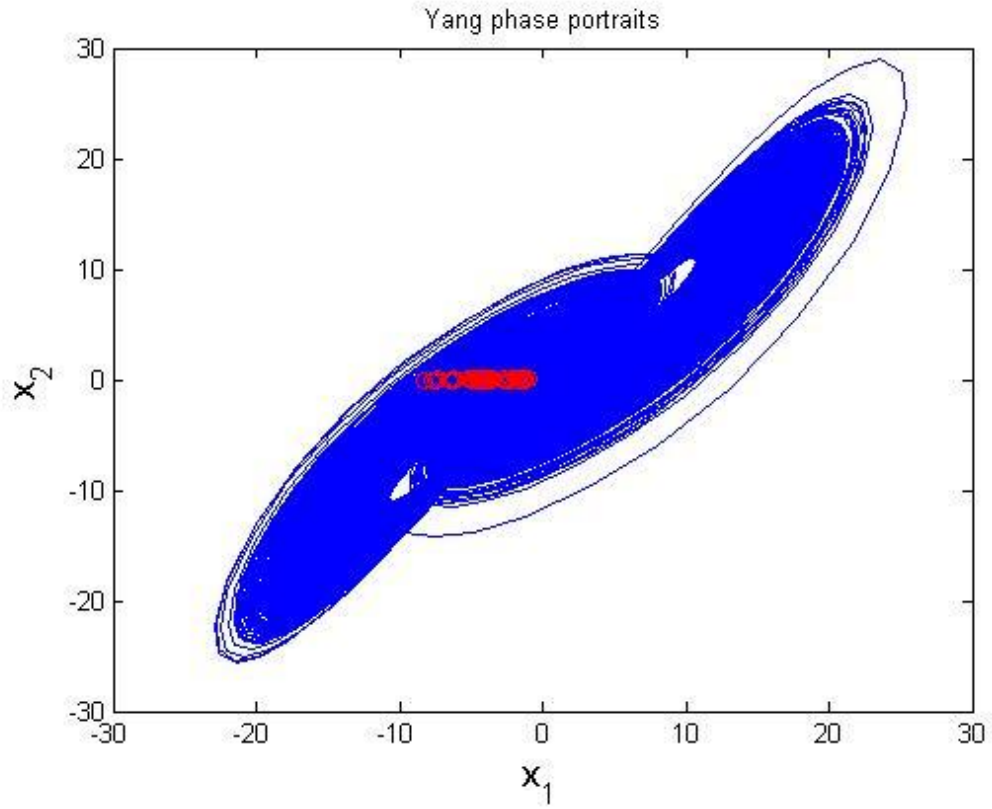

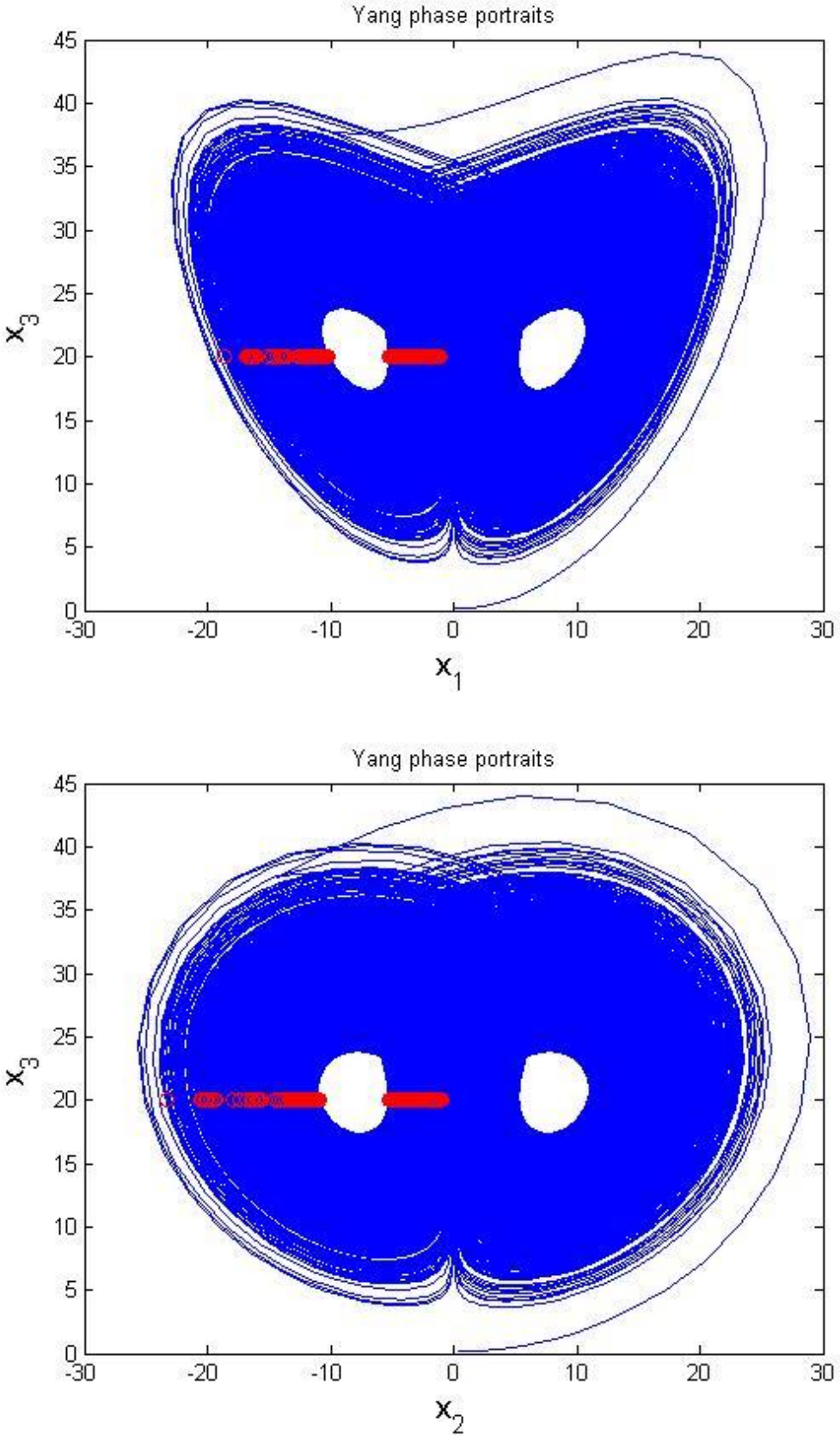

Fig.2 - 2 Projections of Phase portraits and Poincaré maps of Yang Lü chaos with a=35, b=3 and c=27.2.

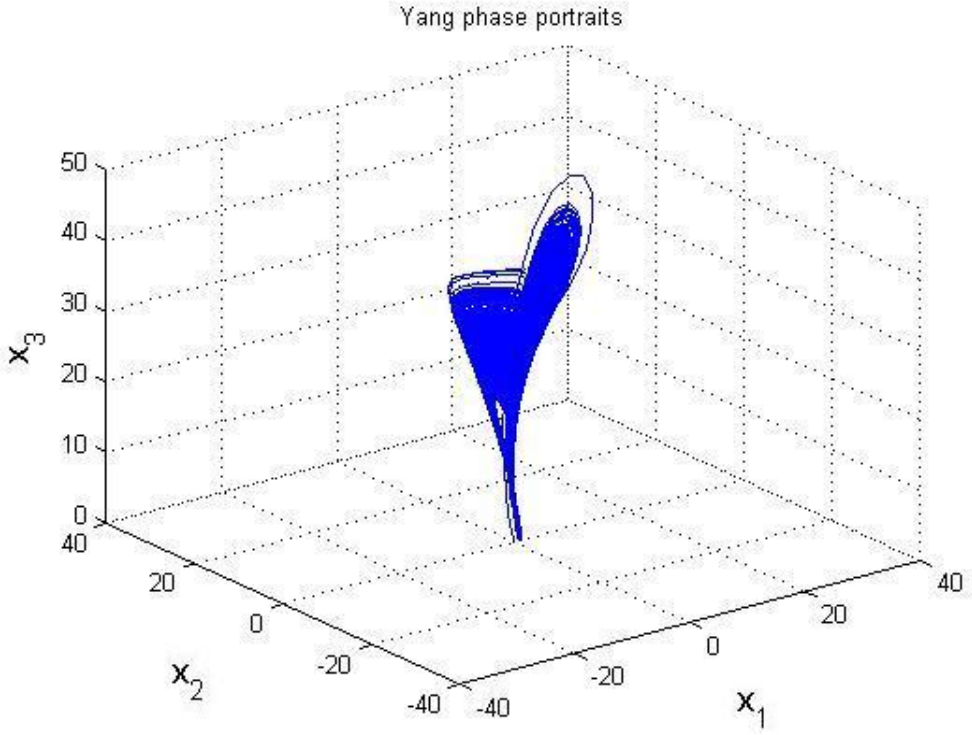

Fig.2 - 3 3D phase portrait of Yang Lü chaos with a=36, b=3 and c=20.

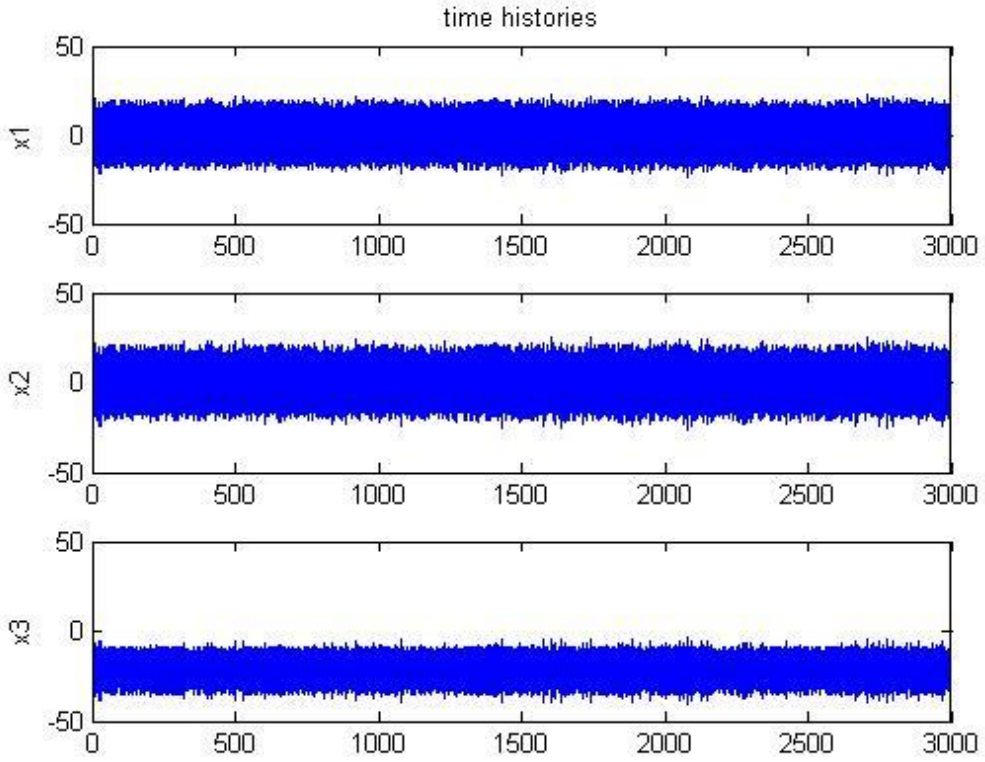

Fig.2 - 4 Time histories of Yin Lü chaos for Yin Lü system with a=-36, b=-3 and c=-20.

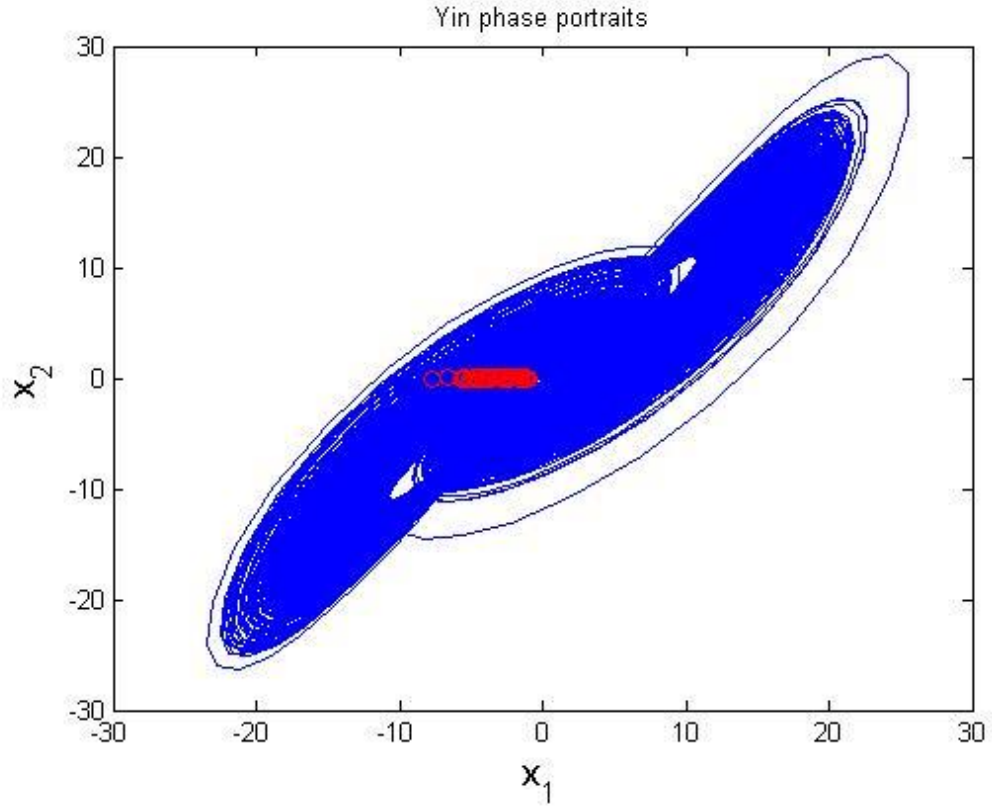
Yin phase portraits
30
20
10
0
-10
-20
-30
-30
-20
-10
0
10
20
30
x2
x1

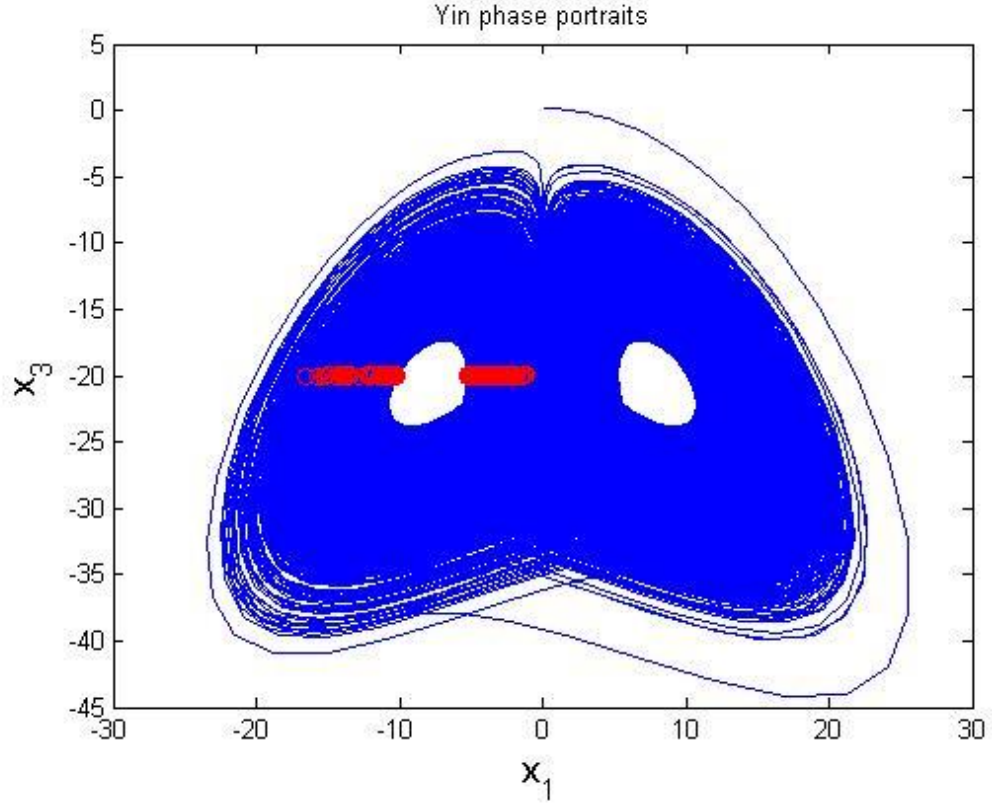
Yin phase portraits
5
0
-5
-10
-15
-20
-25
-30
-35
-40
-45
-30
-20
-10
0
10
20
30
x3
x1

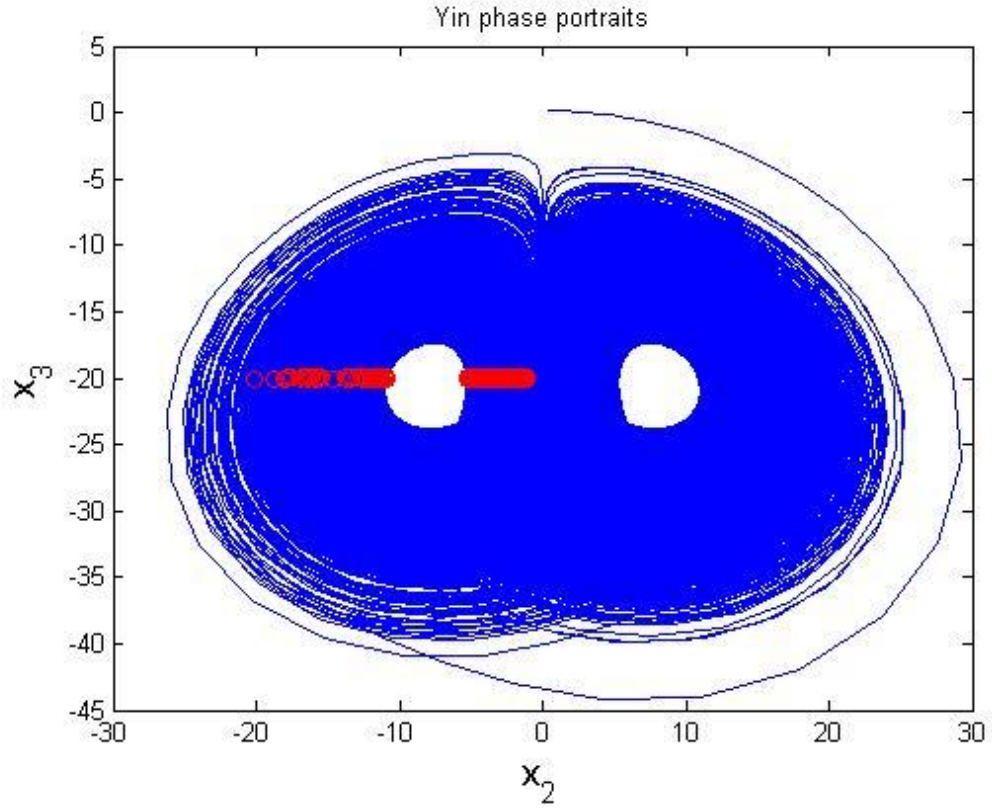

Fig.2 - 5 Projections of Phase portraits and Poincaré maps of Yin Lü chaos with a=-36, b=-3 and c=-20.

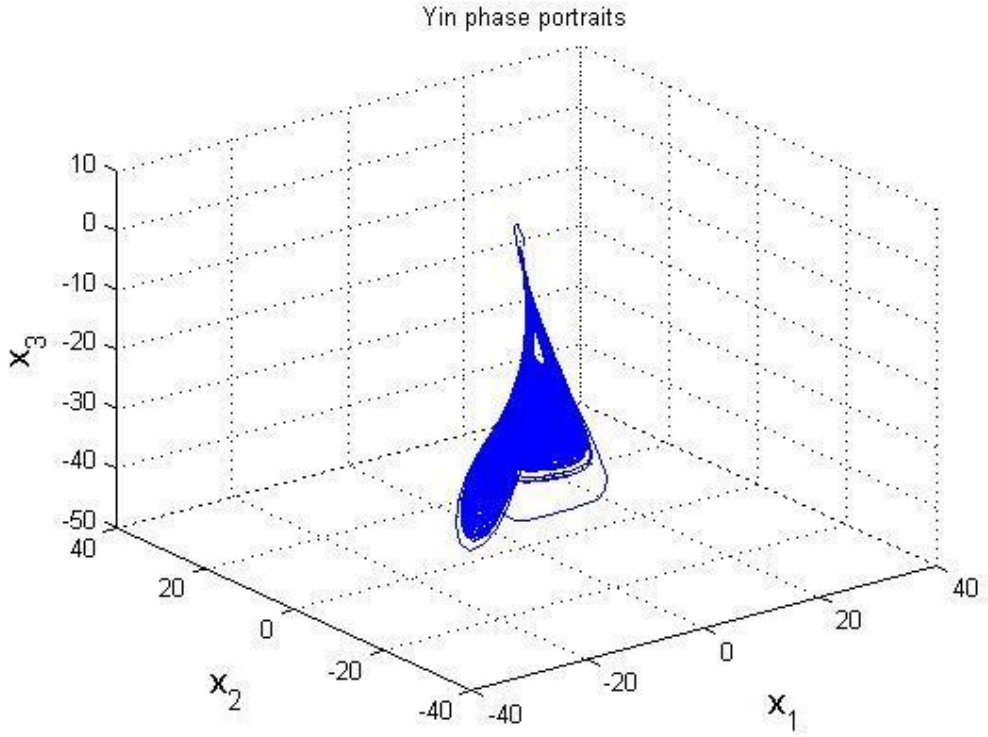

Fig.2 - 6 3D phase portrait of Yin Lü system with a=-36, b=-3 and c=-20.

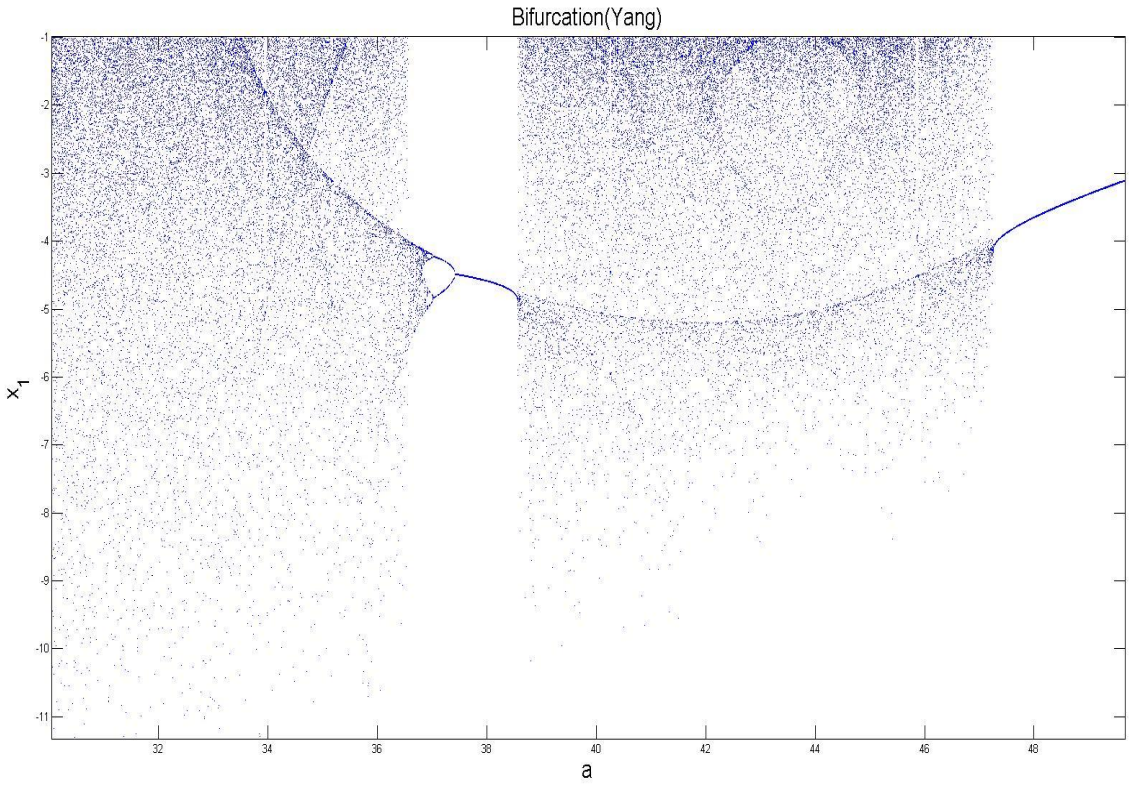

Fig.2 - 7 Bifurcation diagram of chaotic Yang Lü system with b=3 and c=20.

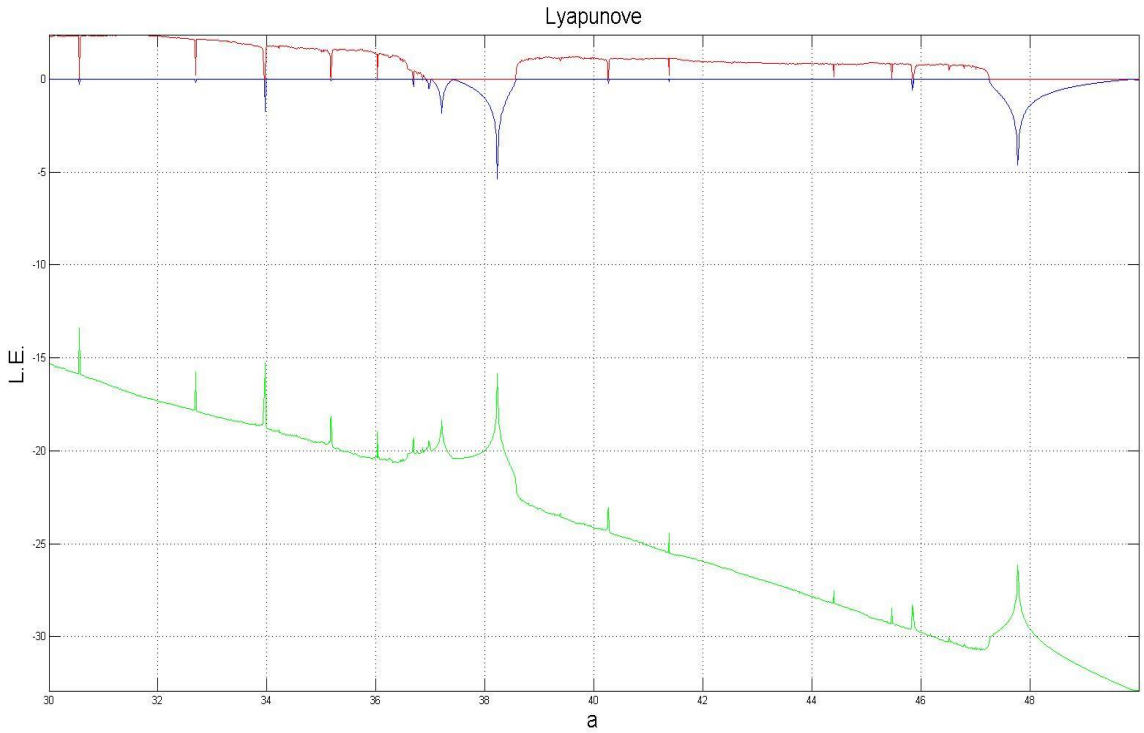

Fig.2 - 8 Lyapunov exponents of chaotic Yang Lü system with b=3 and c=20.

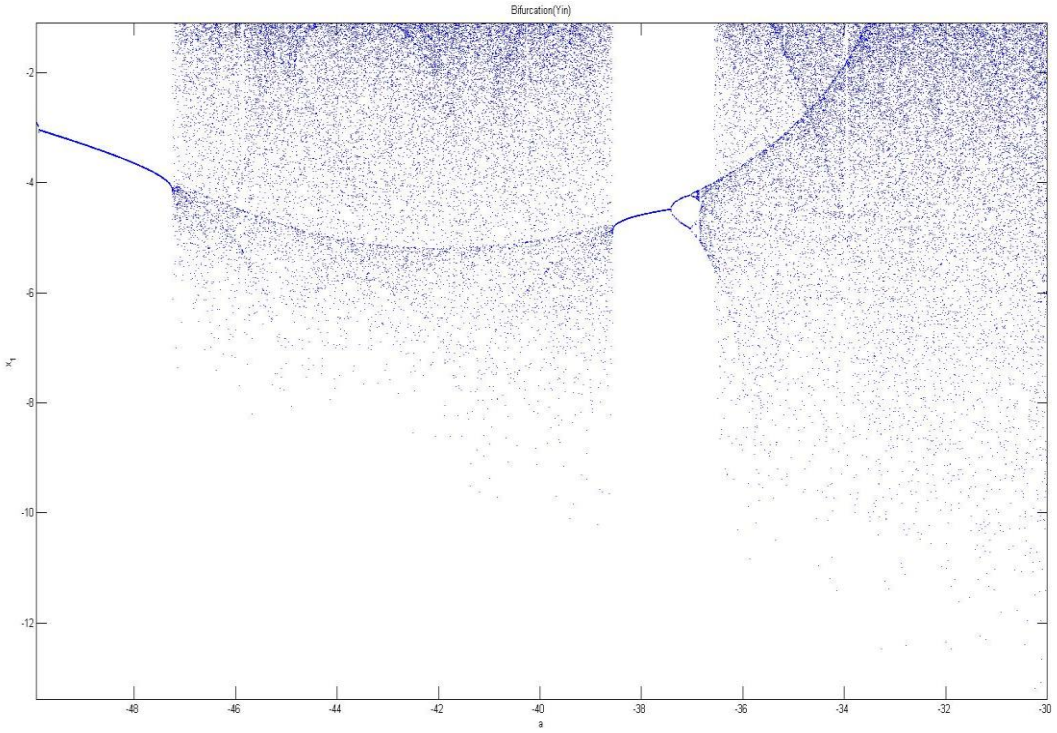

Fig.2 - 9 Bifurcation diagram of chaotic Yin Lü system with b=-3 and c=-20.

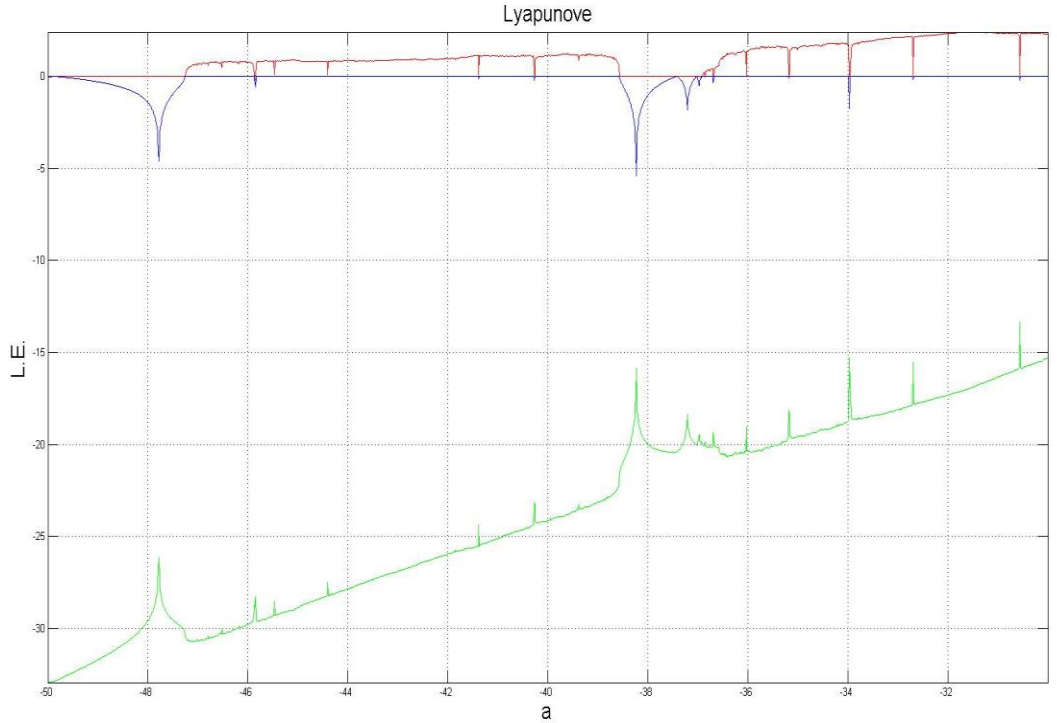

Fig.2 - 10 Lyapunov exponents of chaotic Yin Lü system with b=-3 and c=-20..

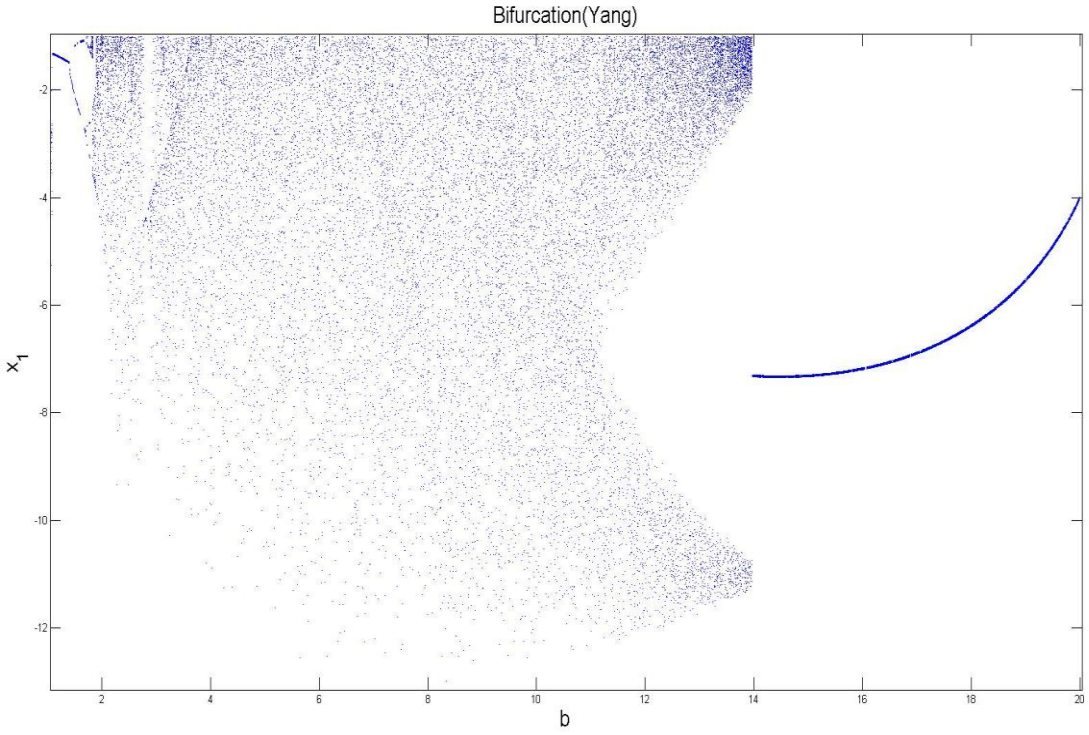

Fig.2 - 11 Bifurcation diagram of chaotic Yang Lü system with a=36 and c=20.

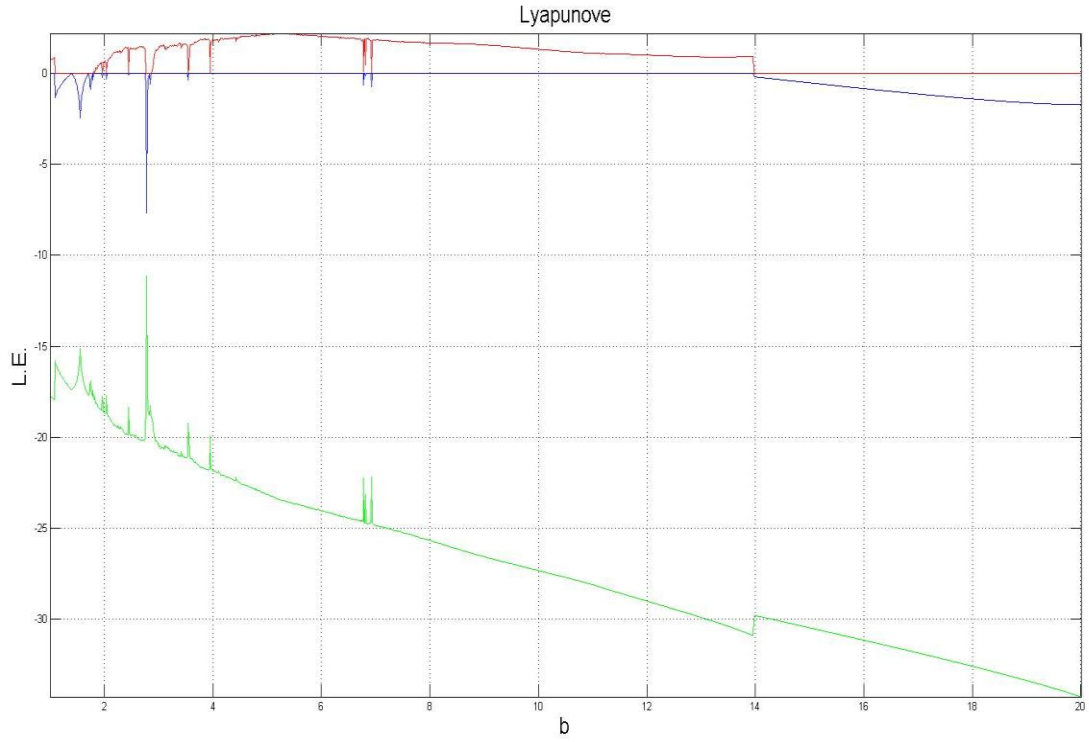

Fig.2 - 12 Lyapunov exponents of chaotic Yang Lü system with a=36 and c=20.

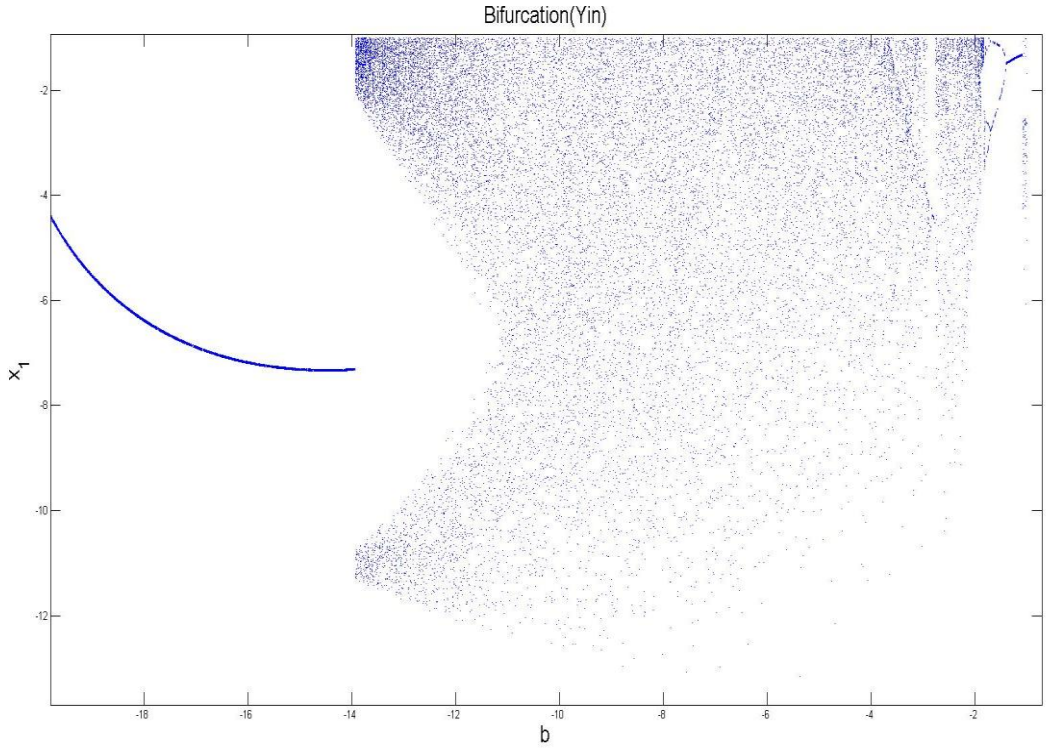

Fig.2 - 13 Bifurcation diagram of chaotic Yin Lü system with a=-36 and c=-20.

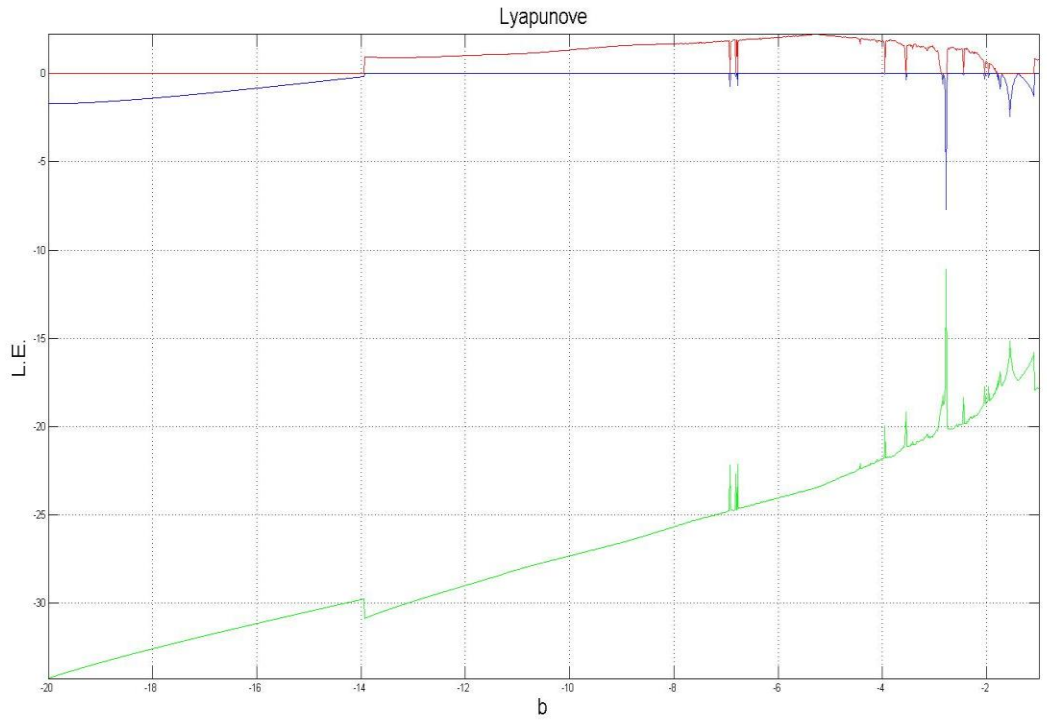

Fig.2 - 14 Lyapunov exponents of chaotic Yin Lü system with a=-36 and c=-20.

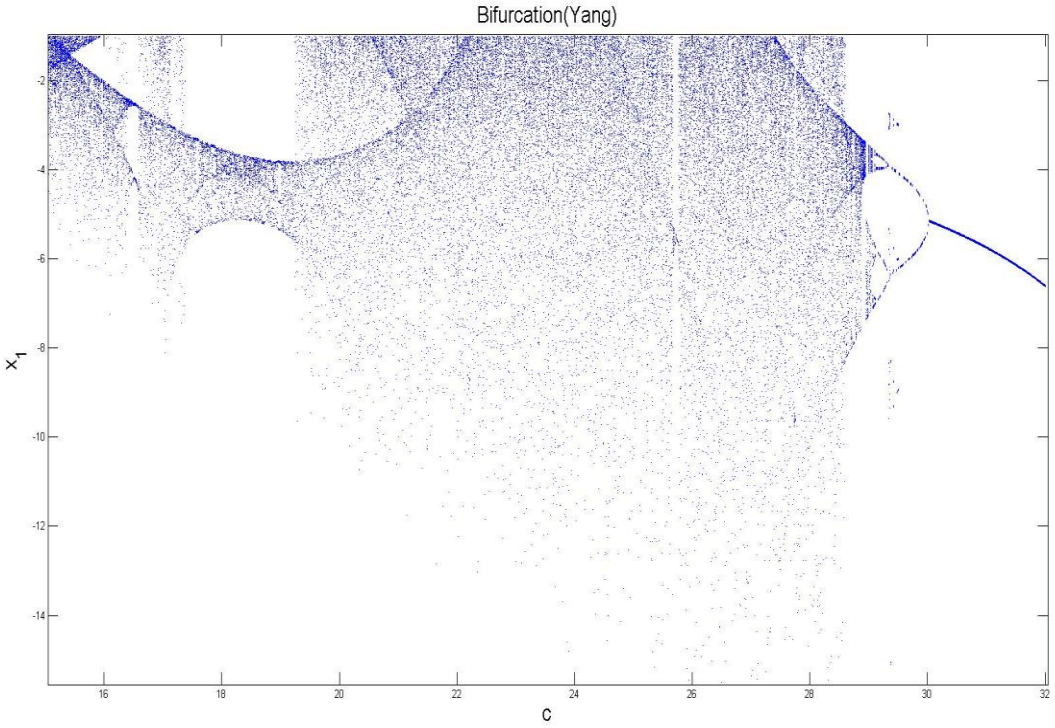

Fig.2 - 15 Bifurcation diagram of chaotic Yang Lü system with a=36 and b=3.

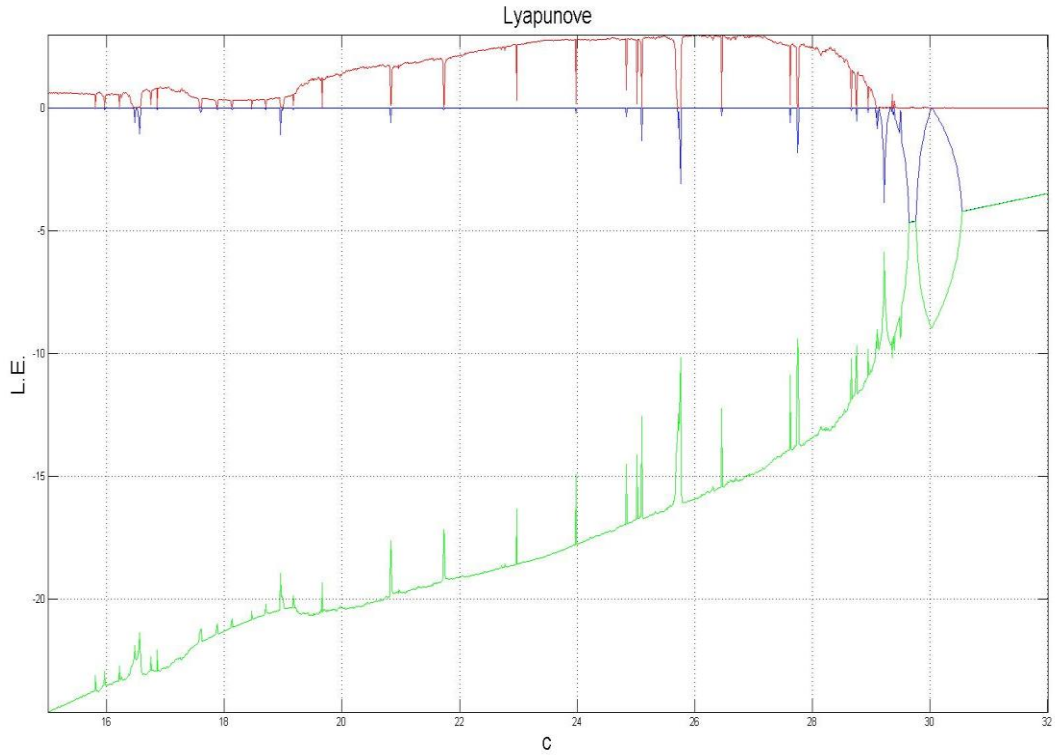

Fig.2 - 16 Lyapunov exponents of chaotic Yang Lü system with a=36 and b=3.

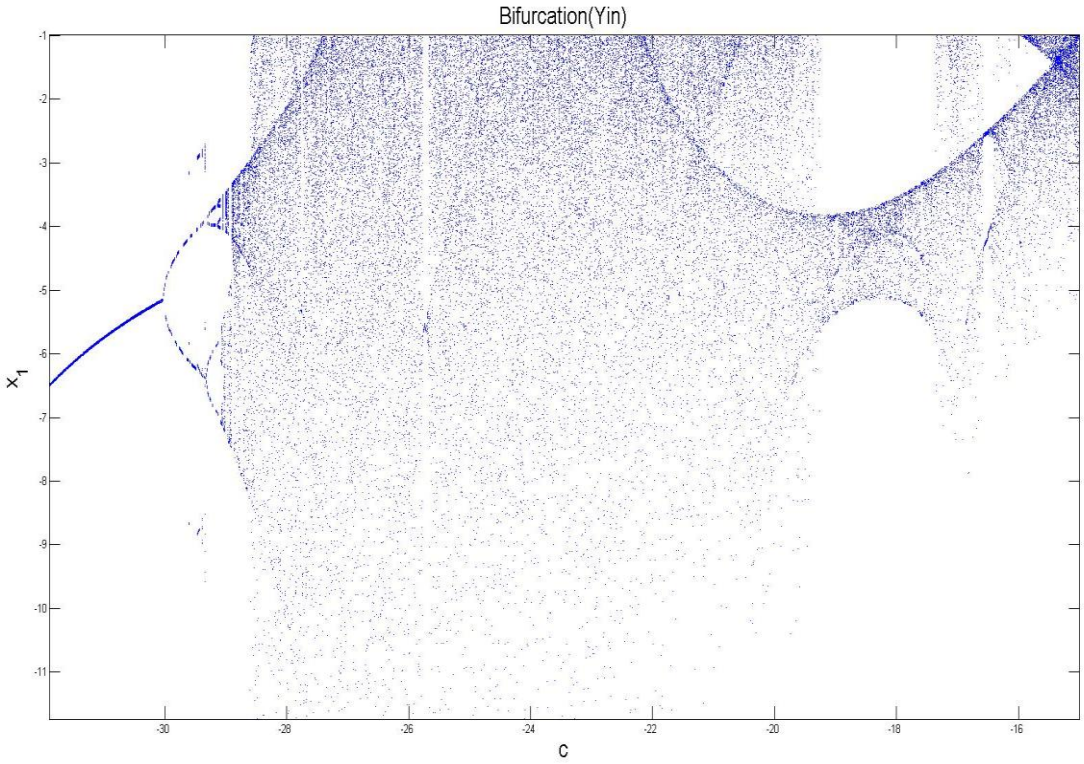

Fig.2 - 17 Bifurcation diagram of chaotic Yin Lü system with a=-36 and b=-3.

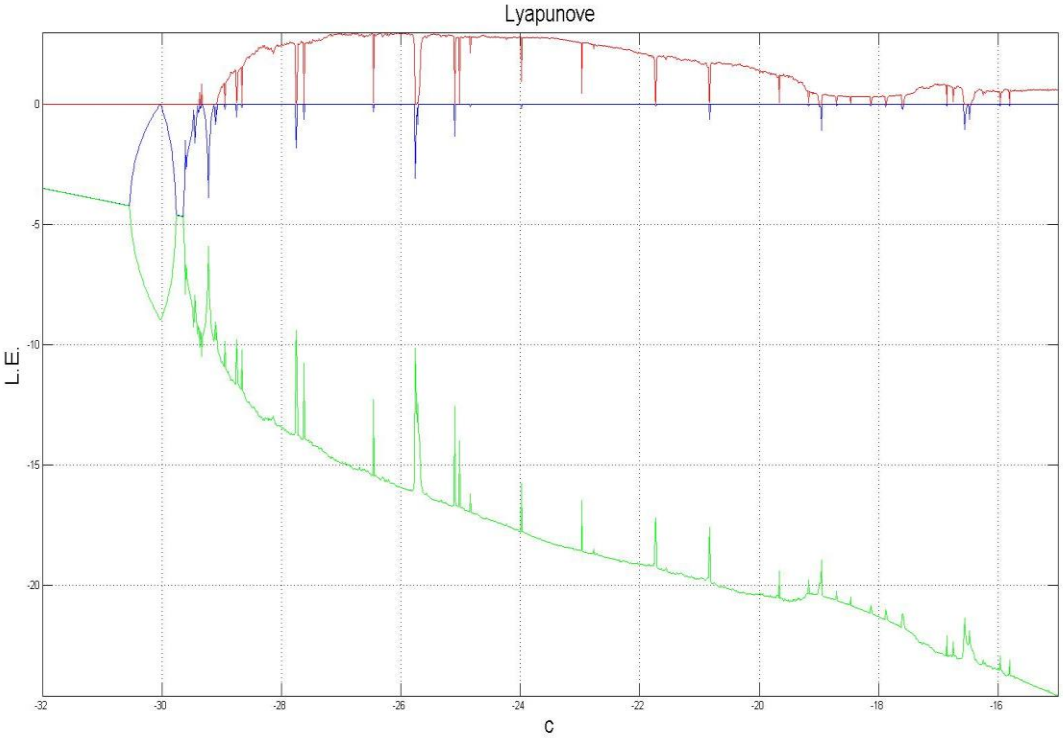

Fig.2 - 18 Lyapunov exponents of chaotic Yin Lü system with a=-36 and b=-3.

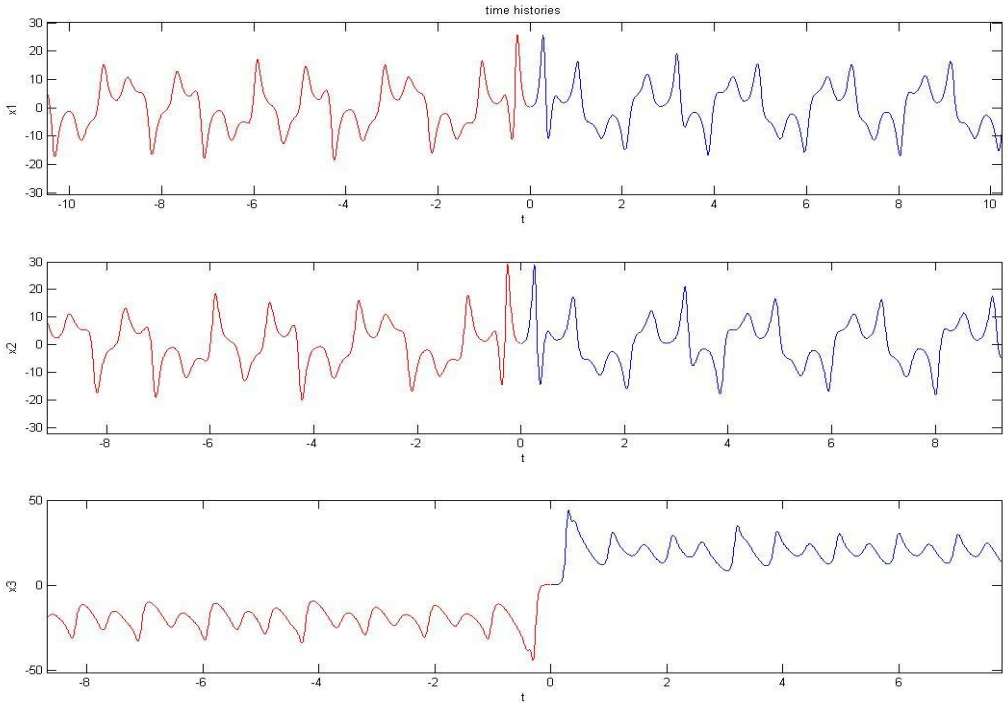

Fig.2 - 19 Time histories of Tai Ji Lü system.

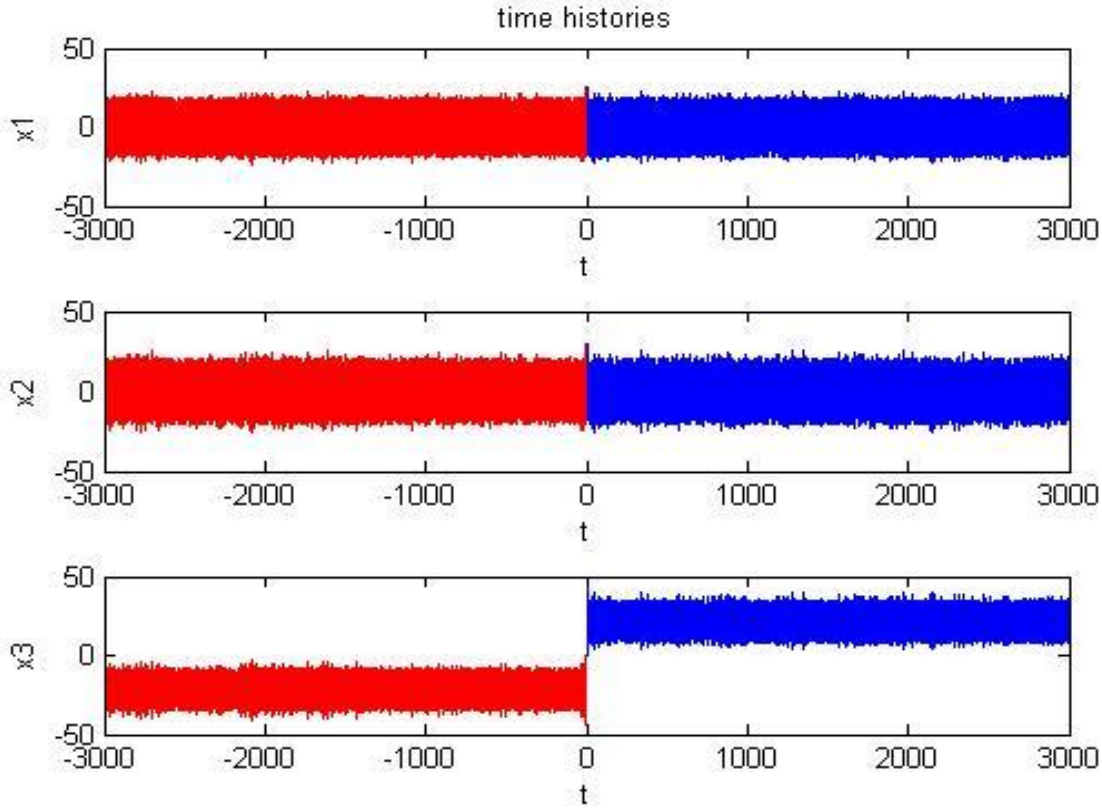

Fig.2 - 20 Time histories of Tai Ji Lü system for -10sec < t < 10sec.

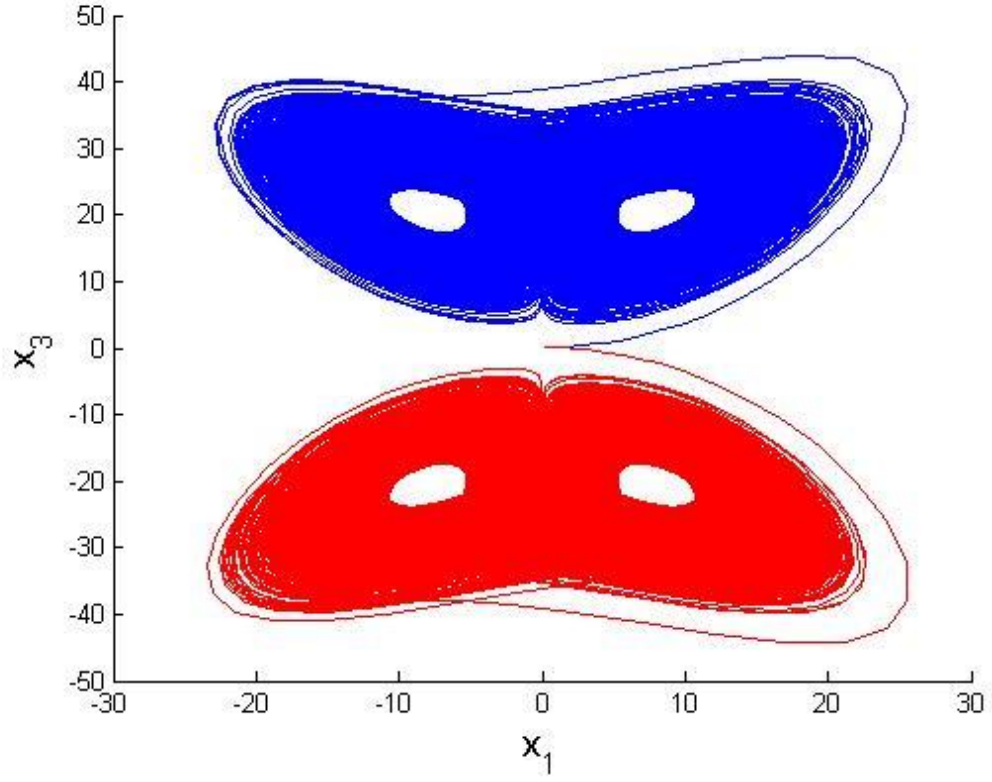
50
40
30
20
10
0
-10
-20
-30
-40
-50
-30
-20
-10
0
10
20
30
x3
x1

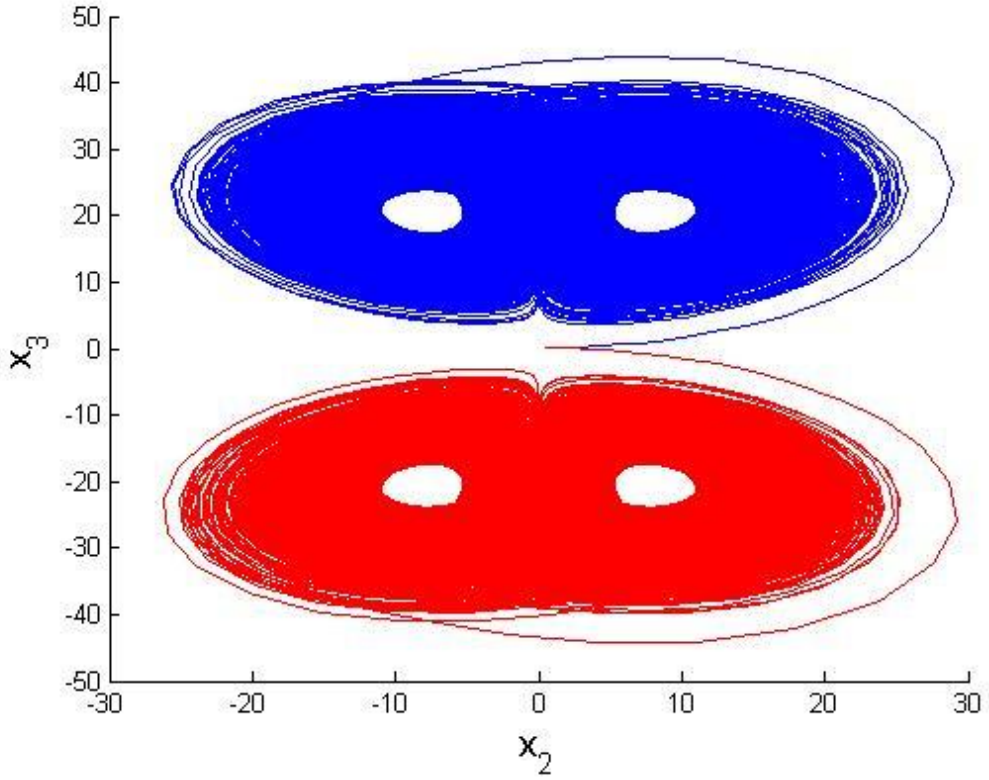
50
40
30
20
10
0
-10
-20
-30
-40
-50
-30
-20
-10
0
10
20
30
x3
x2

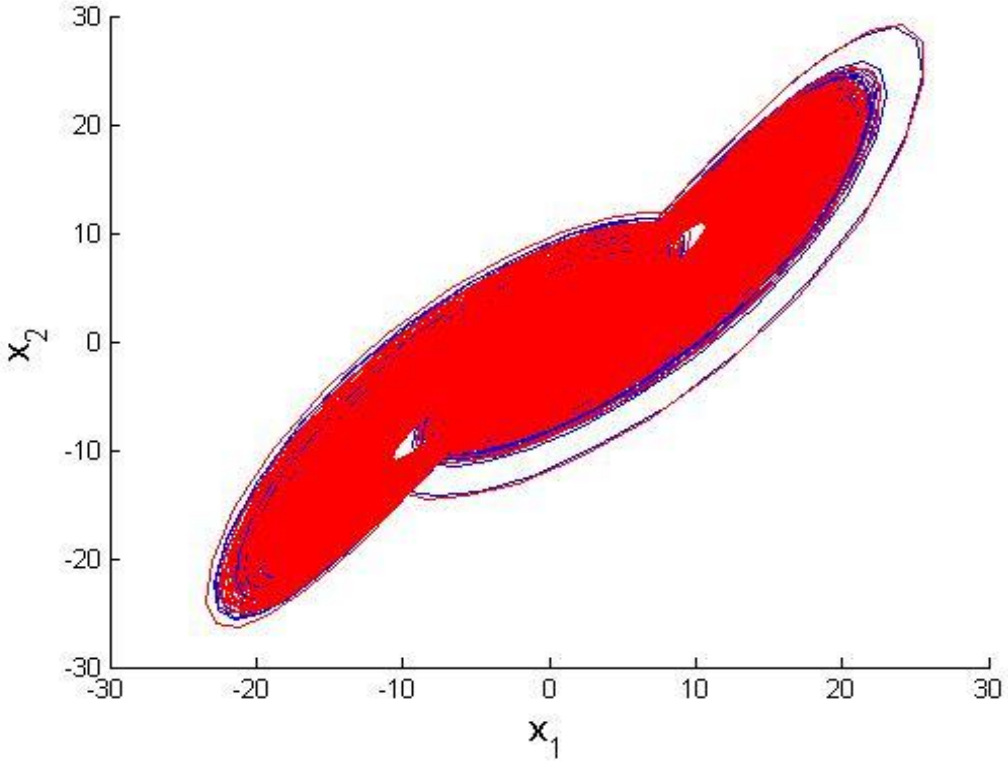

Fig.2 - 21 Projections of phase portraits of Tai Ji Lü system.

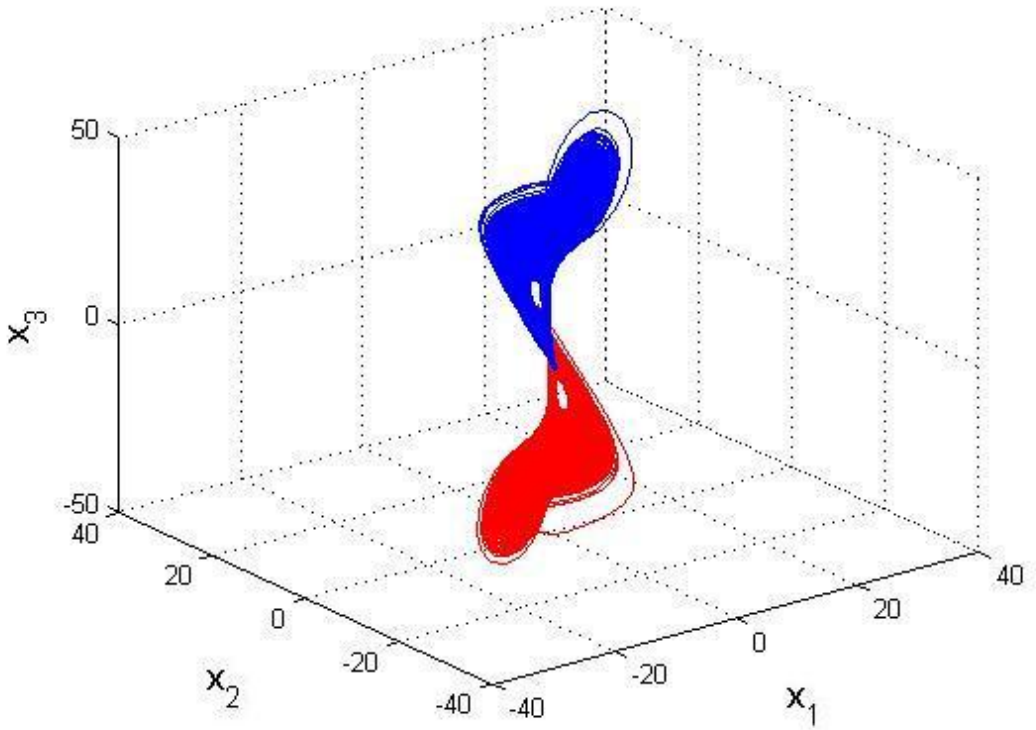

Fig.2 - 22 3D phase portrait of Tai Ji Lü system.

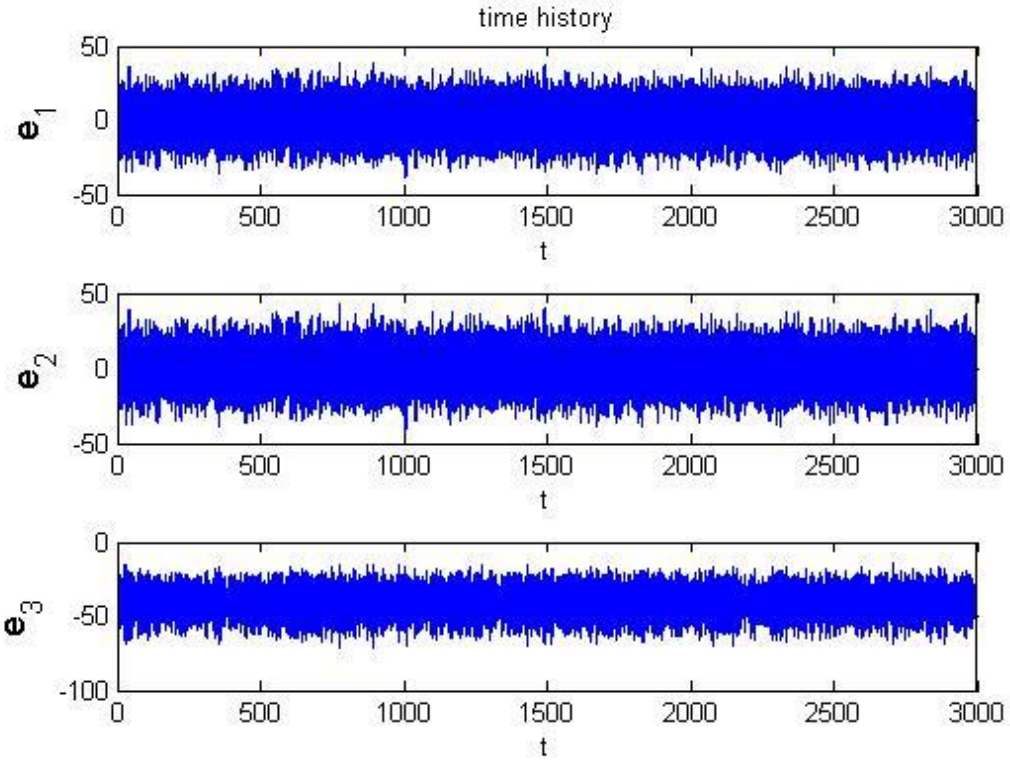

Fig.2 - 23 Time histories of errors for Lü system.

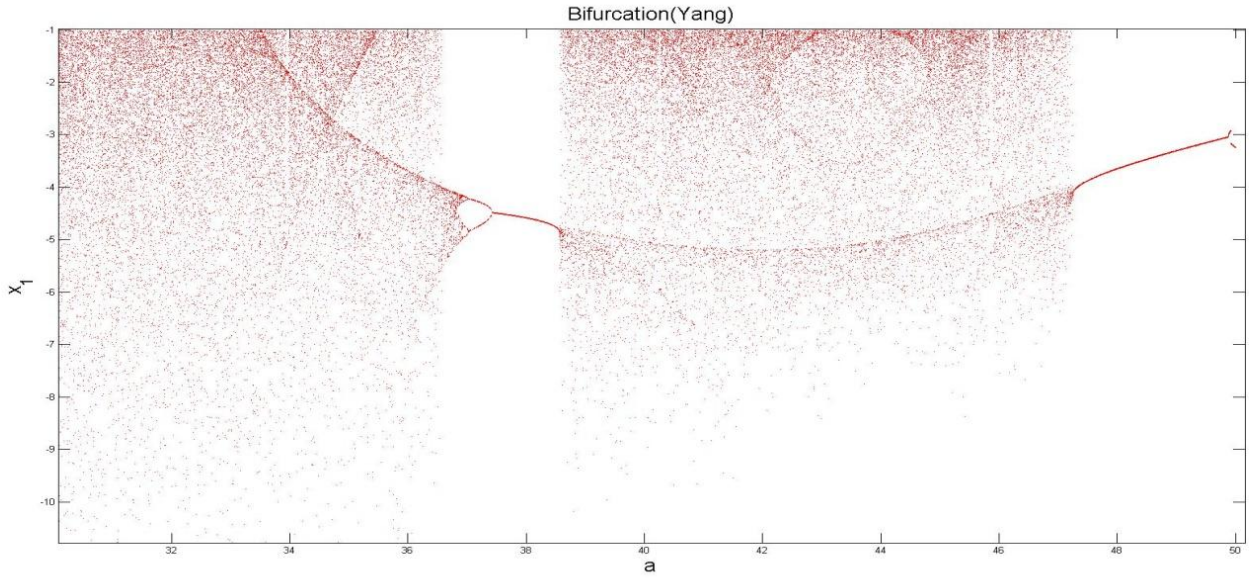

Fig.2 - 24 Bifurcation diagram of chaotic Yang Lü system for varied parameter a.

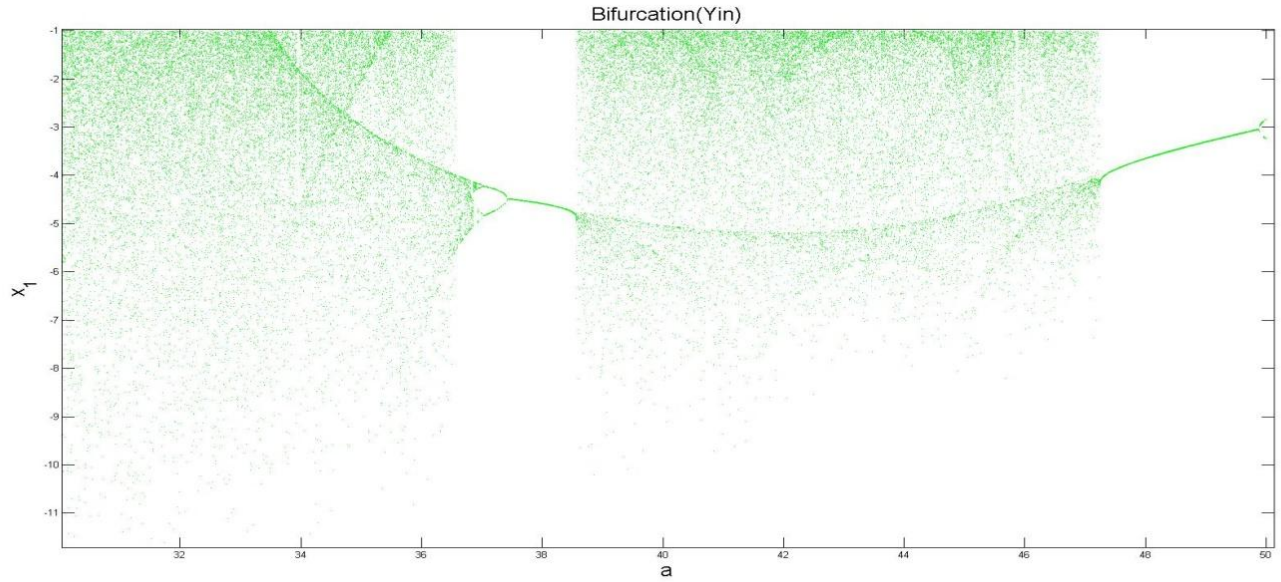

Fig.2 - 25 Bifurcation diagram of chaotic Yin Lü system for varied parameter a.

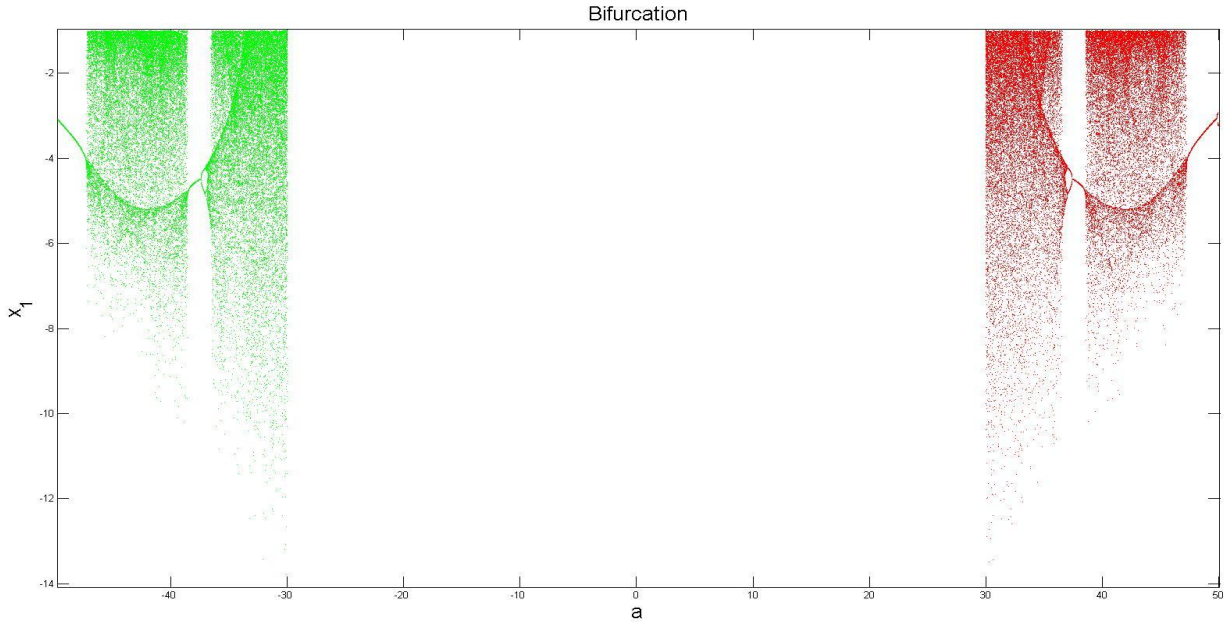

Fig.2 - 26 Bifurcation diagram of chaotic Tai Ji Lü system for varied parameter a.

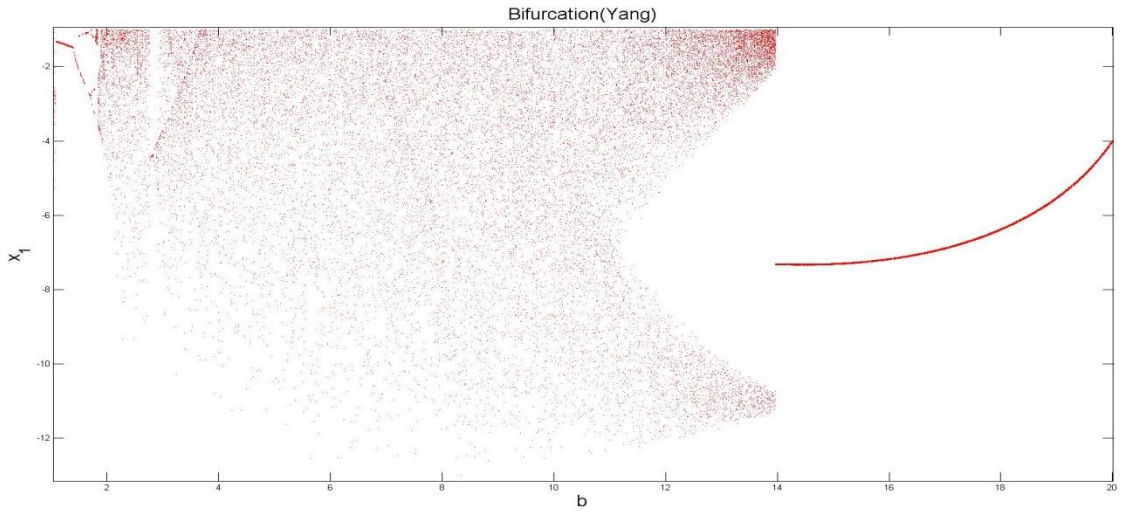

Fig.2 - 27 Bifurcation diagram of chaotic Yang Lü system for varied parameter b.

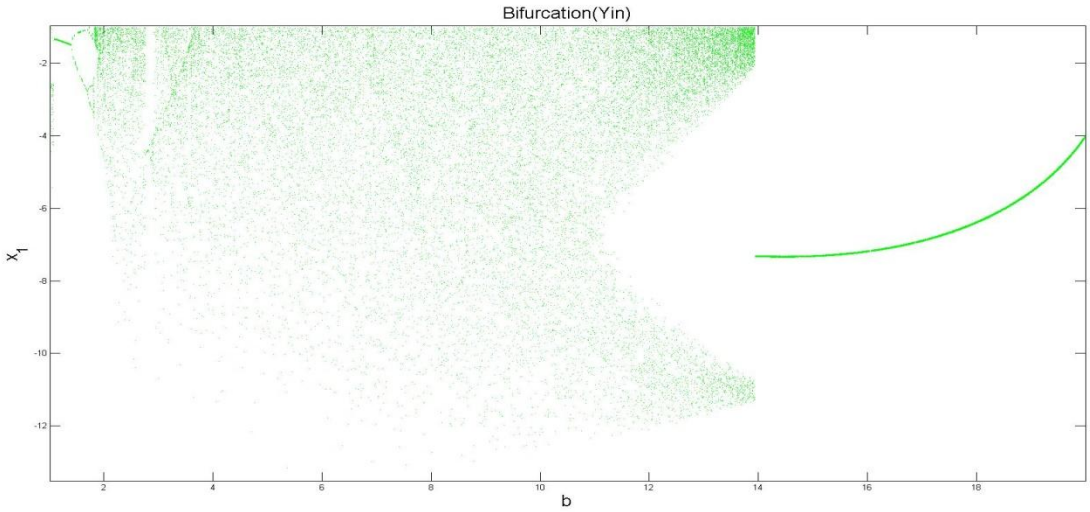

Fig.2 - 28 Bifurcation diagram of chaotic Yin Lü system for varied parameter b.

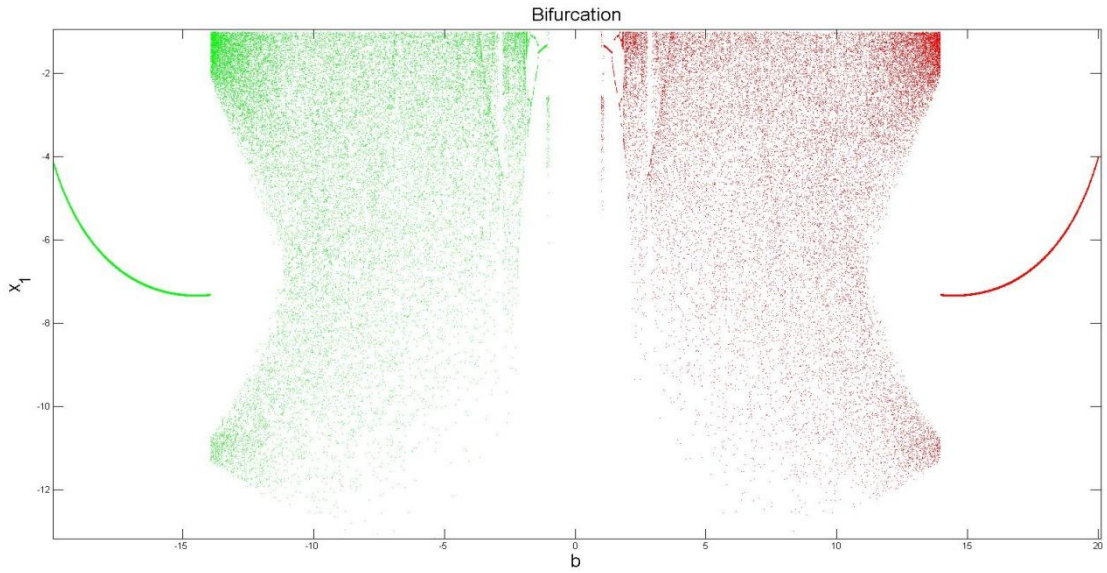

Fig.2 - 29 Bifurcation diagram of chaotic Tai Ji Lü system for varied parameter b.

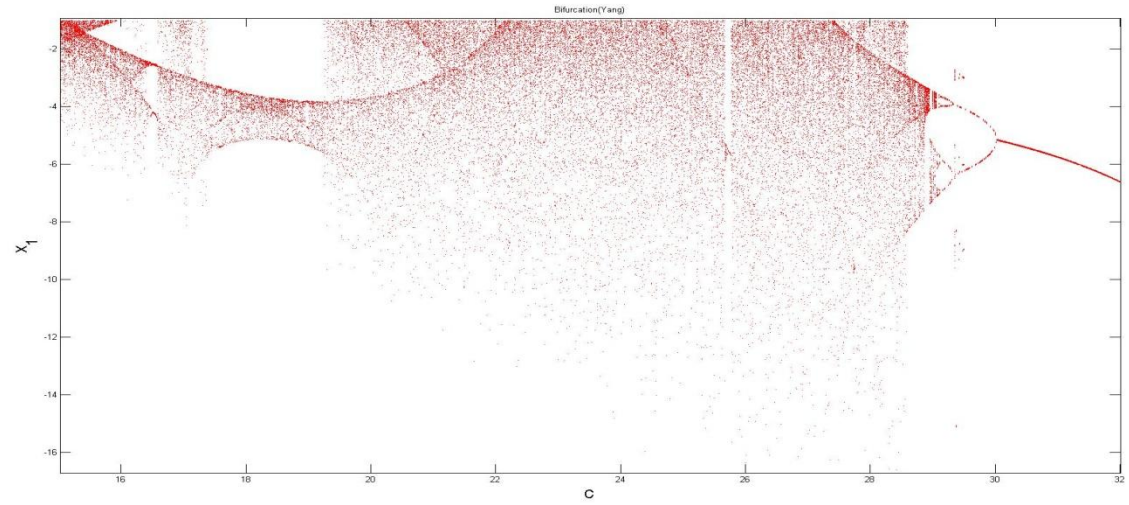

Fig.2 - 30 Bifurcation diagram of chaotic Yang Lü system for varied parameter c.

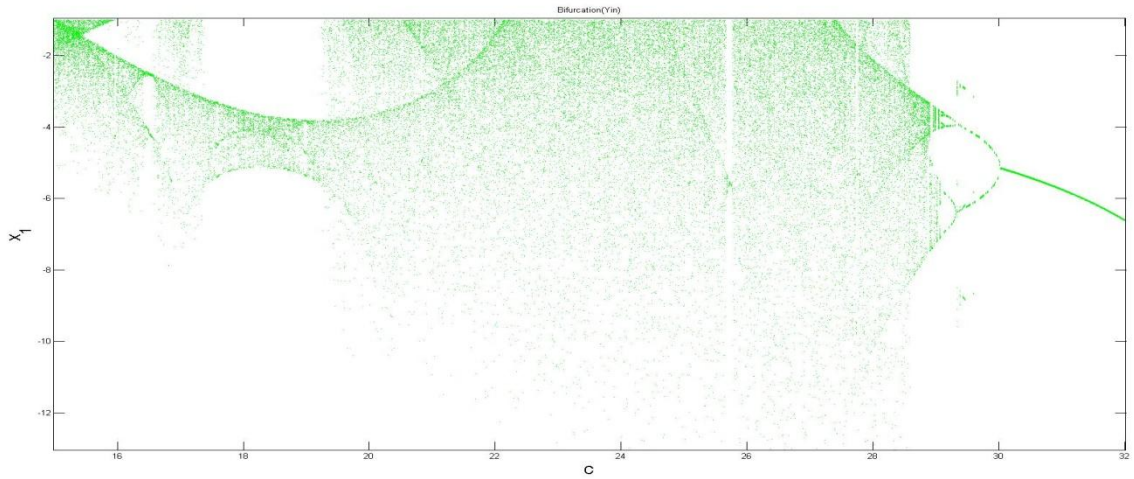

Fig.2 - 31 Bifurcation diagram of chaotic Yin Lü system for varied parameter c.

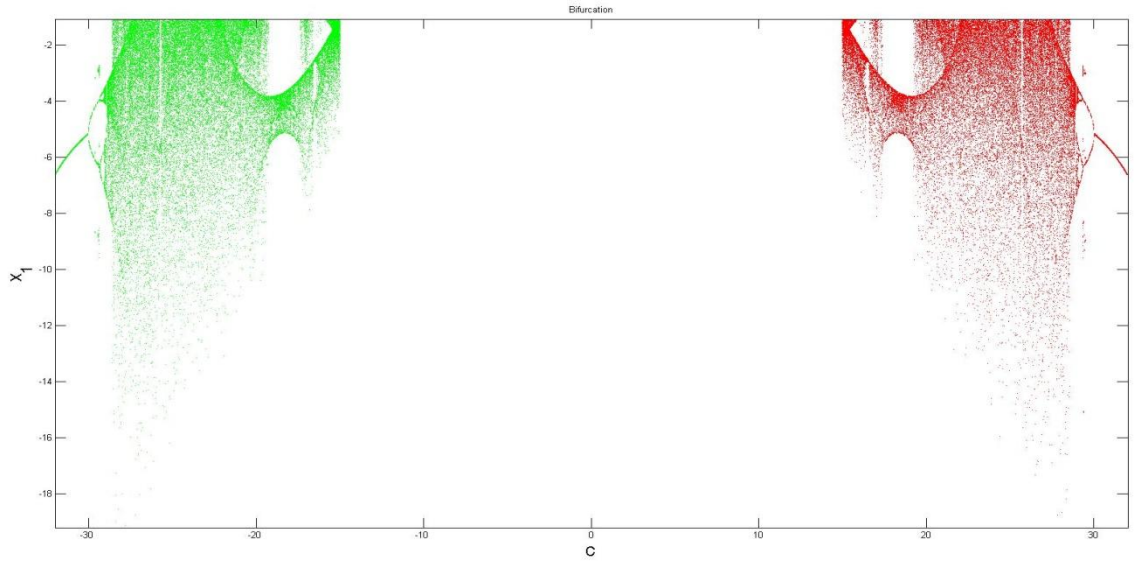

Fig.2 - 32 Bifurcation diagram of chaotic Tai Ji Lü system for varied parameter c.

Chapter 3

Multiple Symplectic Derivative Synchronization of Ge-Ku-Duffing-Lü System with Other Different Systems by Partial Region Stability Theory

3.1 Preliminary

A new type of synchronization, multiple symplectic derivative synchronization is obtained by active control. Next, the partial region stability theory is used for this kind of synchronization. A comparison of errors between new and traditional methods shows that the convergence rate of the new method is much faster than that of the traditional method.

3.2 Strategy of multiple symplectic derivative synchronization

There are two chaotic systems, partner system A and partner system B. The partner A is given by

$$\dot{x} = f(t, x) \tag{3.1}$$

The partner B is given by

$$\dot{y} = g(t, y) \tag{3.2}$$

In order that the error dynamics becomes always positive, the origin of y-coordinate system is translated by a constant vector .

Define $e = G - F + K$ as the error state vector, where $G = G(x, y, \cdots, \dot{x}, \dot{y}, \cdots, \ddot{x}, \ddot{y}, \cdots, t)$ and $F = F(x, y, \cdots, \dot{x}, \dot{y}, \cdots, \ddot{x}, \ddot{y}, \cdots, t)$ are two given functions, and K is positive constant vector to keep the error dynamics always in first quadrant.

Then the error vector derivative is obtained：

$$\dot{e}_i = \dot{G}_i - \dot{F}_i - u_i \tag{3.3}$$

where u_i is a component of the control input vector u, $i = 1, 2, \cdots, n$.

The synchronization can be accomplished when $t \to \infty$, the limit of the error vector $e = [e_1, e_2, \cdots, e_n]^T$ approaches to zero:

$$\lim_{t\to\infty} e = 0 \tag{3.4}$$

3.3 Synchronization by partial region stability theory

Given

$$G(x, y, z, \dot{x}, \dot{y}, \dot{z}, \ddot{x}, \ddot{y}, \ddot{z}, t) = \begin{bmatrix} x_4 \sin x_2 + z_1[\dot{x}_4 - 36(x_5 - x_4)] \\ y_2 \cos y_4 \\ z_2 + z_4 + z_6 + 36(x_5 - x_4) \\ \sin(z_4 + z_6) + \sin \ddot{z}_1 \\ \cos \ddot{x}_4 + \left(x_5 + \frac{x_1}{36} - \frac{\dot{x}_4}{36}\right) + \frac{\dot{y}_4}{y_5} \\ z_4 + \dot{z}_6 + y_2 y_3 + z_6 \end{bmatrix}, \tag{3.5}$$

$$F(x, y, z, \dot{x}, \dot{y}, \dot{z}, \ddot{x}, \ddot{y}, \ddot{z}, t) =$$

$$\begin{bmatrix} x_1 z_1 + \left(x_5 + \frac{x_1}{36} - \frac{\dot{x}_4}{36}\right) \sin \dot{x}_1 \\ x_2 y_2 + (y_1 - \dot{y}_2) \cos y_4 \\ \dot{x}_4 + \dot{z}_5 \\ \sin \ddot{z}_1 \\ x_1 + x_4 + y_6 + \cos[36(-x_4 x_6 + 20x_5) - 36^2(x_5 - x_4) - x_1] \\ \ddot{y}_2 + \dot{z}_5 + \dot{y}_2 \end{bmatrix}, \tag{3.6}$$

Our purpose is to achieve the multiple symplectic derivative synchronization $G(x, \dot{x}, \ddot{x}, y, \dot{y}, \ddot{y}, z, \dot{z}, \ddot{z}, t) = F(x, \dot{x}, \ddot{x}, y, \dot{y}, \ddot{y}, z, \dot{z}, \ddot{z}, t) - K$.

Consider system 1, combining Ge-Ku-Duffing system and Lü system[16] by adding x_1 in the second equation of Lü system, Ge-Ku-Duffing-Lü system is obtained：

$$\begin{cases} \dot{x}_1 = x_2 \\ \dot{x}_2 = -0.1x_2 - x_1[11(40 - {x_1}^2) + 54x_3] \\ \dot{x}_3 = -x_3 - {x_3}^3 - 6x_2 + 30x_1 \\ \dot{x}_4 = 36(x_5 - x_4) + x_1 \\ \dot{x}_5 = -x_4 x_6 + 20x_5 \\ \dot{x}_6 = x_4 x_5 - 3x_6 \end{cases} \tag{3.7}$$

When initial condition（x_{10}、x_{20}、x_{30}）=（2，2.4，5）and（x_{40}、x_{50}、x_{60}）=（0.2，0.35，0.2）, chaos of the Ge-Ku-Duffing-Lü system is appeared. The chaotic attractor of the combination of Ge-Ku-Duffing-Lü system is shown in Fig. 1.

The system 2, combining a Sprott C system[31] and Sprott E system [31] by adding y_3 in the second equation of Sprott E system, Sprott C - E system is obtained：

$$\begin{cases} \dot{y}_1 = y_2 y_3 \\ \dot{y}_2 = y_1 - y_2 \\ \dot{y}_3 = 1 - {y_1}^2 \\ \dot{y}_4 = y_5 y_6 \\ \dot{y}_5 = {y_4}^2 - y_5 + y_3 \\ \dot{y}_6 = 1 - 4y_4 \end{cases} \tag{3.8}$$

When initial condition（y_{10}、y_{20}、y_{30}）=（0.8，1，0.01）and（y_{40}、y_{50}、y_{60}）=（0.2，0.063，0.01）, chaos of the Sprott C - E system is appeared. The chaotic attractor of the combination of Sprott C - E system is shown in Fig. 2.

The system 3, combining a Lorenz system[32] and Sprott D system [31] by adding $0.001z_3$ in the second equation of Sprott D system, Lorenz- Sprott D system is obtained：

$$\begin{cases} \dot{z}_1 = 10(z_2 - z_1) \\ \dot{z}_2 = 28z_1 - z_1 z_3 - z_2 \\ \dot{z}_3 = z_1 z_2 - {}^{8}/_{3}\, z_3 \\ \dot{z}_4 = -z_5 \\ \dot{z}_5 = z_4 + z_6 \\ \dot{z}_6 = z_4 z_6 + 3{z_5}^2 + 0.001z_3 \end{cases} \tag{3.9}$$

When initial condition（z_{10}、z_{20}、z_{30}）=（-0.1，0.2，0.3）and（z_{40}、z_{50}、z_{60}）=（0.1，0.1，0.1）, chaos of the Lorenz- Sprott D system is appeared. The chaotic attractor of the combination of Lorenz and Sprott D is shown in Fig. 3.

The state error is $e = G - F + K$ where $K = [120,100,40,5,300,5]^T$ such that error dynamics always exists in first guardant as shown in Fig. 4 and Fig. 5. Our purpose is

$$\lim_{t\to\infty} e_i = G_i - F_i + K_i = 0, \tag{3.10}$$

where i = 1, 2,⋯ ,6.We obtain the error dynamics:

$$\begin{cases} \dot{e}_1 = \dot{G}_1 - \dot{F}_1 - u_1 \\ \dot{e}_2 = \dot{G}_2 - \dot{F}_2 - u_2 \\ \dot{e}_3 = \dot{G}_3 - \dot{F}_3 - u_3 \\ \dot{e}_4 = \dot{G}_4 - \dot{F}_4 - u_4 \\ \dot{e}_5 = \dot{G}_5 - \dot{F}_5 - u_5 \\ \dot{e}_6 = \dot{G}_6 - \dot{F}_6 - u_6 \end{cases} \tag{3.11}$$

By partial region stability theory, we can choose a Lyapunov function in the form of a positive definite function in first quadrant:

$$V(e) = e_1+e_2+e_3+e_4+e_5+e_6 \tag{3.12}$$

Its time derivative is

$$\dot{V}(e) = \left(\dot{G}_1 - \dot{F}_1 - u_1\right) + \left(\dot{G}_2 - \dot{F}_2 - u_2\right) + \left(\dot{G}_3 - \dot{F}_3 - u_3\right) + \left(\dot{G}_4 - \dot{F}_4 - u_4\right) + \left(\dot{G}_5 - \dot{F}_5 - u_5\right) + \left(\dot{G}_6 - \dot{F}_6 - u_6\right) \tag{3.13}$$

Choose the controller u as

$$u = \begin{bmatrix} e_1 + y_1 - y_2 \\ e_2 + x_4x_5 - 3x_6 \\ e_3 + x_2 \\ e_4 + y_2y_3 \\ e_5 - x_2 \\ e_6 - z_5 \end{bmatrix} \tag{3.14}$$

we obtain

$$\dot{V}(e) = -e_1 - e_2 - e_3 - e_4 - e_5 - e_6 < 0 \tag{3.15}$$

which is negative definite function in first quadrant. Error state time histories are shown in Fig. 6 and Fig. 7.

3.4 Synchronization by traditional method

If the traditional Lyapunov function is used, it means that

$$V(e) = e_1^2 + e_2^2 + e_3^2 + e_4^2 + e_5^2 + e_6^2 \tag{3.16}$$

Its time derivative is

$$\dot{V}(e) = 2(e_1\dot{e}_1 + e_2\dot{e}_2 + e_3\dot{e}_3 + e_4\dot{e}_4 + e_5\dot{e}_5 + e_6\dot{e}_6) \tag{3.17}$$

We want to find u of Eq. (11) such that

$$\dot{V}(e) = -(e_1^2 + e_2^2 + e_3^2 + e_4^2 + e_5^2 + e_6^2) < 0 \quad (3.18)$$

Choose

$$u = \begin{bmatrix} 0.5e_1 + y_1 - y_2 \\ 0.5e_2 + x_4x_5 - 3x_6 \\ 0.5e_3 + x_2 \\ 0.5e_4 + y_2y_3 \\ 0.5e_5 - x_2 \\ 0.5e_6 - z_5 \end{bmatrix}$$

Introduce u into Eq.(11) where i = 1, 2, ⋯, 6, Eq. (3.17) becomes

$$\dot{V}(e) = -(e_1^2 + e_2^2 + e_3^2 + e_4^2 + e_5^2 + e_6^2)$$

which is a negative definite function in all quadrants. Error state time histories are shown in Fig. 8 and Fig. 9.

3.5 Comparison between new strategy and traditional method

From the previous sections, we know that the controllers u of the new strategy and of the traditional method are quite different. Tables and figures for comparing the efficiency of convergence are given as follows. The superiority of new strategy is obvious. The error states of new strategy are much smaller and decay more quickly than that of traditional method.

Table 3. 1. The value of error dynamics at 99.01s ~ 99.10s for traditional method.

t	e_1	e_2	e_3	e_4	e_5	e_6
99.01	0.000000352	0.000000278	0.000000141	0.000000018	0.000007539	0.000000018
99.02	0.000000350	0.000000277	0.000000141	0.000000018	0.000007502	0.000000018
99.03	0.000000348	0.000000275	0.000000140	0.000000018	0.000007464	0.000000018
99.04	0.000000346	0.000000274	0.000000139	0.000000018	0.000007427	0.000000018
99.05	0.000000345	0.000000273	0.000000138	0.000000018	0.000007390	0.000000017
99.06	0.000000343	0.000000271	0.000000138	0.000000018	0.000007353	0.000000017
99.07	0.000000341	0.000000270	0.000000137	0.000000018	0.000007316	0.000000017
99.08	0.000000339	0.000000269	0.000000136	0.000000018	0.000007280	0.000000017
99.09	0.000000338	0.000000267	0.000000136	0.000000018	0.000007244	0.000000017
99.10	0.000000336	0.000000266	0.000000135	0.000000018	0.000007208	0.000000017

Table 3. 2. The value ($\times 10^{-10}$) of error dynamics at 90.01s ~ 90.10s for new strategy.

t	e_1	e_2	e_3	e_4	e_5	e_6
99.01	0. 00441	0. 00597	0. 00341	0. 0000044	0. 01762	0. 0000043
99.02	0. 00441	0. 00597	0. 00341	0. 0000044	0. 01762	0. 0000043
99.03	0. 00441	0. 00597	0. 00341	0. 0000044	0. 01762	0. 0000043
99.04	0. 00441	0. 00597	0. 00341	0. 0000044	0. 01762	0. 0000043
99.05	0. 00441	0. 00597	0. 00341	0. 0000044	0. 01762	0. 0000043
99.06	0. 00441	0. 00597	0. 00341	0. 0000044	0. 01762	0. 0000043
99.07	0. 00441	0. 00597	0. 00341	0. 0000044	0. 01762	0. 0000043
99.08	0. 00441	0. 00597	0. 00341	0. 0000044	0. 01762	0. 0000043
99.09	0. 00441	0. 00597	0. 00341	0. 0000044	0. 01762	0. 0000043
99.10	0. 00441	0. 00597	0. 00341	0. 0000044	0. 01762	0. 0000043

3.6 Summary

In this research, a new synchronization is presented. We not only use the variables but also their derivatives in two given function. New strategy to achieve chaos control by GYC partial region stability is used, by which we can synchronize system quickly comparing with traditional method. Finally, Tables and figures are given to prove that the new strategy do synchronize system more quickly.

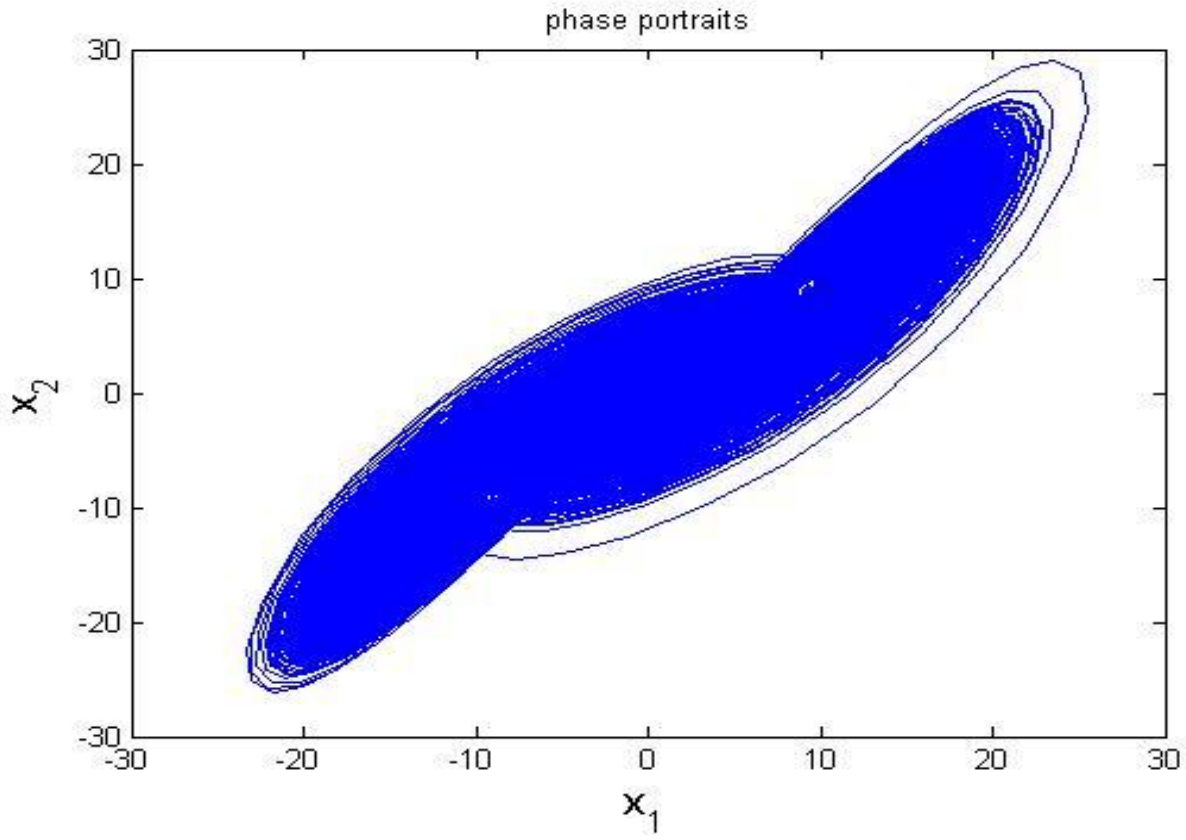

Fig.3 - 1 Phase portrait of Ge-Ku-Duffing-Lü system.

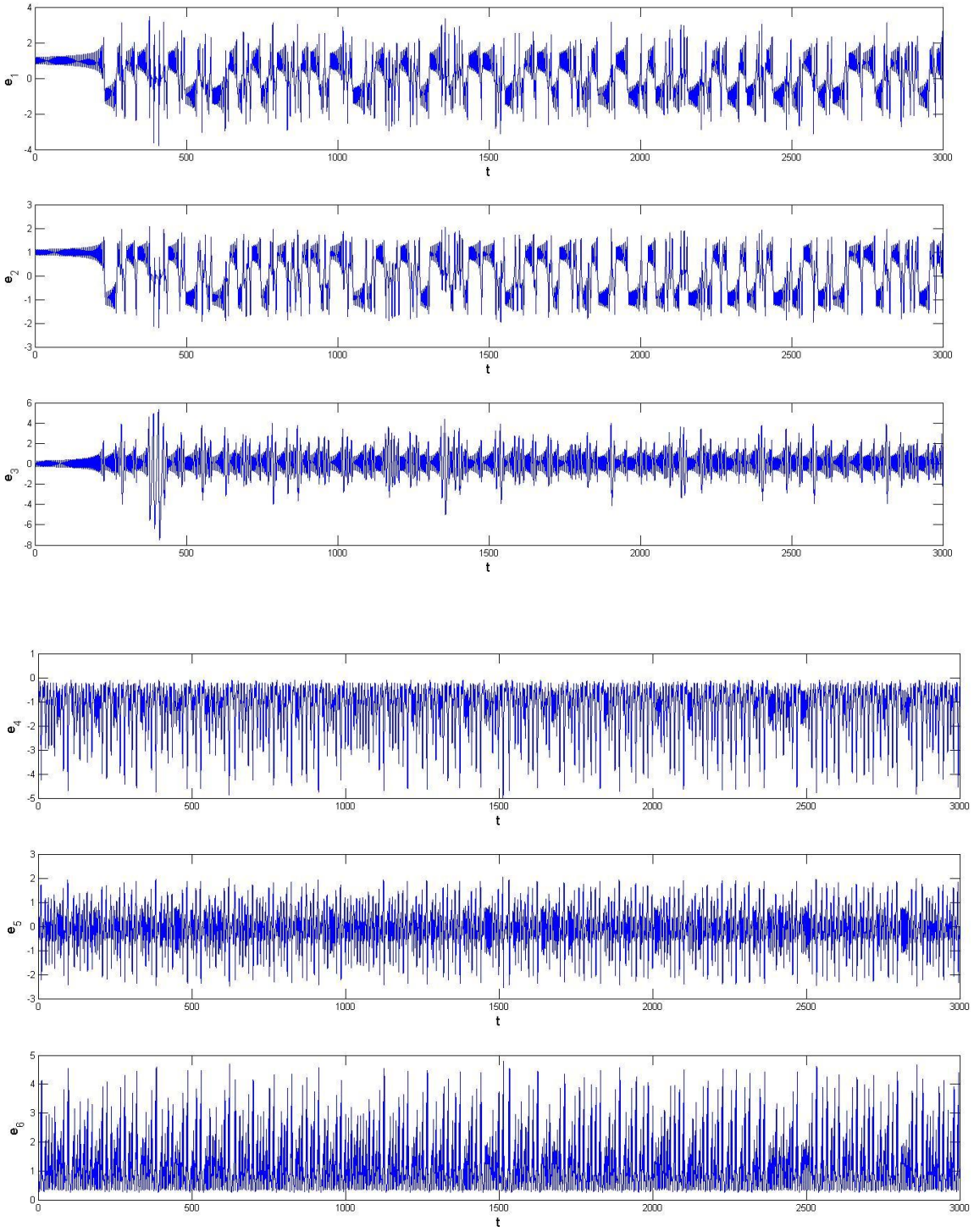

Fig.3 - 2 Time histories of Ge-Ku-Duffing-Lü system.

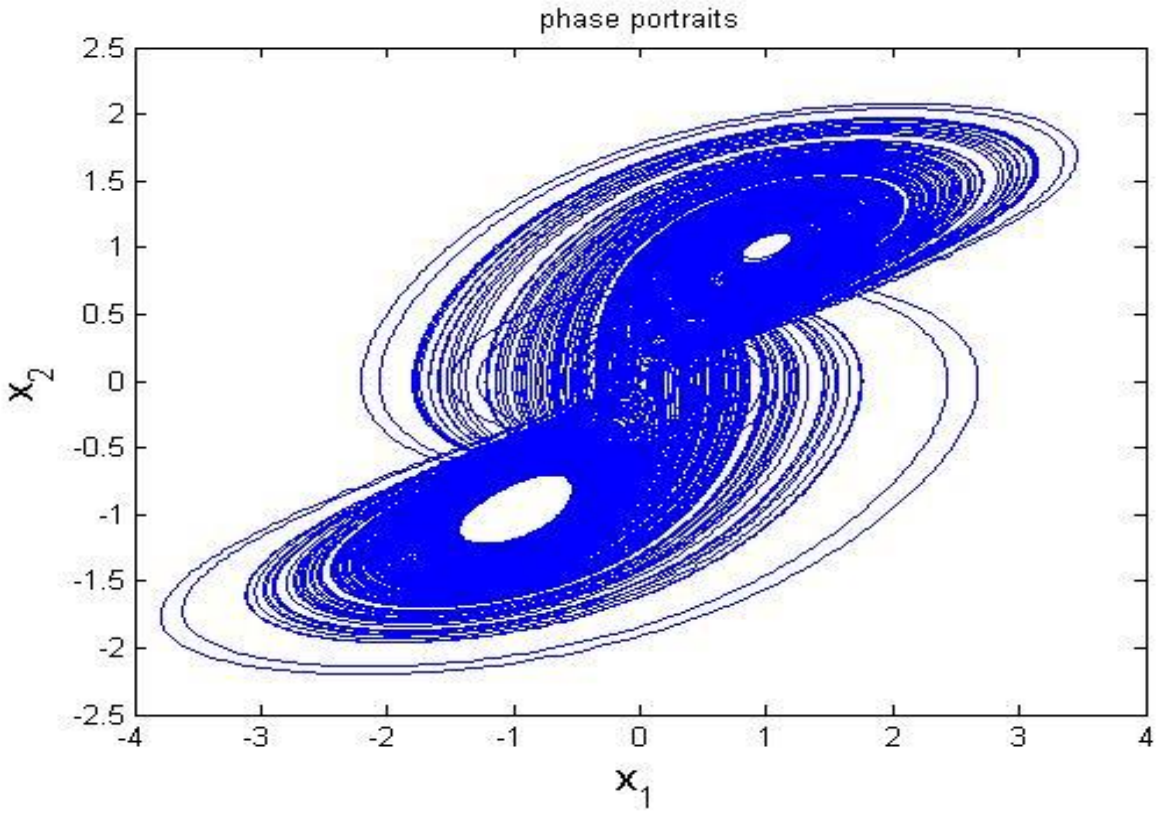

Fig.3 - 3 Phase portrait of Sprott C-E system.

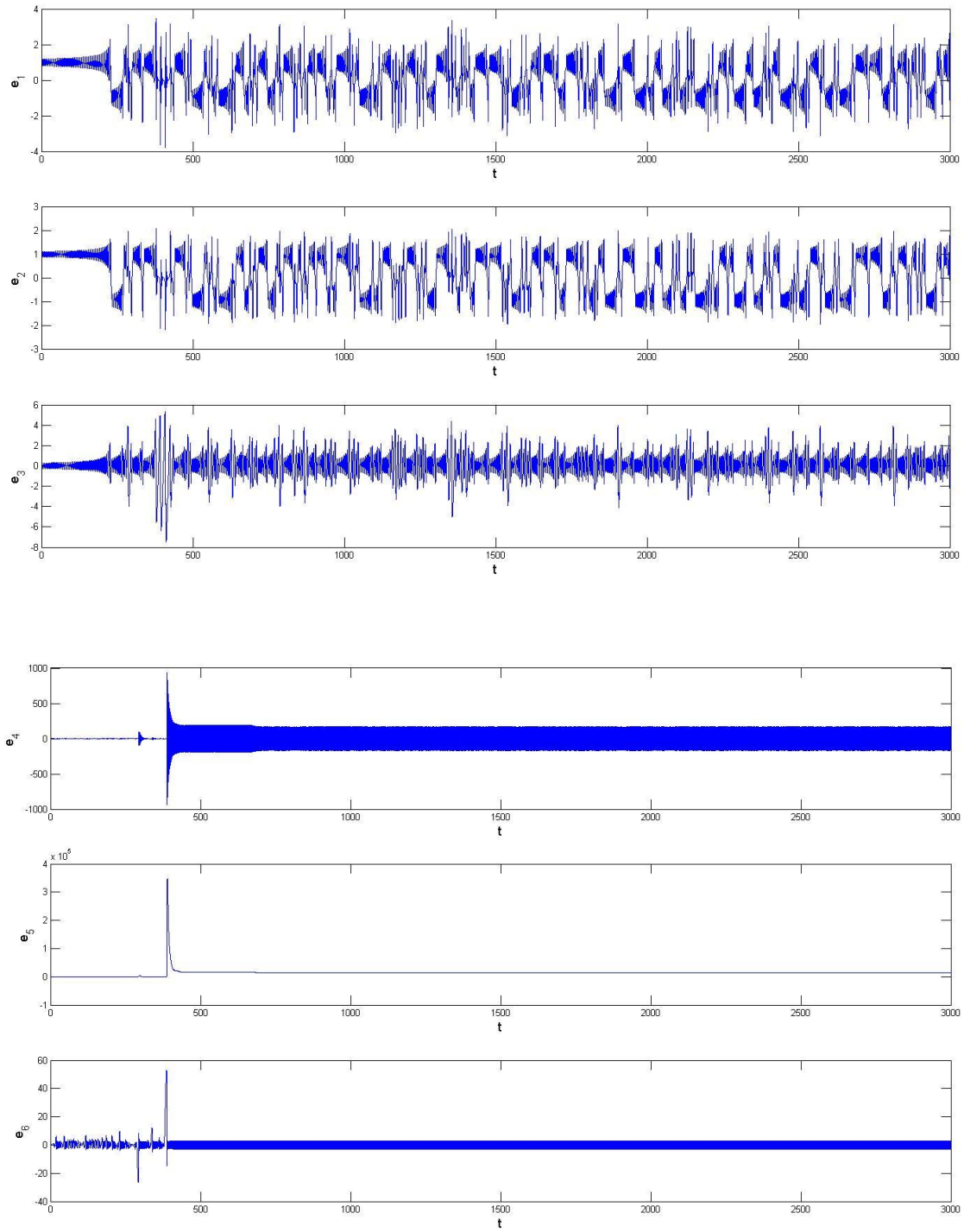

Fig.3 - 4 Time histories of Sprott C-E system.

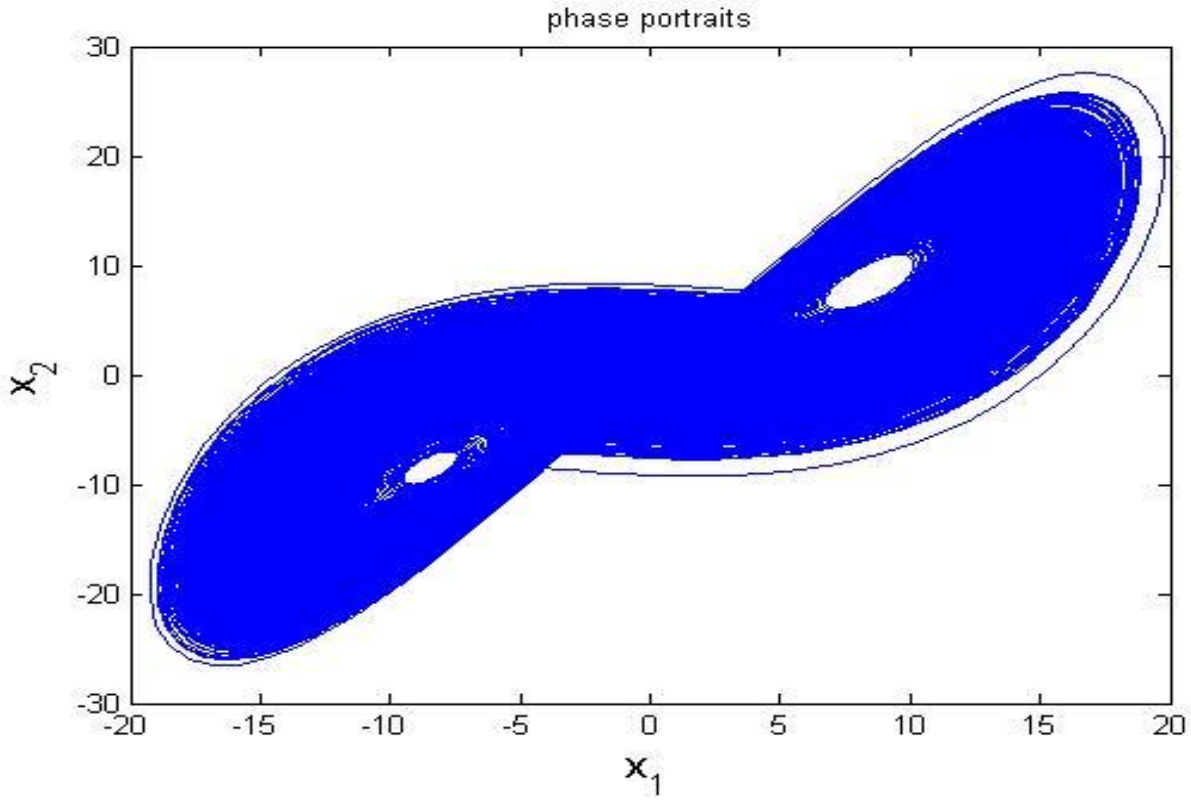

Fig.3 - 5 Phase portrait of Sprott G-H system.

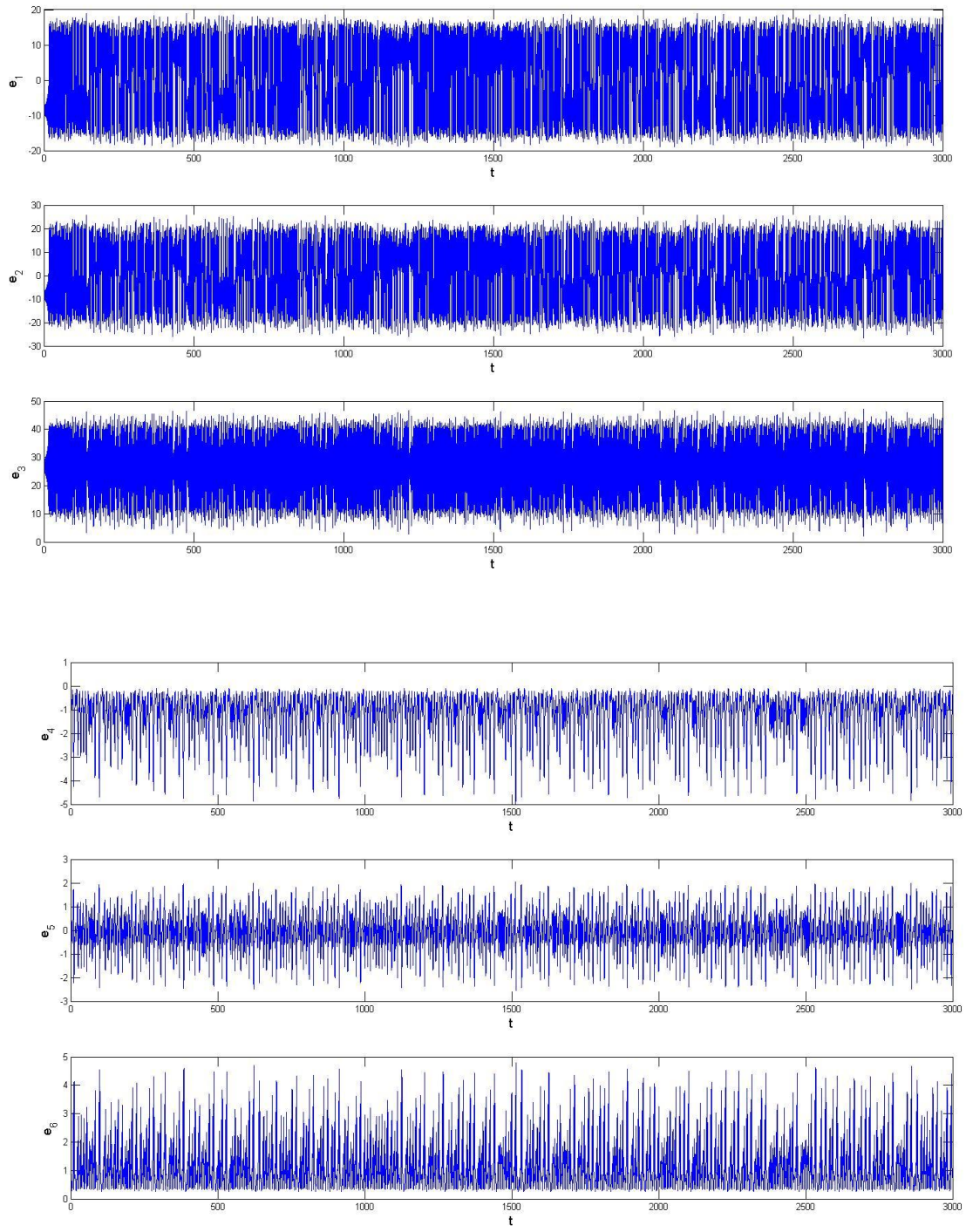

Fig.3 - 6 Time histories of Lorez- Sprott D system system.

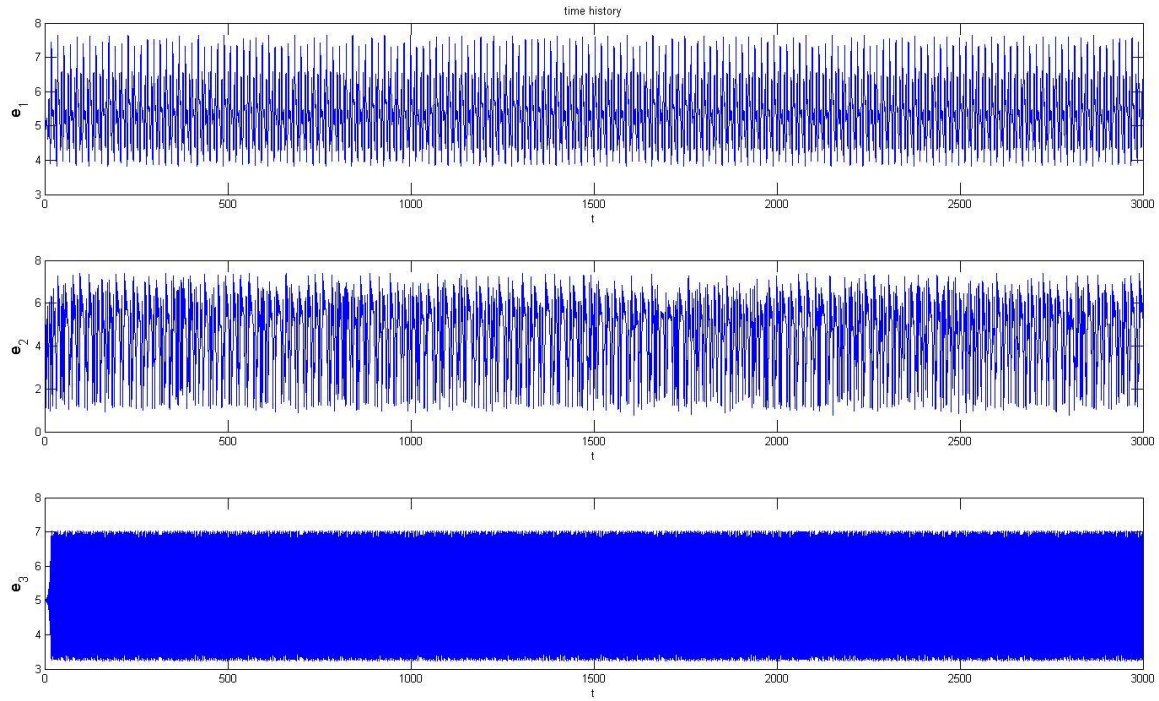

Fig.3 - 7 Time histories of e_1, e_2, e_3 before synchronization.

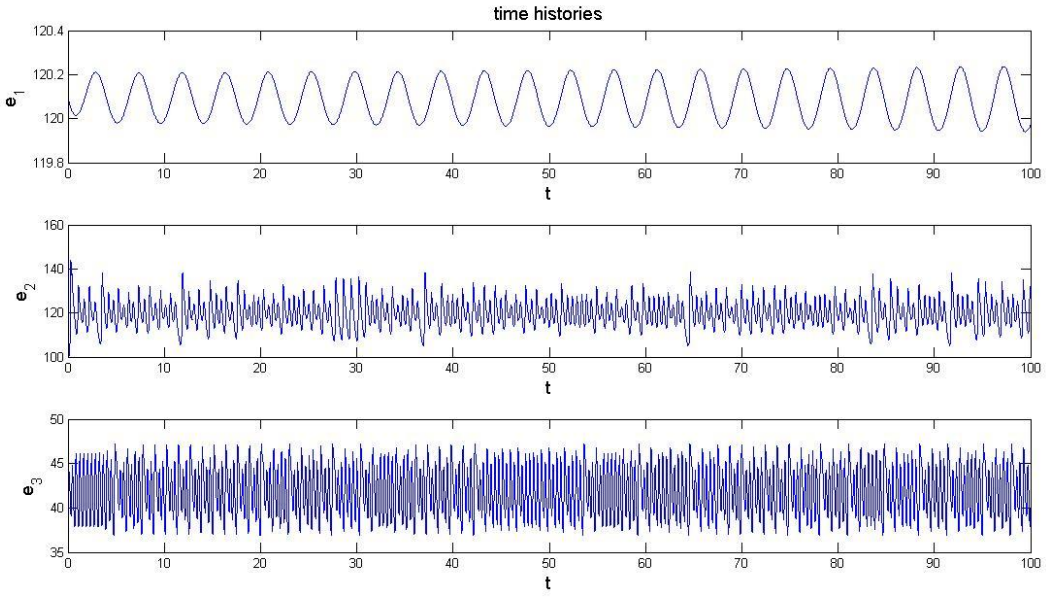

Fig.3 - 8 Time histories of e_1, e_2, e_3 after synchronization for new strategy.

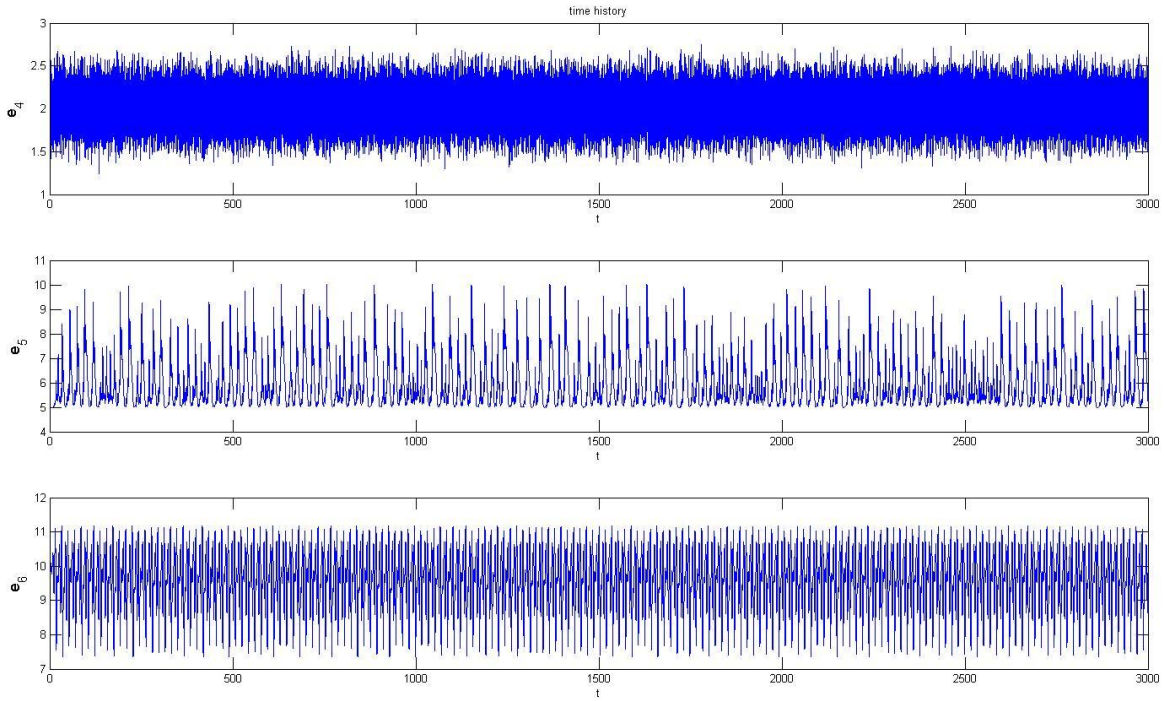

Fig.3 - 9 Time histories of error4~6 before synchronization.

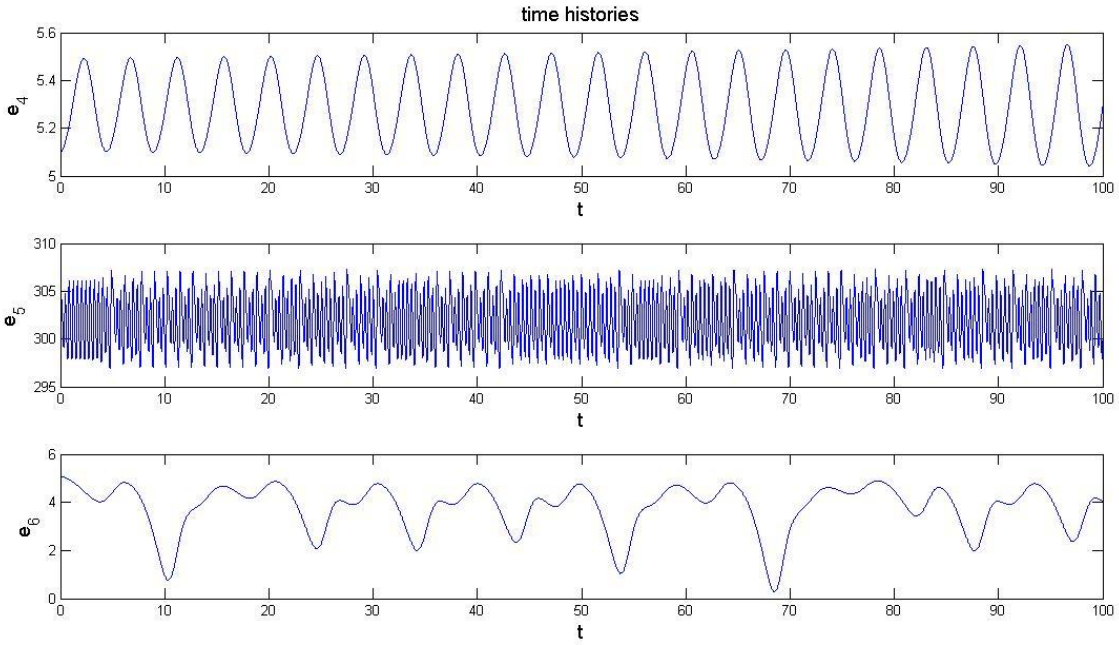

Fig.3 - 10 Time histories of error4~6 after synchronization for new strategy.

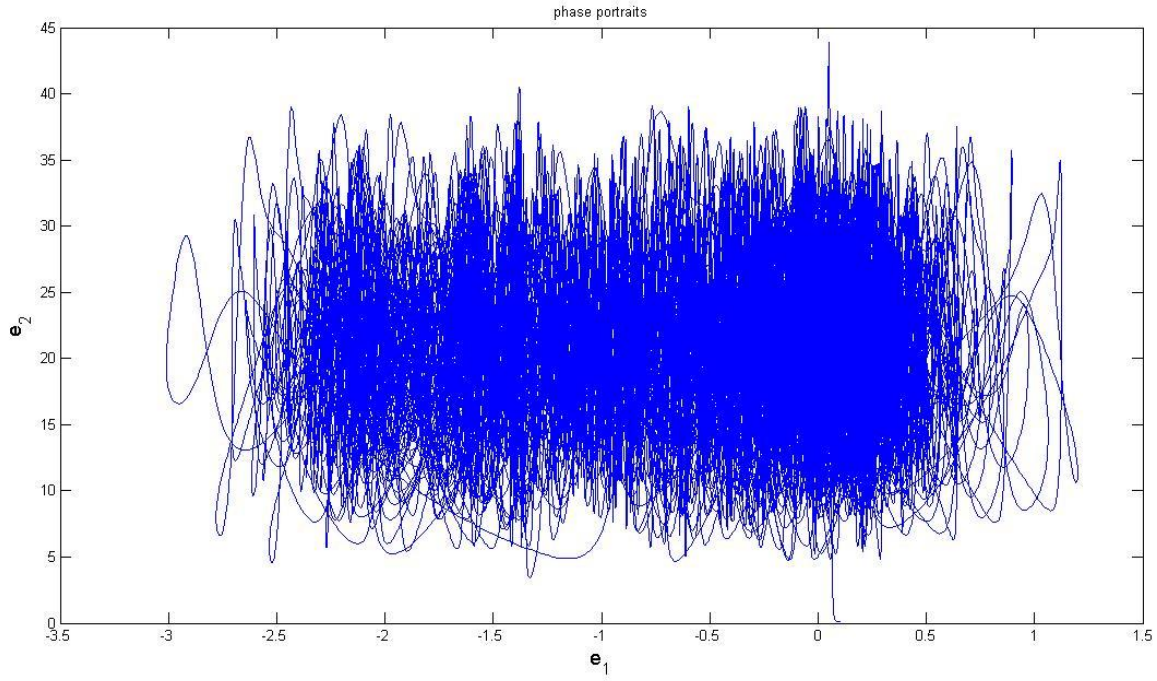

Fig.3 - 11 Phase portrait of e1,e2 before synchronization.

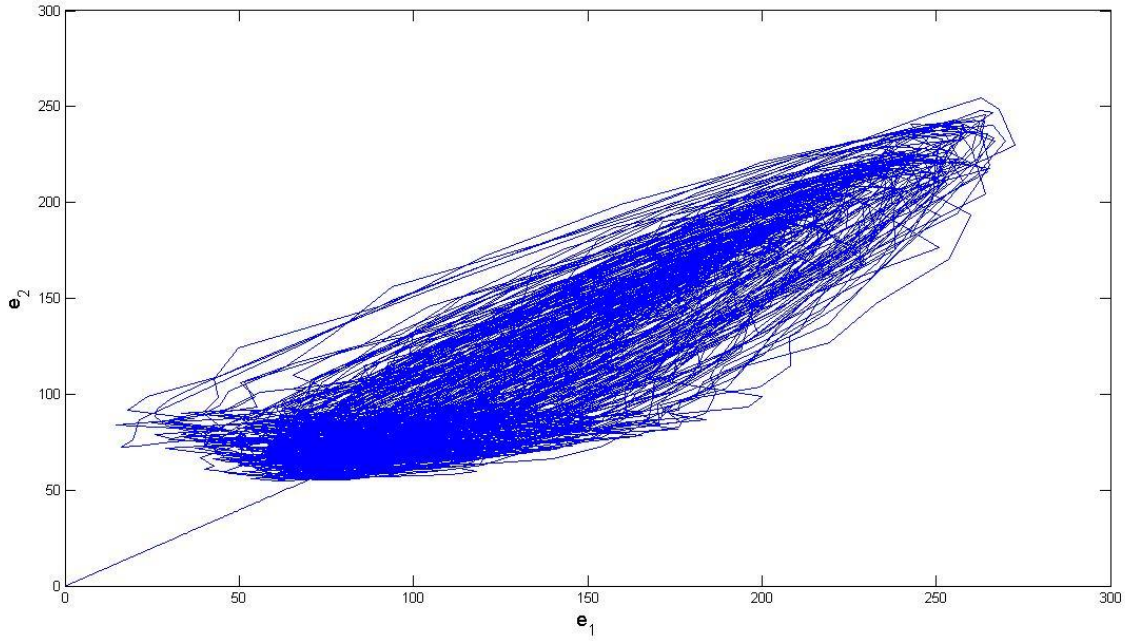

Fig.3 - 12 Phase portrait of e1,e2 after synchronization for new strategy.

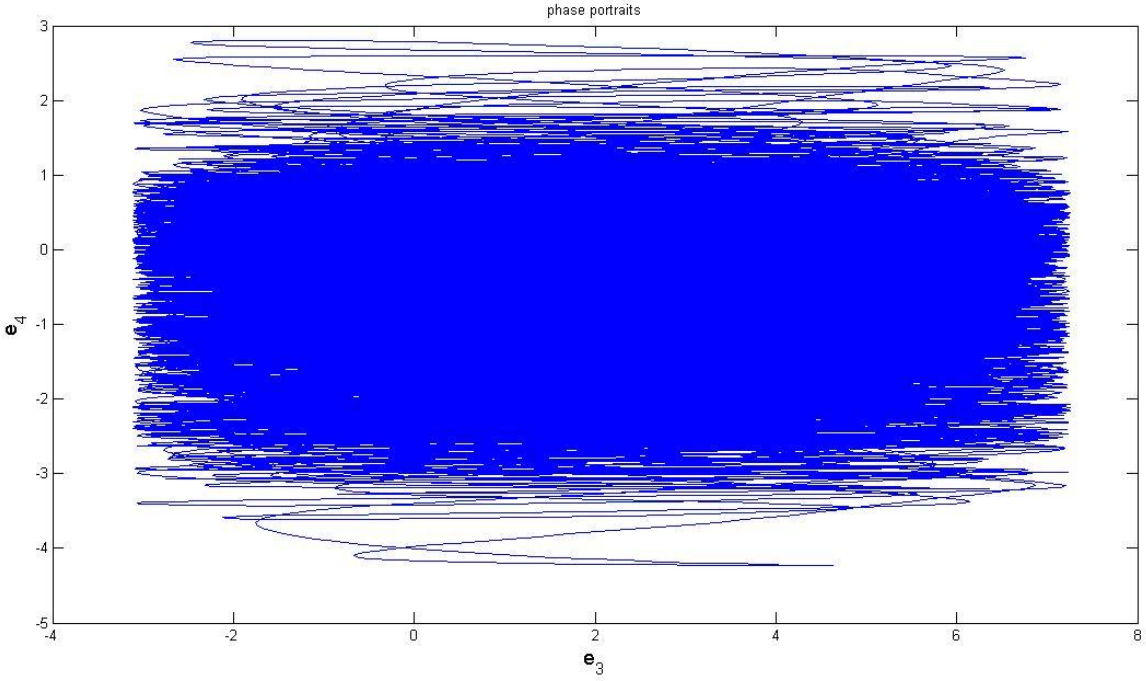

Fig.3 - 13 Phase portrait of e3,e4 before synchronization.

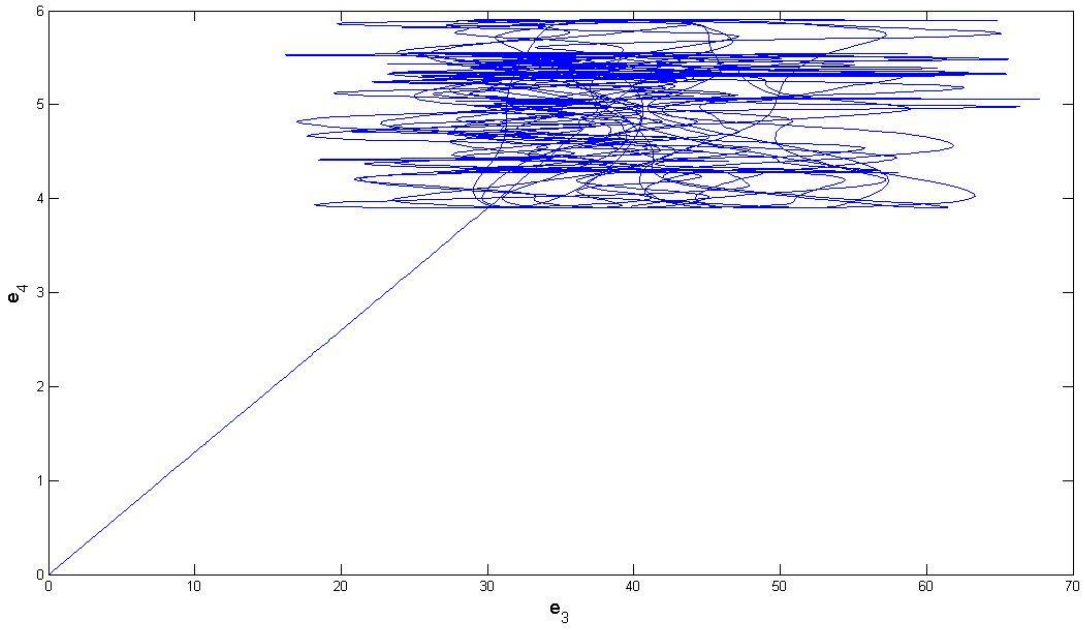

Fig.3 - 14 Phase portrait of e3,e4 after synchronization for new strategy.

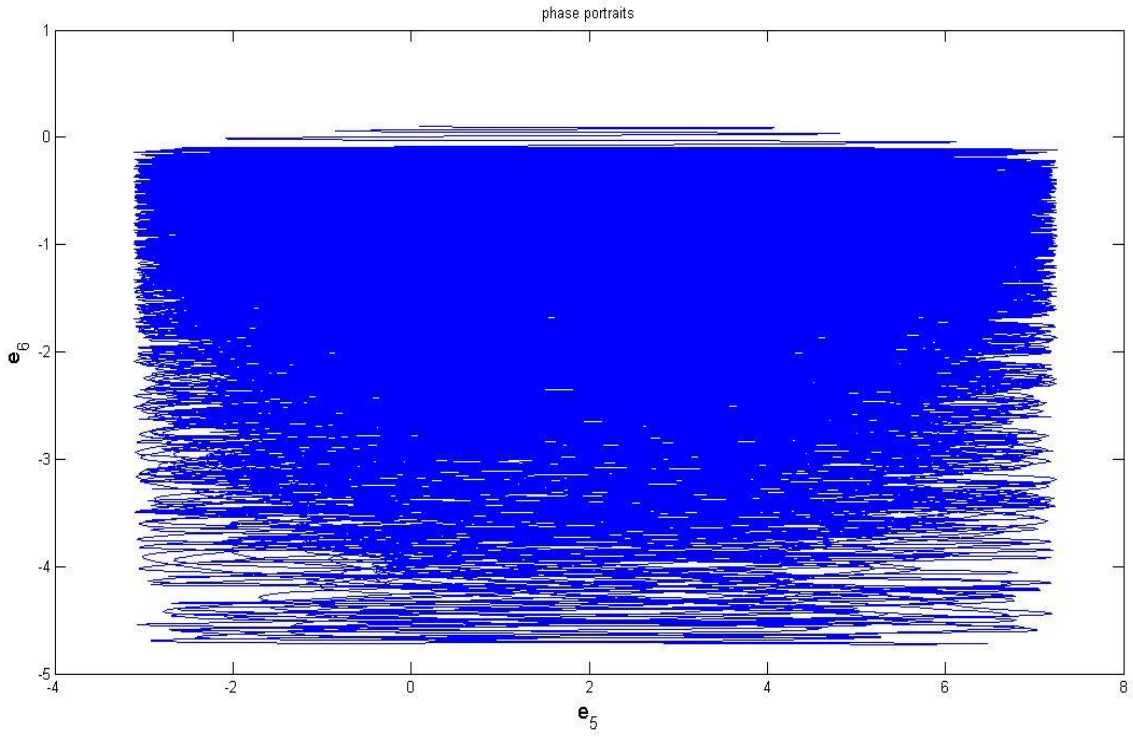

Fig.3 - 15 Phase portrait of e5,e6 before synchronization.

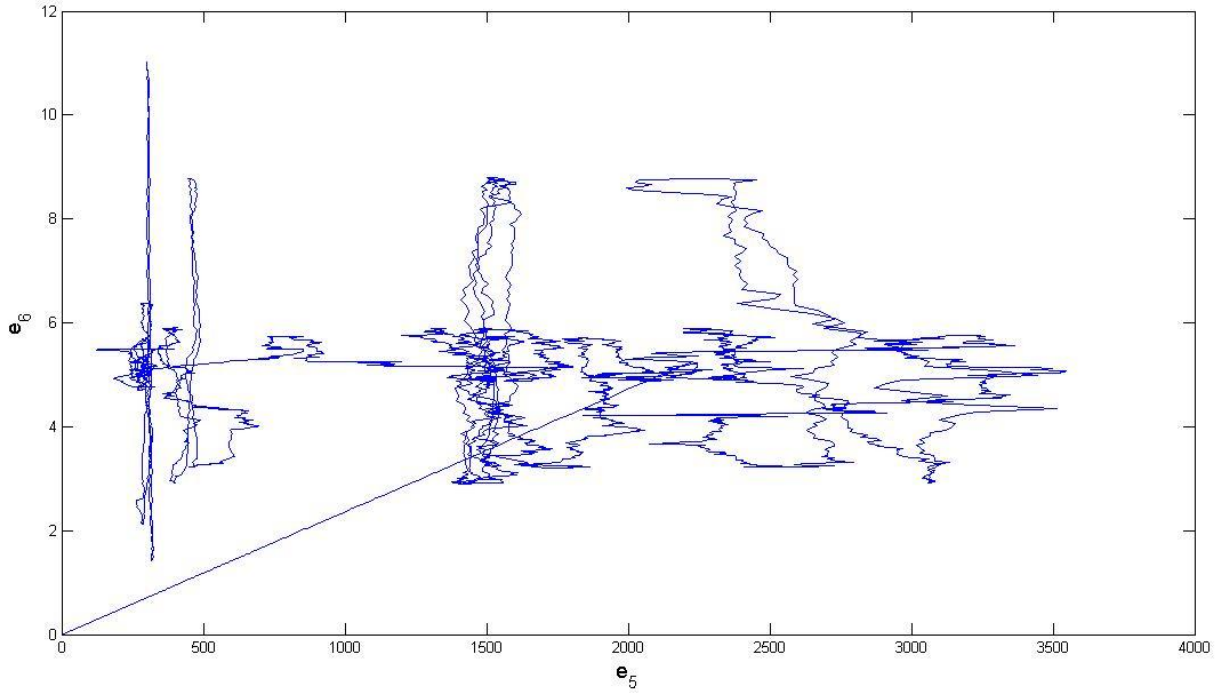

Fig.3 - 16 Phase portrait of e5,e6 before and after control for new strategy.

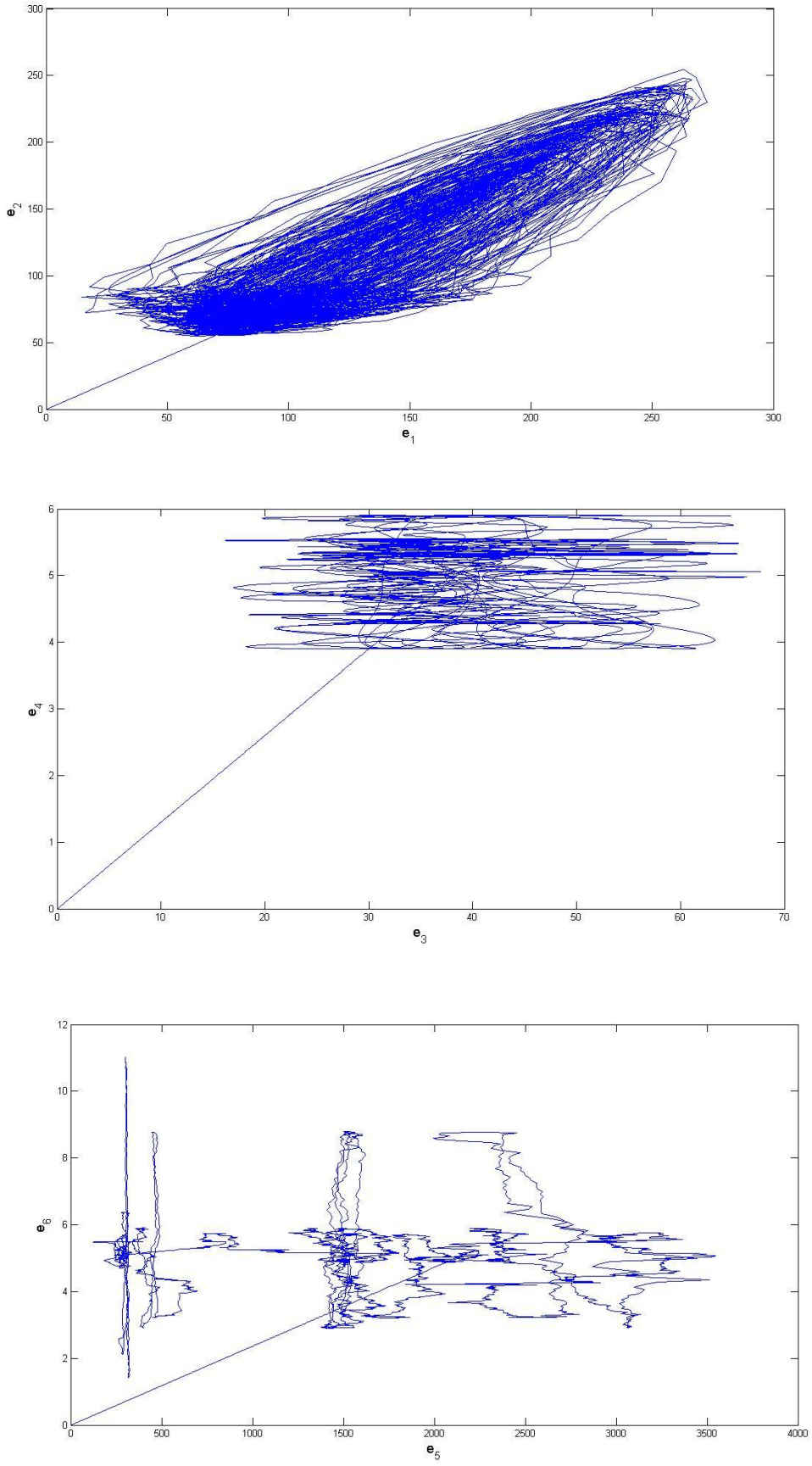

Fig.3 - 17 Phase portrait of e5,e6 before and after control for traditional method.

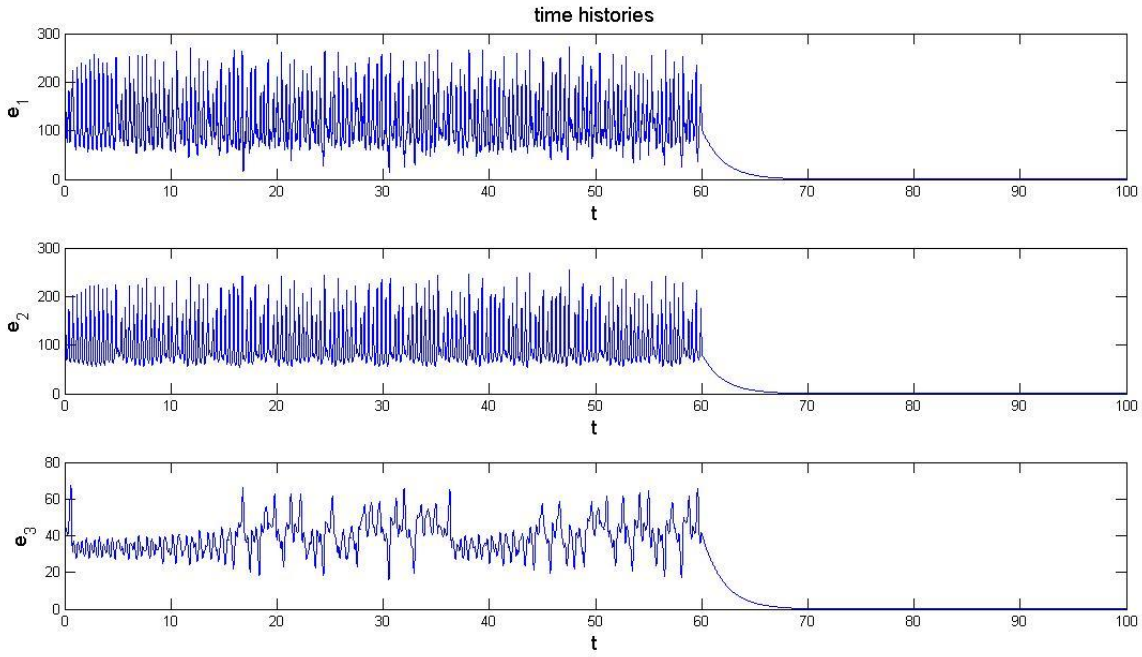

Fig.3 - 18 Time histories of error1~3 before and after control for traditional method.

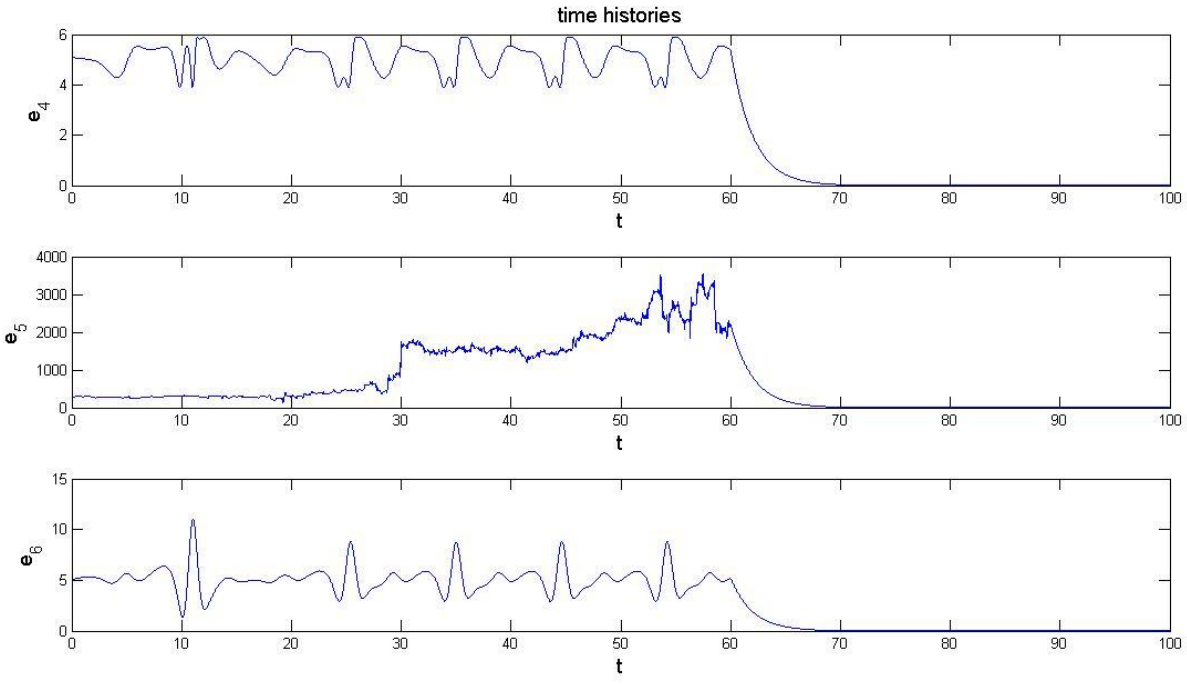

Fig.3 - 19 Time histories of error4~6 before and after control for traditional method.

Chapter 4

Multiple Symplectic Derivative Synchronization of Ge-Ku-Duffing-Lü System with Variable Time Scales by Partial Region Stability Theory

4.1 Preliminary

A new type of synchronization, multiple symplectic derivative synchronization with variable scales is obtained by active control. Next, the partial region stability theory is used for this kind of synchronization. A comparison of errors between new and traditional methods shows that the convergence rate of the new method is much faster than that of the traditional method.

4.2 Strategy of multiple symplectic derivative synchronization with variable time scale

There are two chaotic systems, partner system A and partner system B. The partner A is given by

$$\dot{x} = f(t, x) \tag{4.1}$$

The partner B is given by

$$\dot{y} = g(t, y) \tag{4.2}$$

In order that the error dynamics becomes always positive, the origin of y-coordinate system is translated by a constant vector K.

Define $e = G - F + K$ as the error state vector, where $G = G(x, y, \cdots, \dot{x}, \dot{y}, \dot{x}_\tau, \dot{y}_\tau \cdots, \ddot{x}, \ddot{y}, \ddot{x}_\tau, \ddot{y}_\tau \cdots, t, \tau)$ and

$F = F(x, y, \cdots, \dot{x}, \dot{y}, \dot{x}_\tau, \dot{y}_\tau \cdots, \ddot{x}, \ddot{y}, \ddot{x}_\tau, \ddot{y}_\tau \cdots, t, \tau)$ are two given functions, and K is positive constant vector to keep the error dynamics always in first quadrant.

Then the error vector derivative is obtained：

$$\dot{e}_i = \dot{G}_i - \dot{F}_i - u_i \tag{4.3}$$

where u_i is a component of the control input vector u, $i = 1, 2, \cdots, n$.

The synchronization can be accomplished when $t \to \infty$, the limit of the error vector $e = [e_1, e_2, \cdots, e_n]^T$ approaches to zero:

$$\lim_{t\to\infty} e = 0 \tag{4.4}$$

4.3 Synchronization of different time on other quadrant

Given

$$G(x, y, \dot{x}, \dot{y}, \ddot{x}, \ddot{y}, t, \tau) = \begin{bmatrix} \left[\frac{dy_1}{d\tau} - 36(y_2 - y_1) + x_3\right][x_1 + \dot{x}_3 + {x_3}^2 + 6x_2 - 30x_1] \\ x_1 y_2 + \frac{x_1}{3}(y_1 y_2 - \dot{y}_3) \\ x_1 + x_3 \end{bmatrix},$$

(4.5)

$$F(x, y, \dot{x}, \dot{y}, \ddot{x}, \ddot{y}, t, \tau) = \begin{bmatrix} y_1 + [\frac{dy_1}{d\tau} - 36(y_2 - y_1) + x_3]^2 \\ x_1 y_3 \\ {x_3}^2 + \frac{1}{36}(\dot{x}_4 - x_1) - y_2 \end{bmatrix}, \tag{4.6}$$

Our purpose is to achieve the multiple symplectic derivative synchronization with variable time scale $G(x, \dot{x}, \ddot{x}, y, \dot{y}, \ddot{y}, t, \tau) = F(x, \dot{x}, \ddot{x}, y, \dot{y}, \ddot{y}, t, \tau) - K$.

Combining Ge-Ku-Duffing system and Lü system by adding x_1 in the second equation of Lü system, Ge-Ku-Duffing-Lü system is obtained：

$$\begin{cases} \dot{x}_1 = x_2 \\ \dot{x}_2 = -0.1x_2 - x_1[11(40 - {x_1}^2) + 54x_3] \\ \dot{x}_3 = -x_3 - {x_3}^3 - 6x_2 + 30x_1 \\ \frac{dy_1}{d\tau} = 36(y_2 - y_1) + x_1 \\ \frac{dy_2}{d\tau} = -y_1 y_3 + 20y_2 \\ \frac{dy_3}{d\tau} = y_1 y_2 - 3y_3 \end{cases} \tag{4.7}$$

where $\tau = 4t + 3\sin^2 t$, initial condition（x_{10}，x_{20}，x_{30}）=（2，2.4，5）and（y_{10}，y_{20}，y_{30}）=（0.2，0.35，0.2）. The chaotic attractor of the Ge-Ku-Duffing-Lü system

is shown in Fig. 4.1.

The state error is $e = G - F + K$ where $K = [250, -7000, 50]^T$ such that error dynamics always exists in second guardant as shown in Figs. 4.2 ~4.5.

Ge-Ku-Duffing-Lü system and Chen system have different time scale. To solving this question, transform $\dot{y}$ as

$$\dot{y} = \frac{dy}{dt} = \frac{dy}{d\tau}\frac{d\tau}{dt} = 4 + 3\sin(2t)$$

Our purpose is

$$\lim_{t\to\infty} e_i = G_i - F_i + K_i = 0, \tag{4.8}$$

where i = 1, 2,⋯ ,6.We obtain the error dynamics:

$$\begin{cases} \dot{e}_1 = \dot{G}_1 - \dot{F}_1 - u_1 \\ \dot{e}_2 = \dot{G}_2 - \dot{F}_2 - u_2 \\ \dot{e}_3 = \dot{G}_3 - \dot{F}_3 - u_3 \end{cases} \tag{4.9}$$

By partial region stability theory, we can choose a Lyapunov function in the form of a positive definite function in second quadrant:

$$V(e) = e_1 - e_2 + e_3 \tag{4.10}$$

Its time derivative is

$$\dot{V}(e) = \left(\dot{G}_1 - \dot{F}_1 - u_1\right) + \left(\dot{G}_2 - \dot{F}_2 - u_2\right) + \left(\dot{G}_3 - \dot{F}_3 - u_3\right) \tag{4.11}$$

Choose the controller u as

$$u = \begin{bmatrix} x_2 + e_1 \\ -x_1\frac{dy_2}{d\tau} + e_2 \\ -x_2 y_2 + e_3 \end{bmatrix} \tag{4.12}$$

we obtain

$$\dot{V}(e) = -e_1 + e_2 - e_3 < 0 \tag{4.13}$$

which is negative definite function in second quadrant. Error state time histories are shown in Figs. 4.6~4.8.

In Table 4.1, the sign rule of eight quadrants are shown.

Table 4. 1. The sign rule of eight quadrants

Quadrant Number	Sign Rule
I	$(+,+,+)$
II	$(-,+,+)$
III	$(-,-,+)$
IV	$(+,-,+)$
V	$(+,+,-)$
VI	$(-,+,-)$
VII	$(-,-,-)$
VIII	$(+,-,-)$

Distribution of eight quadrants is shown in Figs. 4.9

4.4 Synchronization by traditional method

If the traditional Lyapunov function is used, it means that

$$V(e) = e_1^2 + e_2^2 + e_3^2 \tag{4.14}$$

Its time derivative is

$$\dot{V}(e) = 2(e_1\dot{e}_1 + e_2\dot{e}_2 + e_3\dot{e}_3) \tag{4.15}$$

We want to find u of Eq. (11) such that

$$\dot{V}(e) = -(e_1^2 + e_2^2 + e_3^2) < 0 \tag{4.16}$$

Choose

$$u = \begin{bmatrix} x_2 + 0.5e_1 \\ -x_1\dfrac{dy_2}{d\tau} + 0.5e_2 \\ -x_2y_2 + 0.5e_3 \end{bmatrix}$$

Introduce u into Eq.(11) where i = 1, 2, ⋯, 6, Eq. (4.15) becomes

$$\dot{V}(e) = -(e_1^2 + e_2^2 + e_3^2)$$

which is a negative definite function in all quadrants. Error state time histories are shown in Fig. 4.10~4.12.

4.4 Synchronization by traditional method

If the traditional Lyapunov function is used, it means that

$$V(e) = e_1^2 + e_2^2 + e_3^2 \tag{4.14}$$

Its time derivative is

$$\dot{V}(e) = 2(e_1\dot{e}_1 + e_2\dot{e}_2 + e_3\dot{e}_3) \tag{4.15}$$

We want to find u of Eq. (11) such that

$$\dot{V}(e) = -(e_1^2 + e_2^2 + e_3^2) < 0 \tag{4.16}$$

Choose

$$u = \begin{bmatrix} x_2 + 0.5e_1 \\ -x_1\dfrac{dy_2}{d\tau} + 0.5e_2 \\ -x_2y_2 + 0.5e_3 \end{bmatrix}$$

Introduce u into Eq.(11) where i = 1, 2, ⋯, 6, Eq. (4.15) becomes

$$\dot{V}(e) = -(e_1^2 + e_2^2 + e_3^2)$$

which is a negative definite function in all quadrants. Error state time histories are shown in Fig. 4.10~4.12.

4.5 Comparison between new strategy and traditional method

From the previous sections, the controllers of the new strategy and the traditional method are similar, but from Table 4.2 and figures the superiority of new strategy is obvious. The error states of new strategy are much smaller and decay more quickly than that of traditional method.

Table 4. 2. The value($\times 10^{-10}$) of error dynamics at 99.01s ~ 99.10s for traditional method and new strategy

Time(s)	Error for traditional method	Error for new method
	e1：	e1：
99.01	0.286	0. 0134
99.02	0.285	0.0134
99.03	0.283	0.0134
99.04	0.282	0.0134
99.05	0.280	0.0134
99.06	0.279	0.0134
99.07	0.277	0.0134
99.08	0.276	0.0134
99.09	0.275	0.0134
99.10	0.273	0.0134
	e2：	e2：
99.01	-3.265	-0.4366
99.02	-3.247	-0.4366
99.03	-3.229	-0.4366
99.04	-3.211	-0.4366
99.05	-3.192	-0.4366
99.06	-3.174	-0.4366
99.07	-3.156	-0.4366
99.08	-3.138	-0.4366
99.09	-3.129	-0.4366
99.10	-3.110	-0.4366
	e3：	e3：
99.01	1.940	0.028
99.02	1.930	0.028
99.03	1.920	0.028
99.04	1.911	0.028
99.05	1.901	0.028
99.06	1.892	0.028
99.07	1.882	0.028
99.08	1.873	0.028
99.09	1.864	0.028
99.10	1.854	0.028

4.6 Summary

A new synchronization is presented that not only use the variable time scale but also their derivatives in two given functions. New strategy to achieve chaos control by GYC partial region stability is used, by which, we can synchronize system much more quickly comparing with traditional method.

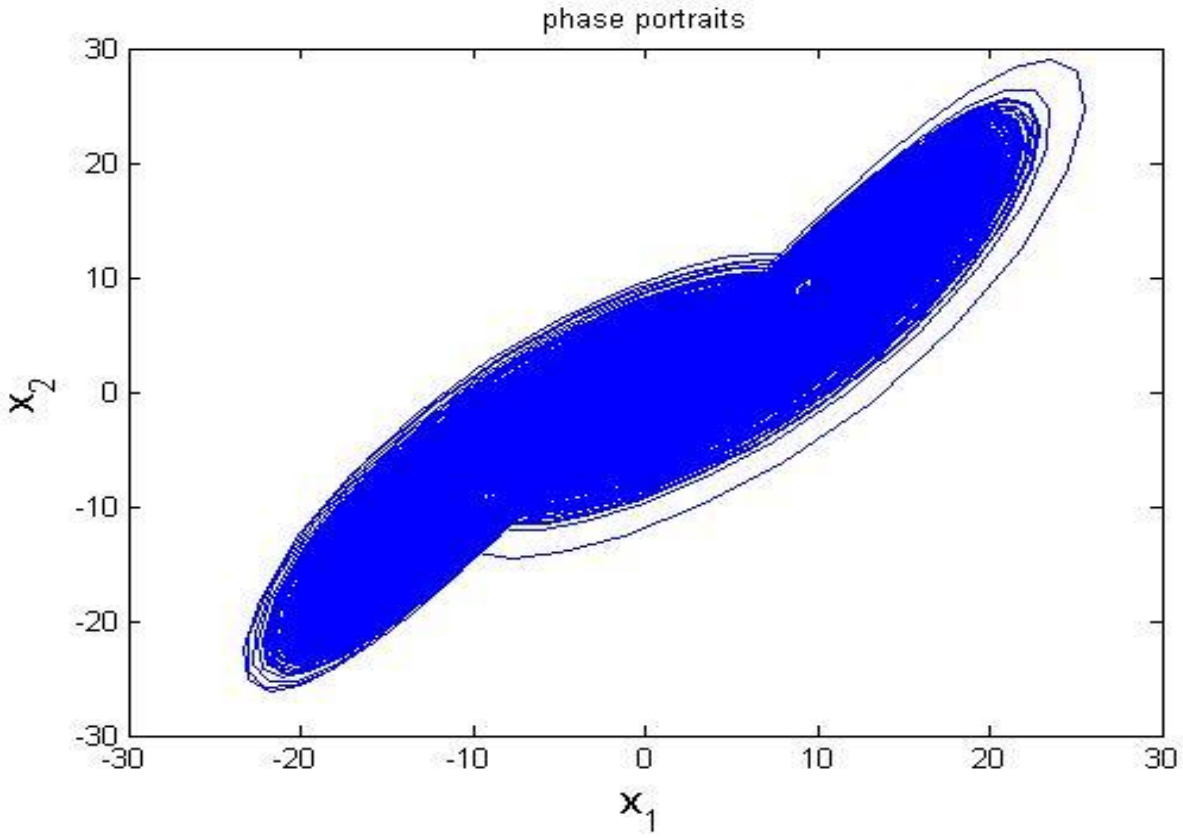

Fig.4 - 1 Phase portrait of Ge-Ku-Duffing-Lü system.

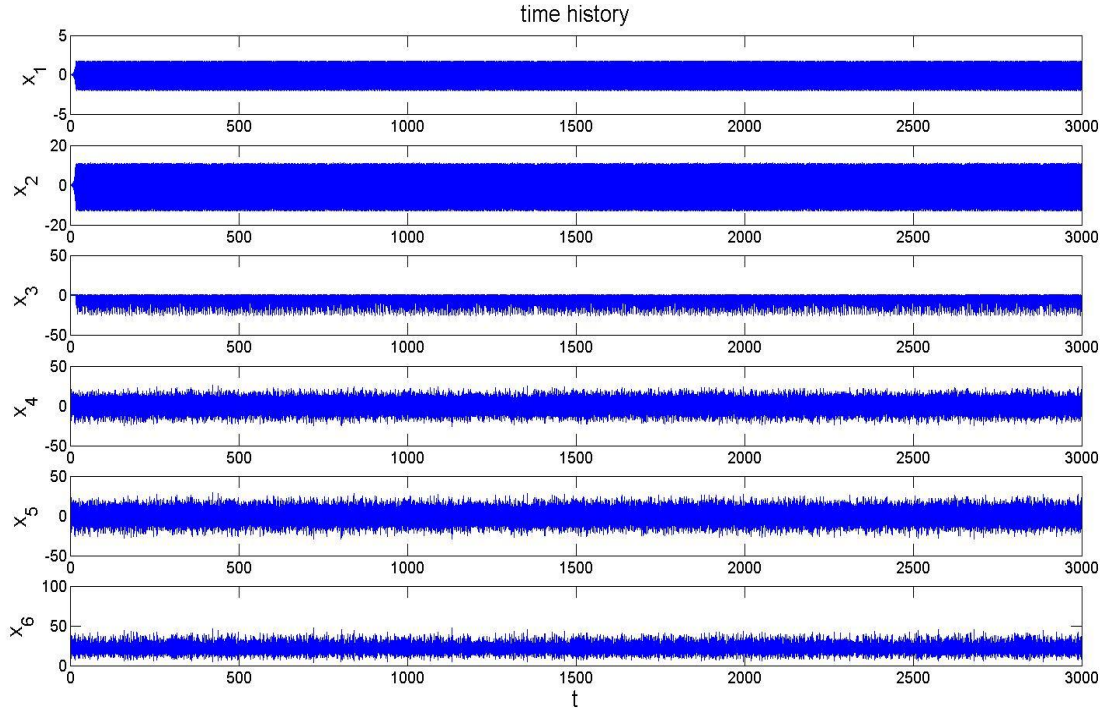

Fig.4 - 2 Time histories of Ge-Ku-Duffing-Lü system.

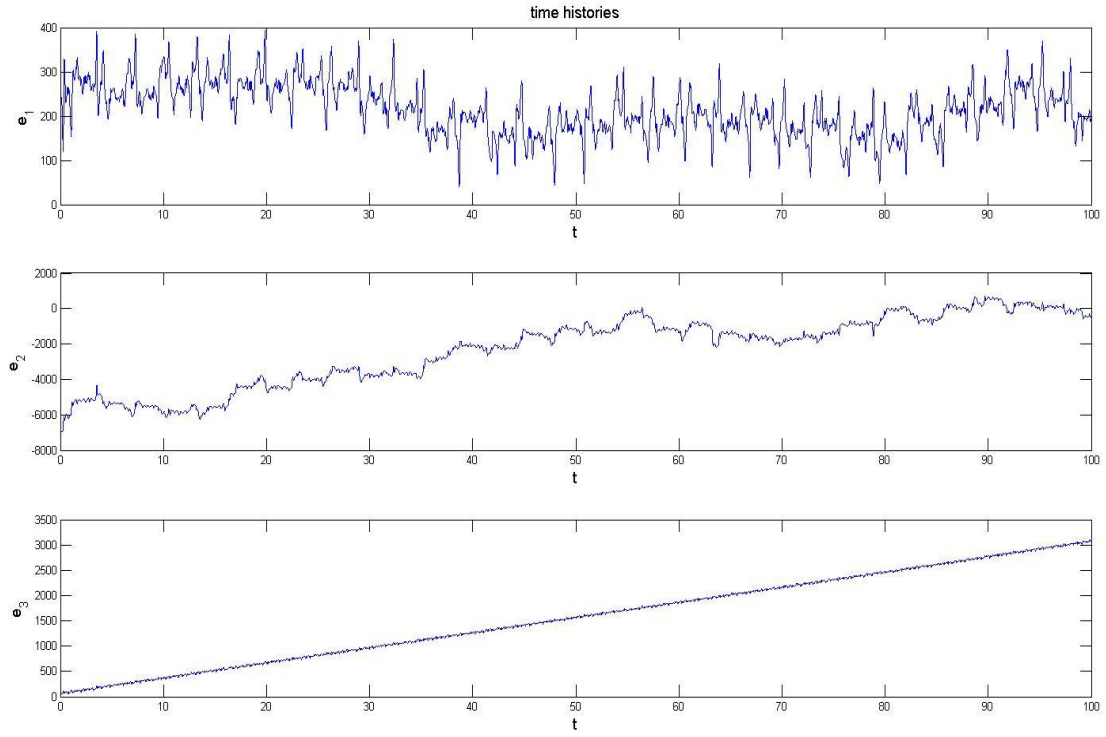

Fig.4 - 3 Time histories of e_1, e_2, e_3 before synchronization.

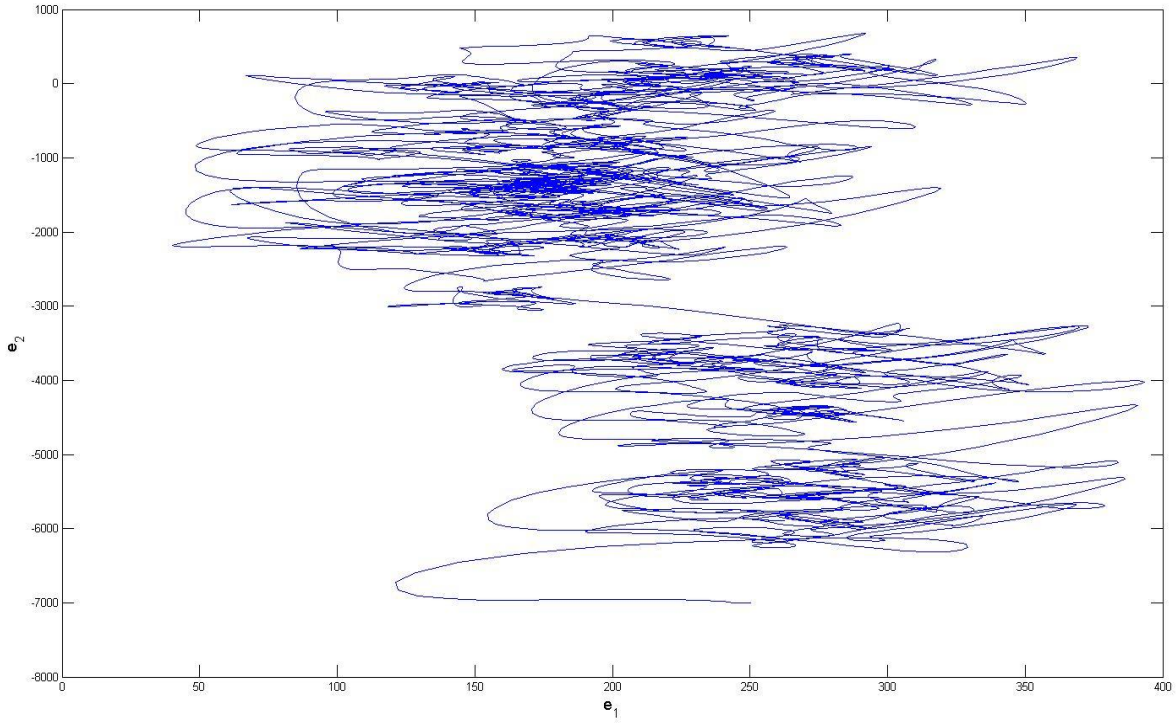

Fig.4 - 4 Phase portrait of e1,e2 before synchronization.

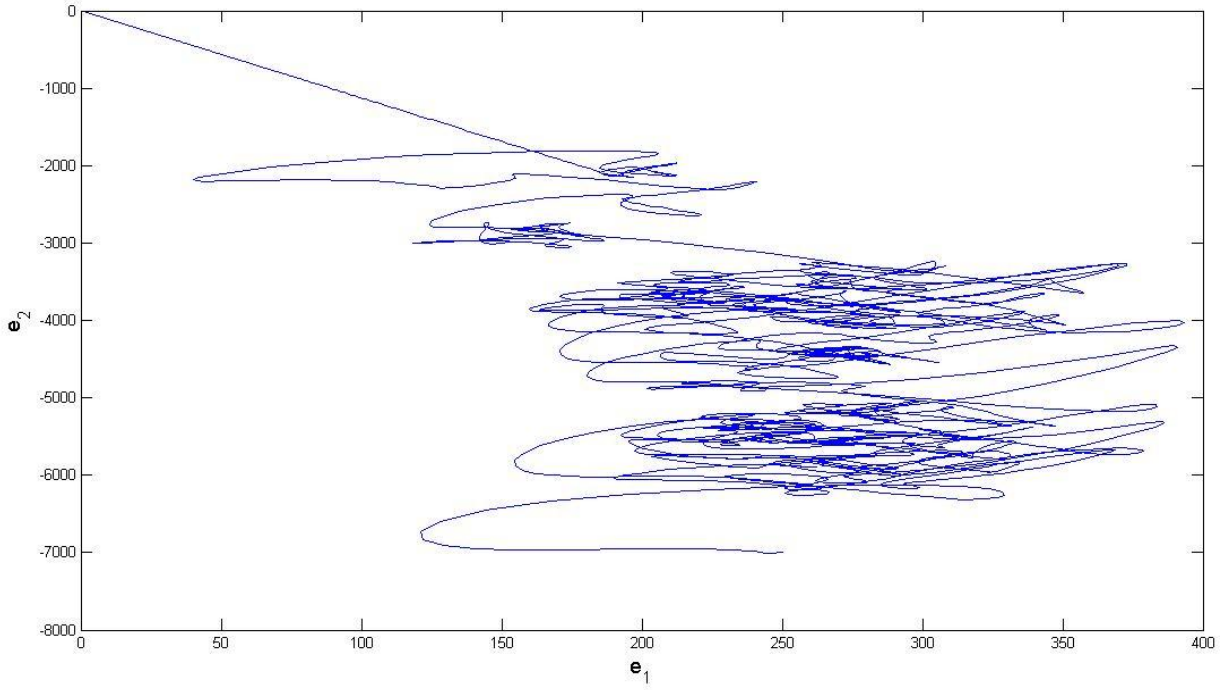

Fig.4 - 5 Phase portrait of e1,e2 before and after control synchronization for new strategy.

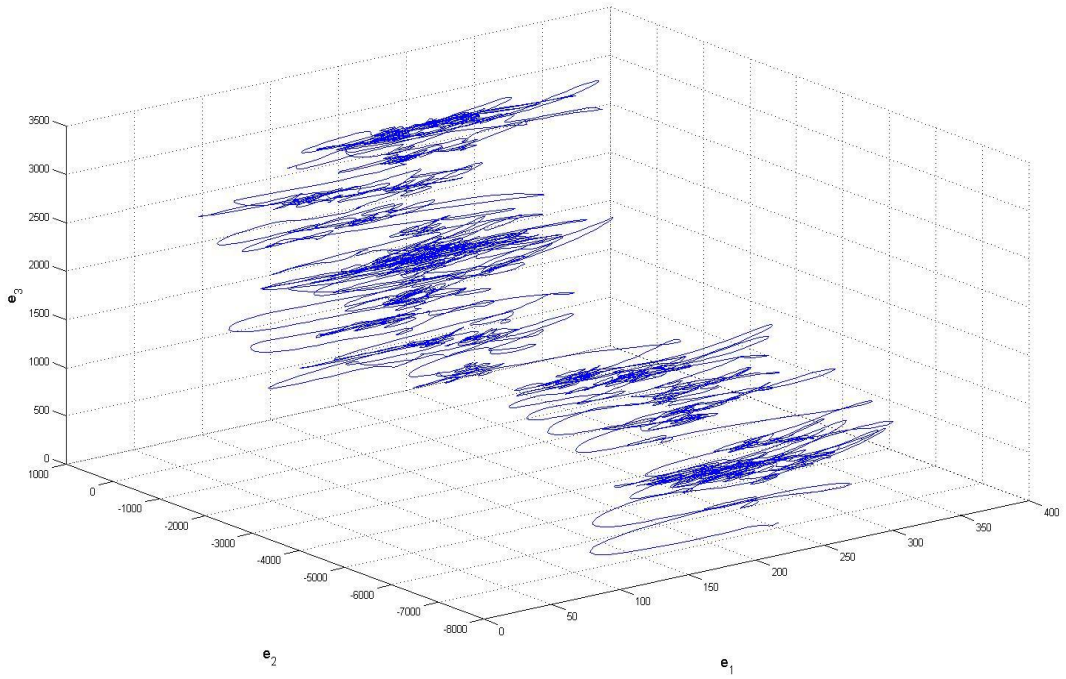

Fig.4 - 6 Phase portrait of e1,e2,e3 before synchronization.

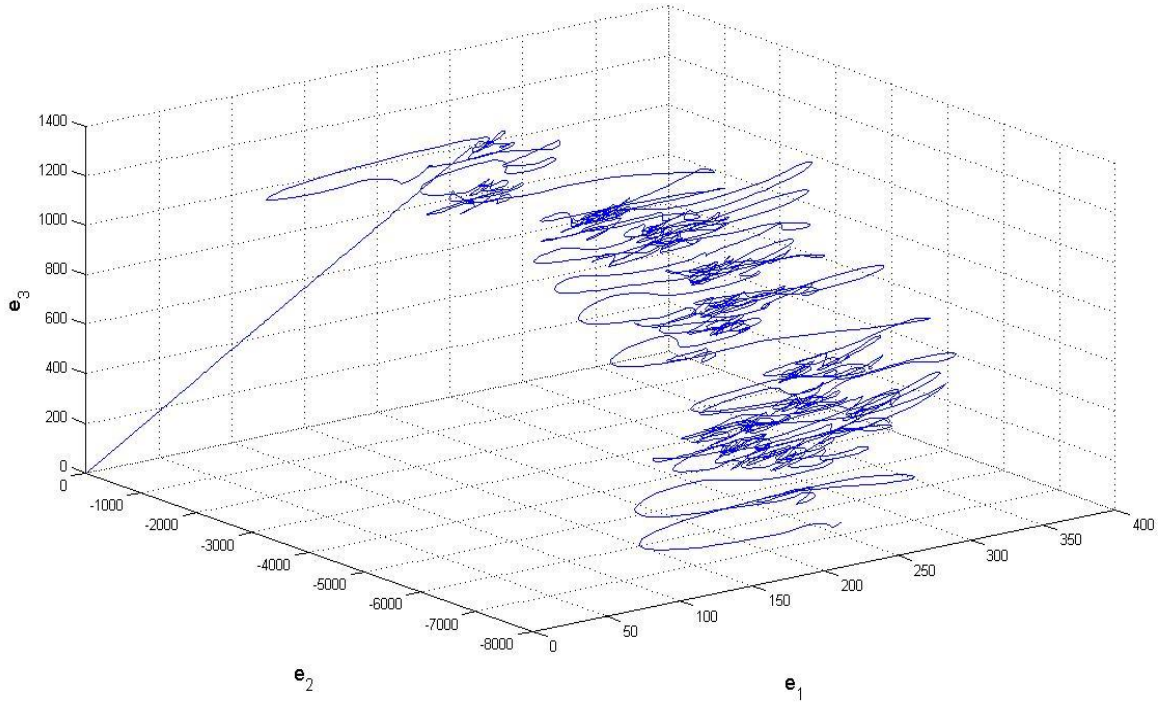

Fig.4 - 7 Phase portrait of e1,e2 ,e3 before and after control synchronization for new strategy.

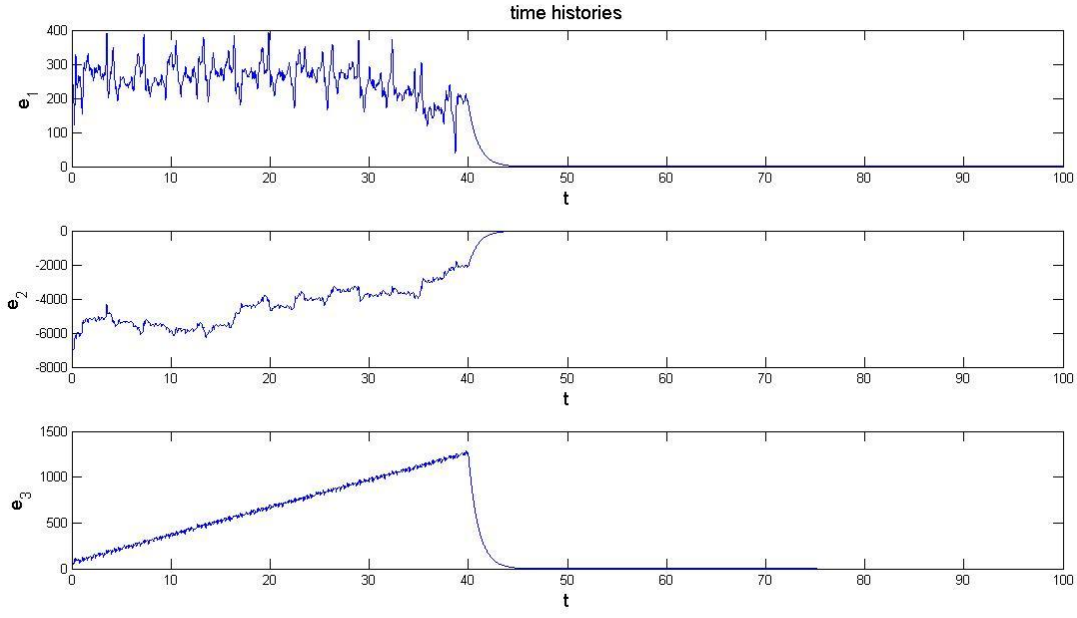

Fig.4 - 8 Time histories of e1,e2,e3 before and after control for new strategy.

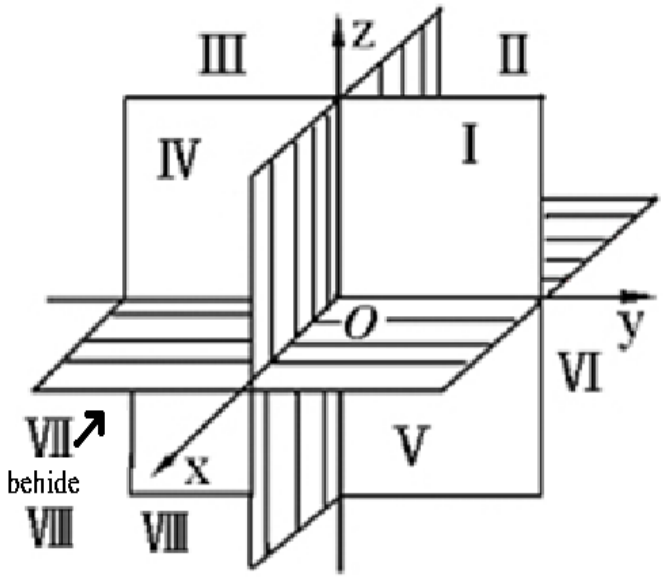

Fig.4 - 9 Definition of the eight quadrants.

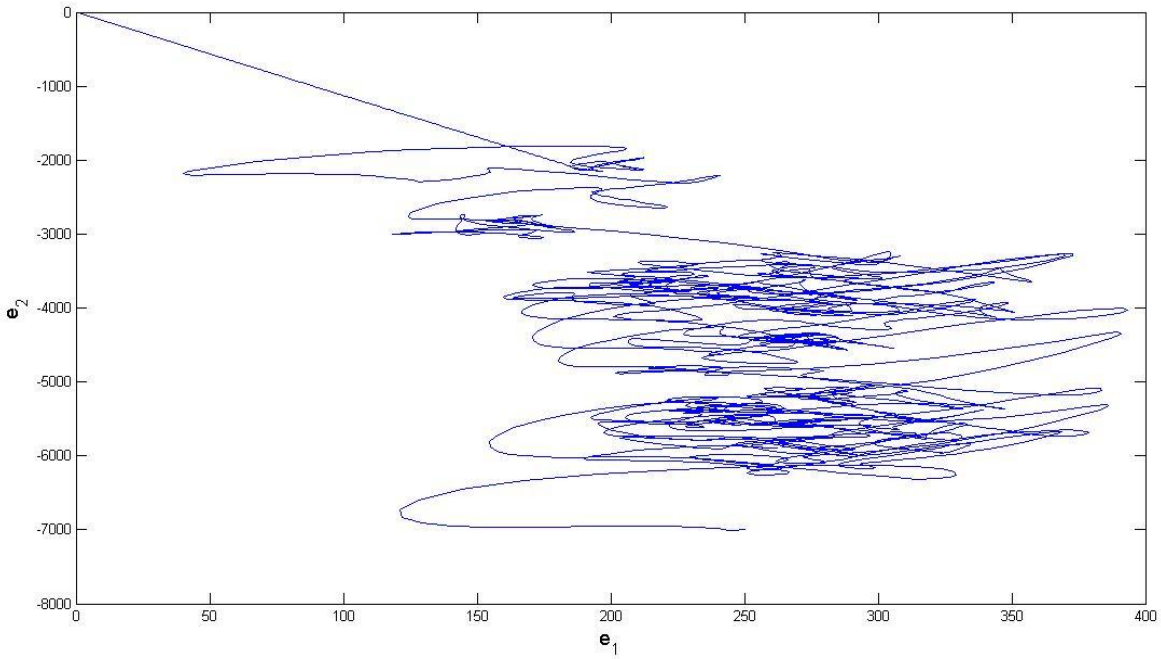

Fig.4 - 10 Phase portrait of e1,e2 before and after control synchronization for traditional method.

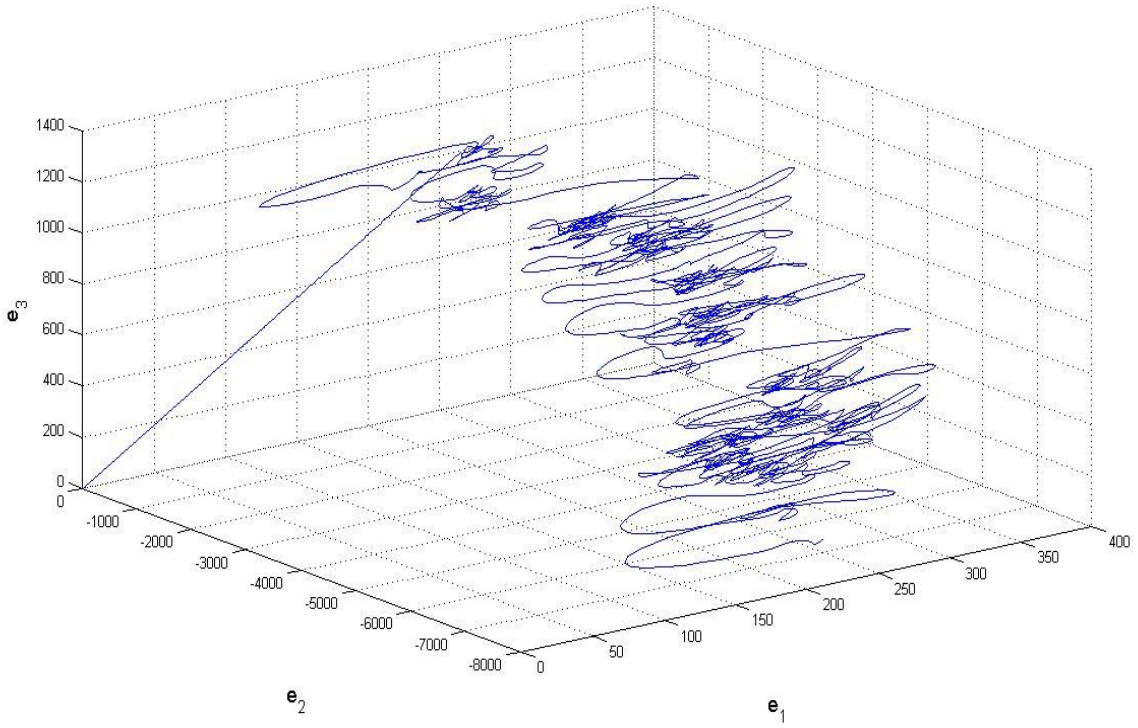

Fig.4 - 11 Phase portrait of e1,e2, e3 before and after control synchronization for traditional method.

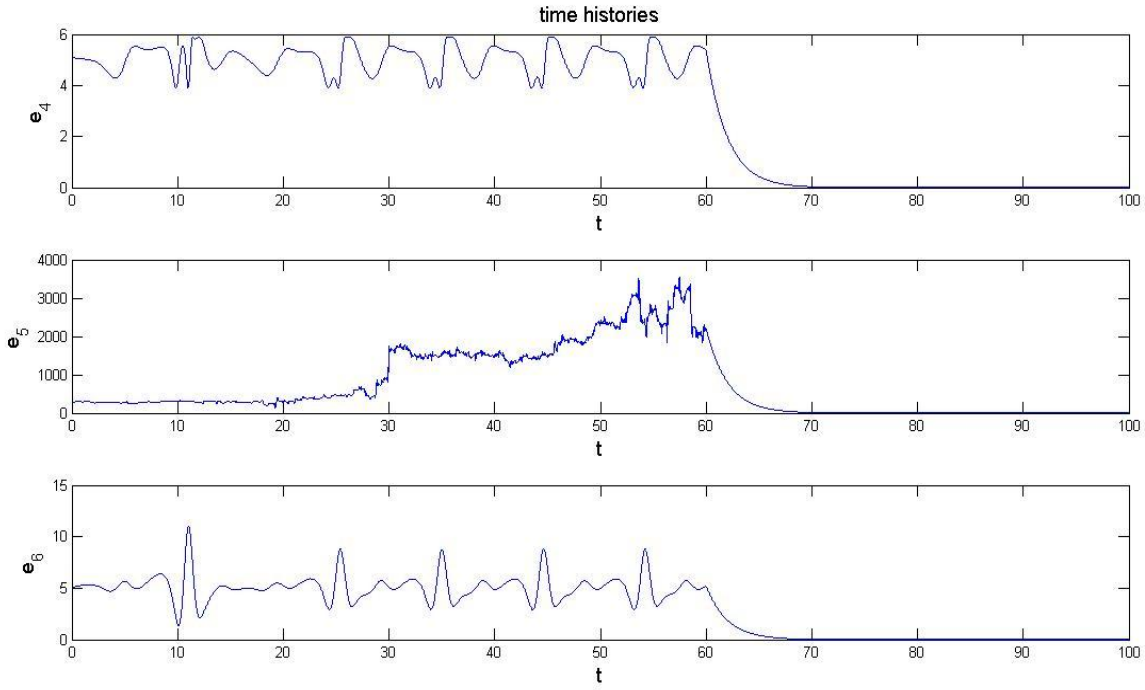

Fig.4 - 12 Time histories of e1,e2,e3 before and after control for traditional method.

Chapter 5

Qian – Dui Hexagram Symplectic Derivative Chaos Synchronization by Partial Region Stability Theory

5.1 Preliminary

The Book of Changes is used the chaos research. The texts of The Book of Changes consist of sixty-four hexagrams. These hexagrams are based on the Eight Trigrams that is shown in Fig. 5.1, each of which consists of three lines, broken or unbroken, the broken representing the weak, or Yin and the unbroken representing the strong, or Yang. Next, choosing two trigrams to research is studied. One is named Qian trigram and another is Dui trigram.

Finally, combining Qian trigram in upper place and Dui trigram in lower place can get Qian-Dui hexagram. Qian-Dui hexagram can be annotated by Chaos and its synchronization.

5.2 "Qian" system and "Dui" system by Yin and Yang results

Consider the first unbroken line, Lü system, is obtained：

$$\begin{cases} \dot{x}_1 = 36(x_2 - x_1) \\ \dot{x}_2 = -x_1 x_3 + 20 x_2 \\ \dot{x}_3 = x_1 x_2 - 3 x_3 \end{cases} \tag{5.1}$$

When initial condition（x_{10}、x_{20}、x_{30}）=（0.2，0.35，0.2）, chaos of the Lü system appears. The chaotic phase portrait of Lü system is shown in Fig. 5.2.

The second unbroken line, Sprott D system, is obtained：

$$\begin{cases} \dot{y}_1 = -y_2 \\ \dot{y}_2 = y_1 + y_3 \\ \dot{y}_3 = y_1 y_3 + 3 {y_2}^2 \end{cases} \tag{5.2}$$

When initial condition（y_{10}、y_{20}、y_{30}）=（0.1，0.1，0.1）, chaos of the Sprott D system is appeared. The chaotic phase portrait of Sprott D system is shown in Fig. 5.3.

The third unbroken line, Sprott E system, is obtained：

$$\begin{cases} \dot{z}_1 = z_2 z_3 \\ \dot{z}_2 = {z_1}^2 + z_2 \\ \dot{z}_3 = 1 - 4z_1 \end{cases} \tag{5.3}$$

When initial condition（z_{10}、z_{20}、z_{30}）=（0.2，0.063，0.01）, chaos of the Sprott E system appears. The chaotic phase portrait of Sprott E is shown in Fig. 5.4.

"Qian" system consists of Yang and Yin system for time $-\infty$ to ∞. Diagrams of chaotic Yang and Yin "Qian" system can be obtained. Put them together, and reverse the time order of Yin chaos, the time histories and phase portraits for time $-\infty$ to ∞ are shown in Figs 5.5~5.7.

Consider the first broken line, Ge-Ku-Duffing system, is obtained：

$$\begin{cases} \dot{x}_1 = x_2 \\ \dot{x}_2 = -0.1x_2 - x_1[11(40 - {x_1}^2) + 54x_3] \\ \dot{x}_3 = -x_3 - {x_3}^3 - 6x_2 + 30x_1 \end{cases} \tag{5.4}$$

When initial condition(x_{10}、x_{20}、x_{30})=（2，2.4，5）, chaos of the Ge-Ku-Duffing system appears. The chaotic phase portrait of Ge-Ku-Duffing system is shown in Fig. 5.8.

Set the Ge-Ku-Duffing system be

$$\begin{cases} \dot{x}_4 = x_5 & + k(x_1 - x_4) \\ \dot{x}_5 = -0.1x_5 - x_4[11(40 - {x_4}^2) + 54x_6] & + k(x_2 - x_5) \\ \dot{x}_6 = -x_6 - {x_6}^3 - 6x_5 + 30x_4 & + k(x_3 - x_6) \end{cases} \tag{5.5}$$

Where x_1, x_2, x_3 are state of Eq.(5.4), k is a positive constant, 100.

The state of linear feedback synchronization for Ge-Ku-Duffing system is obtained.

The second unbroken line, Lorenz system is obtained：

$$\begin{cases} \dot{y}_1 = 10(y_2 - y_1) \\ \dot{y}_2 = 28y_1 - y_1y_3 - y_2 \\ \dot{y}_3 = y_1y_2 - {}^{8}/_{3}\, y_3 \end{cases} \tag{5.6}$$

When initial condition（y_{10}，y_{20}，y_{30}）=（-0.1，0.2，0.3）, chaos of the Lorenz system appears. The chaotic phase portrait of Lorenz system is shown in Fig. 5.9.

The second unbroken line, Sprott C system is obtained：

$$\begin{cases} \dot{z}_1 = z_2z_3 \\ \dot{z}_2 = z_1 - z_2 \\ \dot{z}_3 = 1 - {z_1}^2 \end{cases} \tag{5.7}$$

When initial condition（z_{10}，z_{20}，z_{30}）=（0.8，1，0.01）, chaos of the Sprott C system appears. The chaotic phase portrait of Sprott C is shown in Fig. 5.10.

"Dui" system consists of Yang and Yin system for time $-\infty$ to ∞. Diagrams of chaotic Yang and Yin "Dui" system are almost symmetrical as a whole. Put them together, and reverse the time order of Yin chaos, the time histories and phase portraits for time $-\infty$ to ∞ are shown in Figs 5.11~5.13.

5.3 The strategy of multiple symplectic derivative synchronization

There are two chaotic systems, partner system A and partner system B. The partner A is given by

$$\dot{x} = f(t, x) \tag{5.8}$$

The partner B is given by

$$\dot{y} = g(t, y) \tag{5.9}$$

In order that the error dynamics becomes always positive, the origin of y-coordinate system is translated by a constant vector .

Define $e = G - F + K$ as the error state vector, where $G = G(x, y, \cdots, \dot{x}, \dot{y}, \cdots, \ddot{x}, \ddot{y}, \cdots, t)$ and $F = F(x, y, \cdots, \dot{x}, \dot{y}, \cdots, \ddot{x}, \ddot{y}, \cdots, t)$ are two given

functions, and K is positive constant vector to keep the error dynamics always in first quadrant.

Then the error vector derivative is obtained：

$$\dot{e}_i = \dot{G}_i - \dot{F}_i - u_i \tag{5.10}$$

where u_i is a component of the control input vector u, $i = 1, 2, \cdots, n$.

The synchronization can be accomplished when $t \to \infty$, the limit of the error vector $e = [e_1, e_2, \cdots, e_n]^T$ approaches to zero:

$$\lim_{t\to\infty} e = 0 \tag{5.11}$$

5.4 Synchronization of Qian and Dui trigrams by partial region stability theory

Given G.F.K of Qian trigram for time interval $0 \to +\infty$

$$\begin{cases} G_1 = x_1 y_2 + \frac{1}{36}\dot{x}_1 y_2 \\ G_2 = x_2 y_3 - x_2 \dot{y}_2 + \dot{y}_1 \\ G_3 = \sin y_2 + \frac{1}{20}\dot{x}_2 - \dot{y}_2 \\ G_4 = \cos y_2 - \dot{y}_1 y_3 - y_2 y_3 \\ G_5 = y_3 z_2 - \dot{z}_2 + {z_1}^2 \\ G_6 = \sin y_1 + \dot{y}_2 \end{cases} \tag{5.12}$$

$$\begin{cases} F_1 = \dot{y}_2 + x_2 y_2 + x_1 y_2 \\ F_2 = \frac{1}{3}x_1 x_2 - x_2 x_1 + \frac{1}{3}\dot{x}_3 \\ F_3 = \sin(-\dot{y}_1) - y_1 - \frac{1}{20}x_1 x_3 \\ F_4 = \cos(-\dot{y}_1) - \frac{1}{4}\dot{z}_3 - \frac{1}{4} \\ F_5 = \dot{y}_2 z_2 - y_1 z_2 - y_3 + \dot{y}_2 \\ F_6 = \sin(\dot{y}_2 - y_3) + y_1 \end{cases} \tag{5.13}$$

$$\begin{cases} k_1 = 5 \\ k_2 = 40 \\ k_3 = 40 \\ k_4 = 5 \\ k_5 = 5 \\ k_6 = 5 \end{cases} \tag{5.14}$$

Given G.F.K of Qian trigram for time interval $0 \to -\infty$

$$\begin{cases} G_1 = x_2 y_2 - x_1 y_2 \\ G_2 = x_2 \dot{y}_2 + x_2 y_3 - \dot{y}_1 \\ G_3 = \sin y_2 - \sin(-\dot{y}_1) + y_3 \\ G_4 = \cos y_2 - \dot{y}_1 y_3 - y_2 y_3 \\ G_5 = z_2 - y_3 z_2 + \dot{y}_2 \\ G_6 = \sin y_1 + \dot{y}_2 \end{cases} \quad (5.15)$$

$$\begin{cases} F_1 = \dot{y}_2 + \frac{1}{36}\dot{x}_1 y_2 \\ F_2 = \frac{1}{3}(x_1 x_2 - \dot{x}_3) + x_2 y_1 \\ F_3 = \dot{y}_2 - \frac{1}{20}(\dot{x}_2 + x_1 x_3) \\ F_4 = \cos(-\dot{y}_1) - \dot{y}_1 y_3 \\ F_5 = \dot{z}_2 - {z_1}^2 - \dot{y}_2 z_2 + y_1 z_2 \\ F_6 = \sin(\dot{y}_2 - y_3) \end{cases} \quad (5.16)$$

$$\begin{cases} k_1 = 5 \\ k_2 = 40 \\ k_3 = 40 \\ k_4 = 5 \\ k_5 = 5 \\ k_6 = 5 \end{cases} \quad (5.17)$$

Our purpose is to achieve the multiple symplectic derivative synchronization

$G(x, \dot{x}, y, \dot{y}, z, \dot{z}, t) = F(x, \dot{x}, y, \dot{y}, z, \dot{z}, , t) - K.$

The state error is $e = G - F + K$ such that error dynamics always exists in first guardant as shown in Fig. 5.14. Our purpose is

$$\lim_{t=-\infty \to +\infty} e_i = G_i - F_i + K_i = 0, \quad (5.18)$$

where i = 1, 2,3.We obtain the error dynamics:

$$\begin{cases} \dot{e}_1 = \dot{G}_1 - \dot{F}_1 - u_1 \\ \dot{e}_2 = \dot{G}_2 - \dot{F}_2 - u_2 \\ \dot{e}_3 = \dot{G}_3 - \dot{F}_3 - u_3 \end{cases} \quad (5.19)$$

The state error is $e = G - F + K$ such that error dynamics always exists in first guardant as shown in Fig. 5.15. Our purpose is

$$\lim_{t=-\infty \to +\infty} e_i = G_i - F_i + K_i = 0,$$

where i = 4, 5,6.We obtain the error dynamics:

$$\begin{cases} \dot{e}_4 = \dot{G}_4 - \dot{F}_4 - u_4 \\ \dot{e}_5 = \dot{G}_5 - \dot{F}_5 - u_5 \\ \dot{e}_6 = \dot{G}_6 - \dot{F}_6 - u_6 \end{cases} \tag{5.20}$$

By partial region stability theory, we can choose a Lyapunov function in the form of a positive definite function in first quadrant:

$$V(e) = e_1+e_2+e_3+e_4+e_5+e_6 \tag{5.21}$$

Its time derivative is

$$\dot{V}(e) = \left(\dot{G}_1 - \dot{F}_1 - u_1\right) + \left(\dot{G}_2 - \dot{F}_2 - u_2\right) + \left(\dot{G}_3 - \dot{F}_3 - u_3\right) + \left(\dot{G}_4 - \dot{F}_4 - u_4\right) + \left(\dot{G}_5 - \dot{F}_5 - u_5\right) + \left(\dot{G}_6 - \dot{F}_6 - u_6\right) \tag{5.22}$$

Choose the controller of Yang and Yin u as

$$\begin{cases} u_1 = \dot{y}_1 + \dot{y}_3 + e_1 \\ u_2 = \dot{y}_2 - \dot{x}_3 + e_2 \\ u_3 = \dot{y}_3 - \dot{x}_2 + e_3 \\ u_4 = \dot{z}_3 + e_4 \\ u_5 = \dot{z}_2 - \dot{y}_1 + e_5 \\ u_6 = -\dot{y}_3 + e_6 \end{cases} \tag{5.23}$$

and the controller of Yin u as

$$\begin{cases} u_1 = \dot{y}_1 + \dot{y}_3 + e_1 \\ u_2 = \dot{y}_2 - \dot{x}_3 + e_2 \\ u_3 = \dot{y}_1 - \dot{x}_2 + e_3 \\ u_4 = \dot{z}_1 + e_4 \\ u_5 = \dot{y}_3 - \dot{y}_1 + e_5 \\ u_6 = -\dot{y}_1 - \dot{y}_3 + e_6 \end{cases} \tag{5.24}$$

Given G.F.K of Dui trigram for time interval $0 \rightarrow +\infty$

$$\begin{cases} G_1 = -y_1y_3 + \frac{8}{3}y_1y_2 \\ G_2 = -\frac{1}{30}{x_3}^3 - \dot{y}_2 \\ G_3 = y_2 - \frac{1}{10}\dot{y}_1 \\ G_4 = \dot{z}_2 - \dot{y}_3 \\ G_5 = \dot{y}_2 - y_2y_3 \\ G_6 = \frac{1}{10}\dot{y}_1y_3 + y_1y_3 \end{cases} \tag{5.25}$$

$$\begin{cases} F_1 = \dot{x}_1 + \dot{x}_1 x_3 \\ F_2 = \frac{1}{30} x_3 + \frac{3}{8} \dot{y}_3 \\ F_3 = \frac{1}{30} \dot{x}_3 + x_1 \dot{x}_1 \\ F_4 = \dot{z}_2 - y_1 y_3 \\ F_5 = y_2 - y_1 \\ F_6 = 28 y_1 y_3 - \dot{y}_2 y_3 \end{cases} \tag{5.26}$$

$$\begin{cases} k_1 = 5 \\ k_2 = 40 \\ k_3 = 40 \\ k_4 = 5 \\ k_5 = 5 \\ k_6 = 5 \end{cases} \tag{5.27}$$

Given G.F.K of Dui trigram for time interval $0 \to -\infty$

$$\begin{cases} G_1 = 0 \\ G_2 = 0 \\ G_3 = 0 \\ G_4 = \dot{z}_2 + \dot{y}_3 \\ G_5 = \dot{y}_2 + y_2 y_3 \\ G_6 = -\frac{1}{10} \dot{y}_1 y_3 + y_1 y_3 \end{cases} \tag{5.28}$$

$$\begin{cases} F_1 = 0 \\ F_2 = 0 \\ F_3 = 0 \\ F_4 = \dot{z}_2 - y_1 y_3 \\ F_5 = y_2 - y_1 \\ F_6 = -28 y_1 y_3 + \dot{y}_2 y_3 \end{cases} \tag{5.29}$$

$$\begin{cases} k_1 = 5 \\ k_2 = 40 \\ k_3 = 40 \\ k_4 = 5 \\ k_5 = 5 \\ k_6 = 5 \end{cases} \tag{5.30}$$

Our purpose is to achieve the multiple symplectic derivative synchronization

$G(x, \dot{x}, y, \dot{y}, z, \dot{z}, t) = F(x, \dot{x}, y, \dot{y}, z, \dot{z}, , t) - K.$

The state error is $e = G - F + K$ such that error dynamics always exists in first guardant as shown in Fig. 5.16. Our purpose is

$$\lim_{t \to \infty} e_i = G_i - F_i + K_i = 0, \tag{5.31}$$

where i = 1, 2,3.We obtain the error dynamics:

$$\begin{cases} \dot{e}_1 = \dot{G}_1 - \dot{F}_1 - u_1 \\ \dot{e}_2 = \dot{G}_2 - \dot{F}_2 - u_2 \\ \dot{e}_3 = \dot{G}_3 - \dot{F}_3 - u_3 \end{cases} \quad (5.32)$$

The state error is $e = G - F + K$ such that error dynamics always exists in first guardant as shown in Fig. 5.17. Our purpose is

$\lim_{t\to\infty} e_i = G_i - F_i + K_i = 0,$

where i = 4, 5,6.We obtain the error dynamics:

$$\begin{cases} \dot{e}_4 = \dot{G}_4 - \dot{F}_4 - u_4 \\ \dot{e}_5 = \dot{G}_5 - \dot{F}_5 - u_5 \\ \dot{e}_6 = \dot{G}_6 - \dot{F}_6 - u_6 \end{cases} \quad (5.33)$$

By partial region stability theory, we can choose a Lyapunov function in the form of a positive definite function in first quadrant:

$$V(e) = e_1+e_2+e_3+e_4+e_5+e_6 \quad (5.34)$$

Its time derivative is

$$\dot{V}(e) = \left(\dot{G}_1 - \dot{F}_1 - u_1\right) + \left(\dot{G}_2 - \dot{F}_2 - u_2\right) + \left(\dot{G}_3 - \dot{F}_3 - u_3\right) + \left(\dot{G}_4 - \dot{F}_4 - u_4\right) + \left(\dot{G}_5 - \dot{F}_5 - u_5\right) + (\dot{G}_6 - \dot{F}_6 - u_6) \quad (5.35)$$

Choose the controller of Yang and Yin u as

$$\begin{cases} u_1 = \frac{1}{30}\dot{x}_3 + e_1 \\ u_2 = \frac{1}{5}\dot{x}_2 - \dot{x}_1 + e_2 \\ u_3 = \dot{x}_3 - 28\dot{y}_1 + e_3 \\ u_4 = \frac{11}{3}\dot{y}_3 - \dot{z}_2 + e_4 \\ u_5 = 28\dot{y}_1 - \dot{z}_1 + e_5 \\ u_6 = \dot{y}_2 - \dot{z}_3 + e_6 \end{cases} \quad (5.36)$$

and the controller of Yin u as

$$\begin{cases} u_1 = 0 \\ u_2 = 0 \\ u_3 = 0 \\ u_4 = -\frac{5}{3}\dot{y}_3 - \dot{z}_2 + e_4 \\ u_5 = 28\dot{y}_1 - \dot{z}_1 + e_5 \\ u_6 = \dot{y}_2 - \dot{z}_3 + e_6 \end{cases} \quad (5.37)$$

we obtain

$$\dot{V}(e) = -e_1 - e_2 - e_3 - e_4 - e_5 - e_6 < 0 \tag{5.38}$$

which is negative definite function in first quadrant.

5.5 Qian-Dui Hexagram Multiple Symplectic Derivative Synchronization by Partial Region Stability Theory

Qian-Dui Hexagram is used for synchronization.

Given

$G(x,y,z,\ldots,\dot{x},\ ,\dot{y},\ ,\dot{z},\ldots\ddot{x},\ddot{y},\ddot{z}\ldots,t)$:

$$\begin{cases} G_1 = x_2y_2 - x_1y_2 \\ G_2 = x_2\dot{y}_2 + x_2y_3 - \dot{y}_1 \\ G_3 = \sin y_2 - \sin(-\dot{y}_1) + y_3 \end{cases} \tag{5.39}$$

$F(x,y,z,\ldots,\dot{x},\ ,\dot{y},\ ,\dot{z},\ldots\ddot{x},\ddot{y},\ddot{z}\ldots,t)$:

$$\begin{cases} F_1 = \dot{x}_1 + \dot{x}_1x_3 \\ F_2 = \frac{1}{30}x_3 + \frac{3}{8}\dot{y}_3 \\ F_3 = \frac{1}{30}\dot{x}_3 + x_1\dot{x}_1 \end{cases} \tag{5.40}$$

Our goal is to achieve the multiple symplectic derivative synchronization.

Define error function as

e = $G(x,y,z,\ldots,\dot{x},\ ,\dot{y},\ ,\dot{z},\ldots\ddot{x},\ddot{y},\ddot{z}\ldots,t)$-$F(x,y,z,\ldots,\dot{x},\ ,\dot{y},\ ,\dot{z},\ldots\ddot{x},\ddot{y},\ddot{z}\ldots,t)$+$\boldsymbol{K}$.

(5.41)

where $\boldsymbol{K}=[200,1000,1000]^T$ keep the error dynamics always in first guardant. Our goal is

$$\lim_{t\to\infty} e_i = \lim_{t\to\infty}(G_i - F_i + K_i) = 0, (i = 1,2,3) \tag{5.42}$$

Thus we design the controller as

$$\begin{cases} u_1 = \frac{1}{30}\dot{x}_3 + e_1 \\ u_2 = \frac{1}{5}\dot{x}_2 - \dot{x}_1 + e_2 \\ u_3 = \dot{x}_3 - 28\dot{y}_1 + e_3 \end{cases} \tag{5.43}$$

The error dynamics becomes

$$\dot{\mathbf{e}} = \dot{\mathbf{G}} - \dot{\mathbf{F}} - \mathbf{u} \tag{5.44}$$

Using partial region stability theory we can choose a Lyapunov function in the form of a positive definite function in first quadrant.

$$V(e) = e_1+e_2+e_3 > 0 \tag{5.45}$$

By adding u ,we obtain

$$\dot{V}(e) = -e_1 - e_2 - e_3 < 0 \tag{5.46}$$

which is a negative definite function in first quadrant. The results are shown in Fig.5.18

5.6 Summary

A synchronization of "Qian" system and "Dui" system are presented. Qian trigram is one of Eight trigrams. which consists of three unbroken lines. Dui Trigram is one broken line and two unbroken lines. Qian-Dui Hexagram has two parts, upper is Qian Trigram, and low is Dui trigram.

The chaotic behaviors for time $0 \rightarrow +\infty$ are shown by time histories. The multiple derivative synchronizations of Qian and Dui trigrams are given by partial stability theory. Finally, Qian-Dui hexagram is produced by synchronizations of Qian trigram and Dui trigram.

From the previous sections, symplectic derivative chaos synchronization by partial region stability theory is shown. To achieve chaos control by GYC partial region stability theory is used for searching controller easily and synchronizing system quickly. The new synchronization seems be rather complex, and the confidential property would be difficult to decipher.

Fig.5 - 1 The eight trigrams.

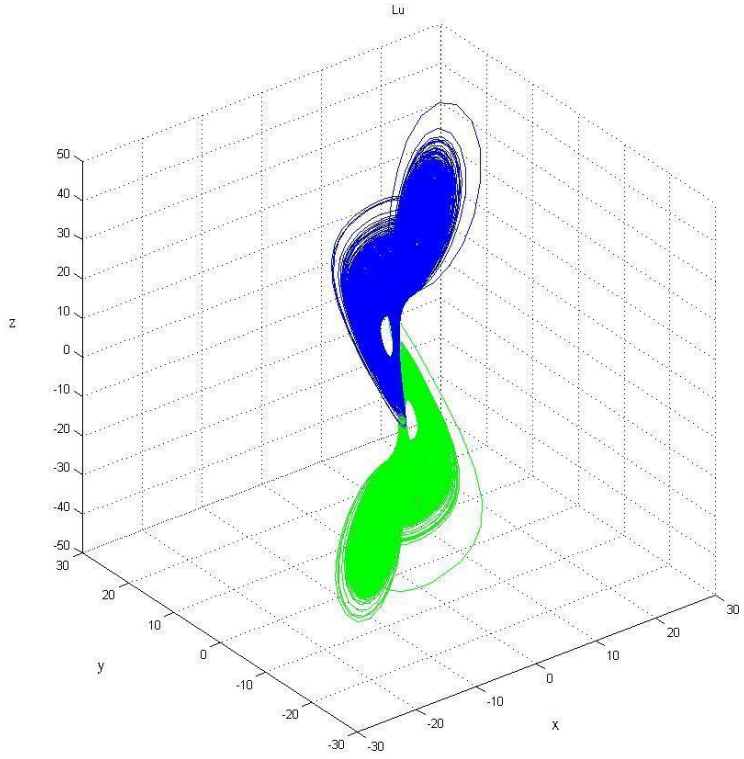

Fig.5 - 2 3D phase portrait of Lü system.

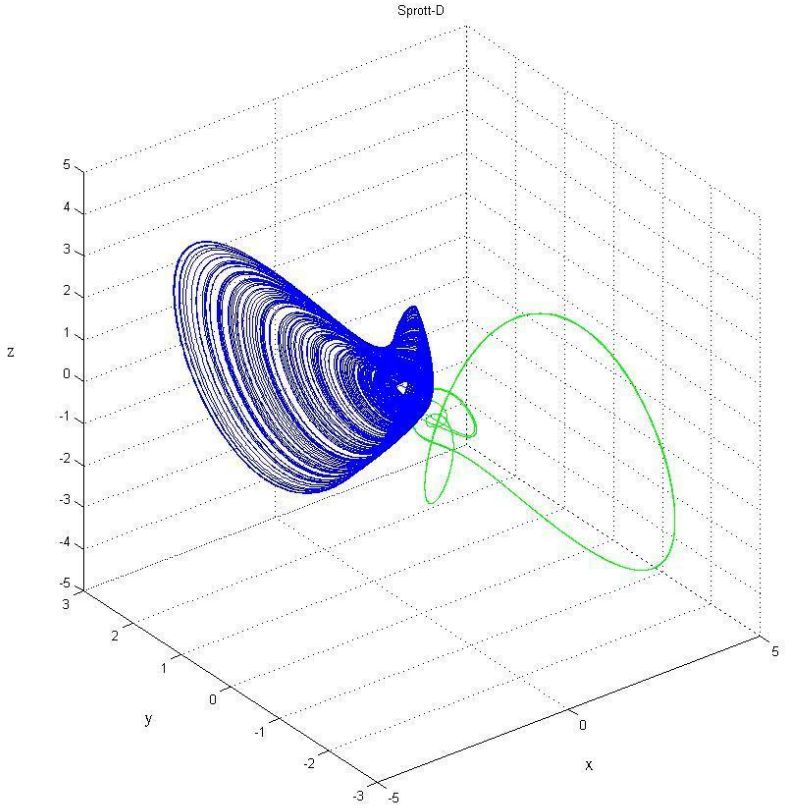

Fig.5 - 3 3D phase portrait of Sprott-D system.

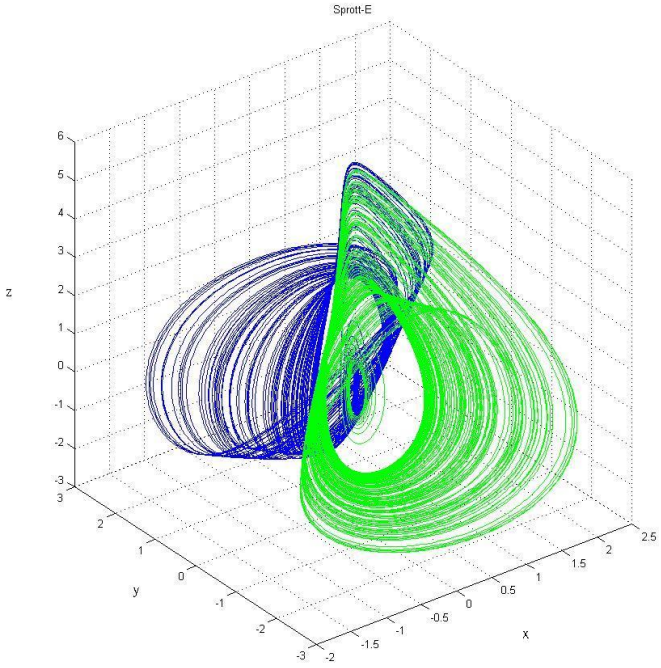

Fig.5 - 4 3D phase portrait of Sprott-E system.

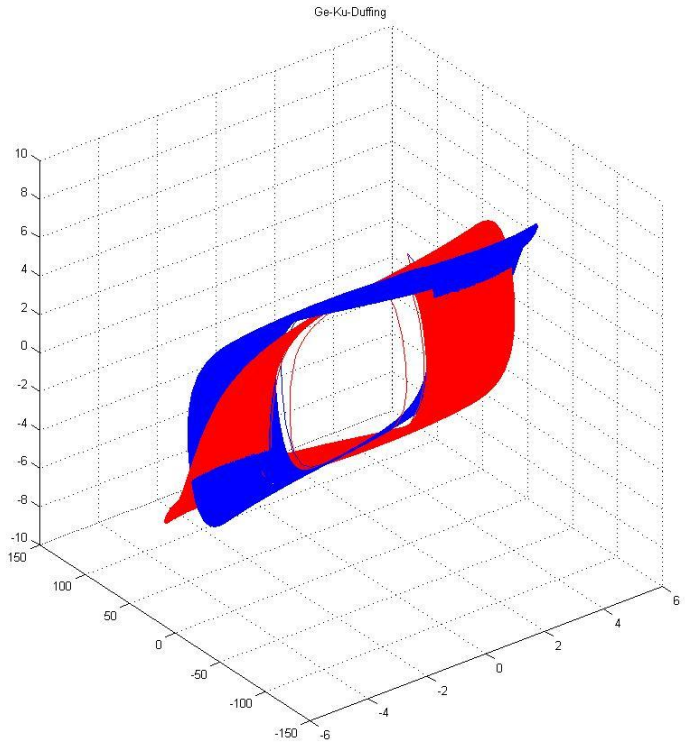

Fig.5 - 5 3D phase portrait of Ge-Ku-Duffing system.

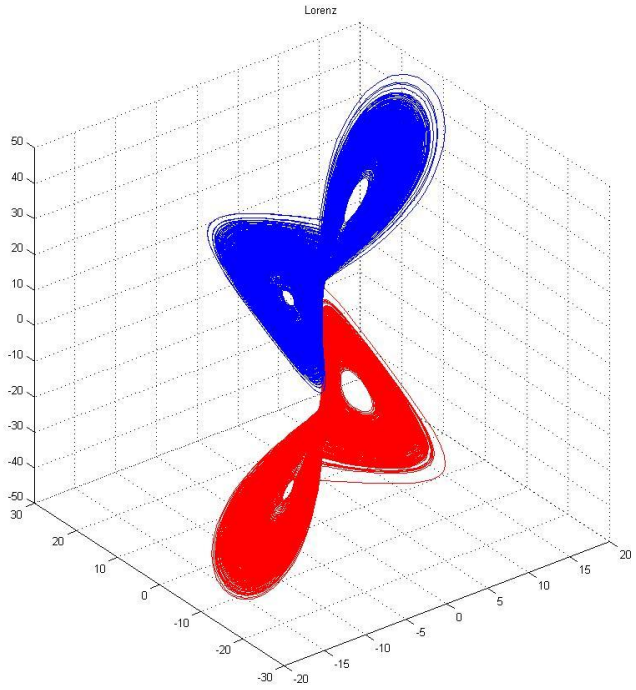

Fig.5 - 6 3D phase portrait of Lorenz system.

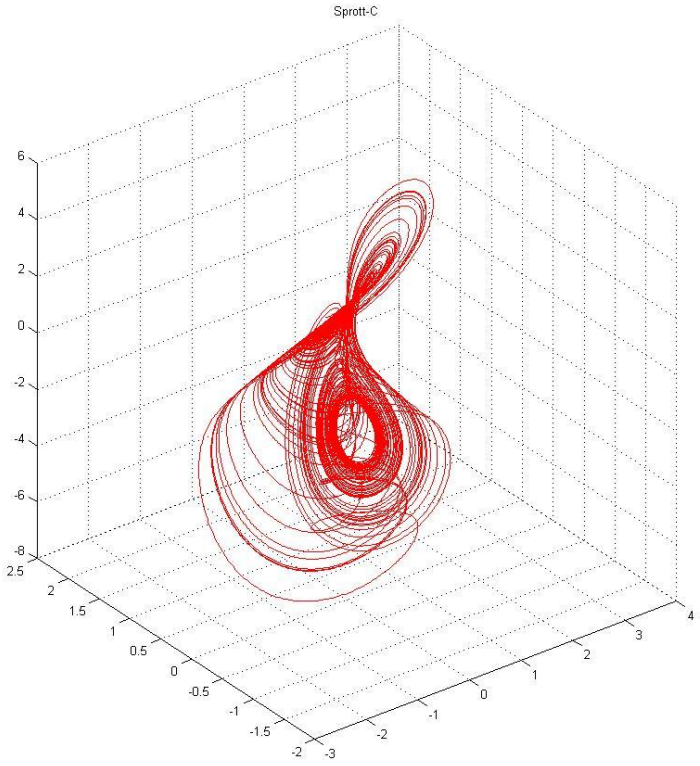

Fig.5 - 7 3D phase portrait of Sprott C system.

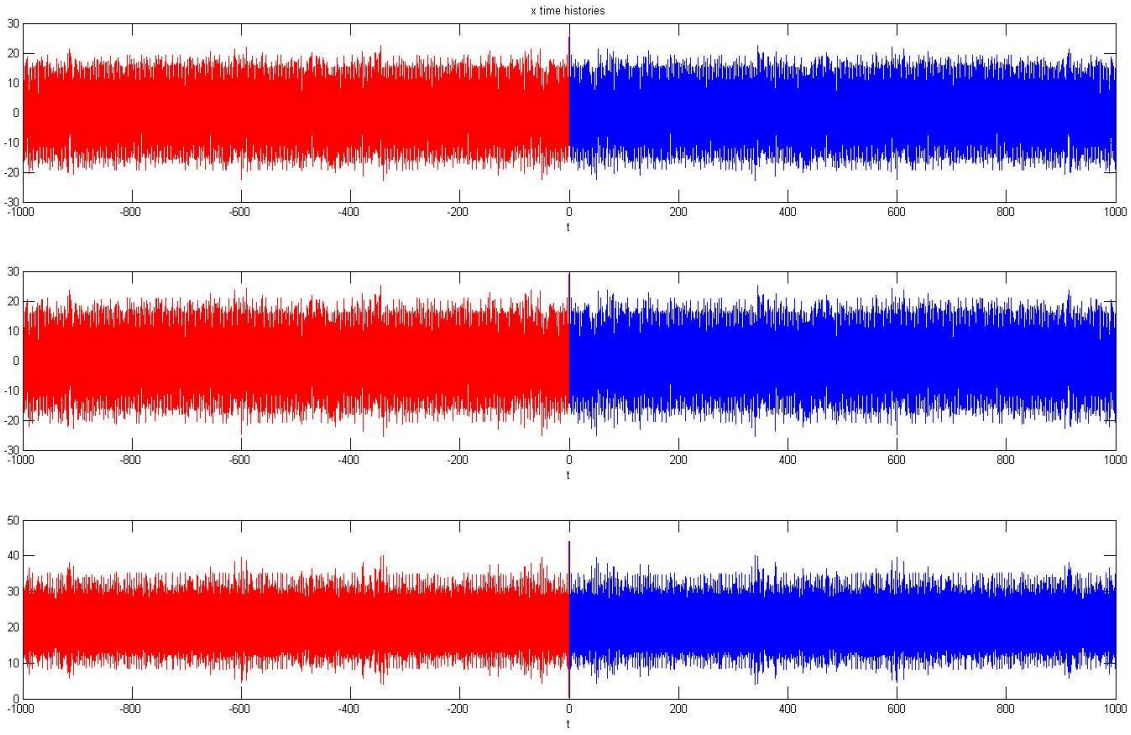

Fig.5 - 8 Time histories of parameter $x_1. x_2. x_3.$

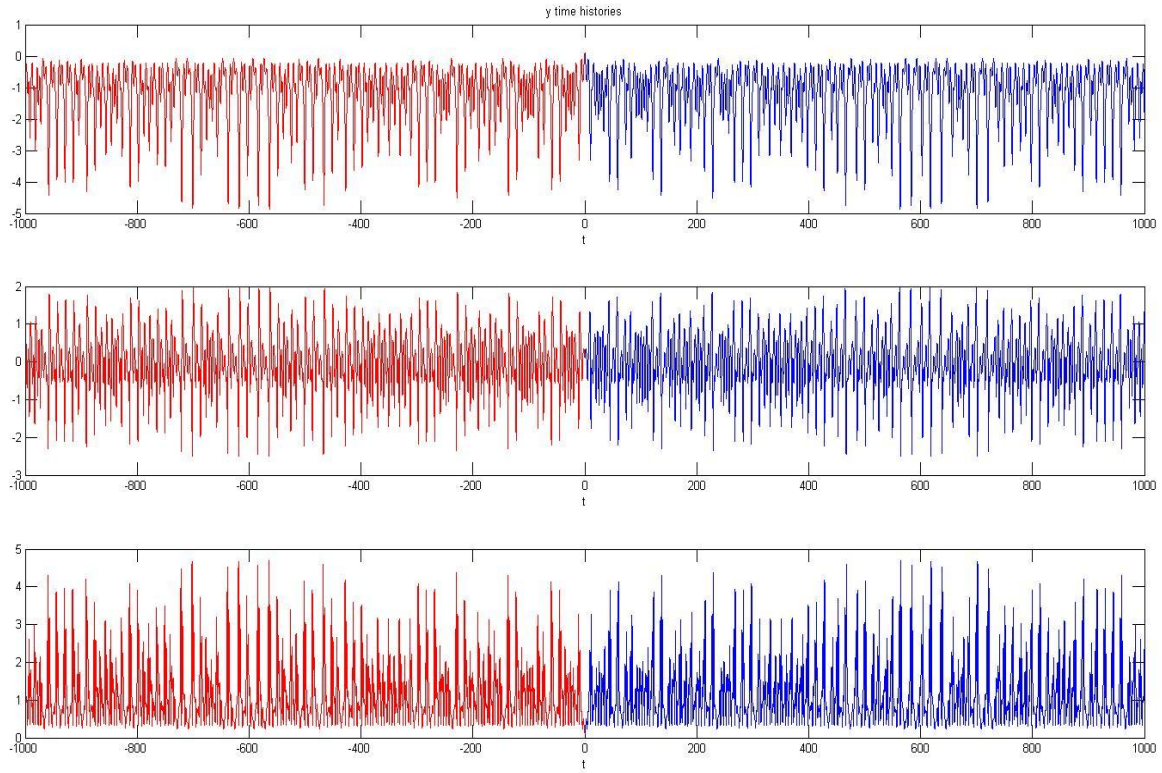

Fig.5 - 9 Time histories of parameter $y_1. y_2. y_3.$

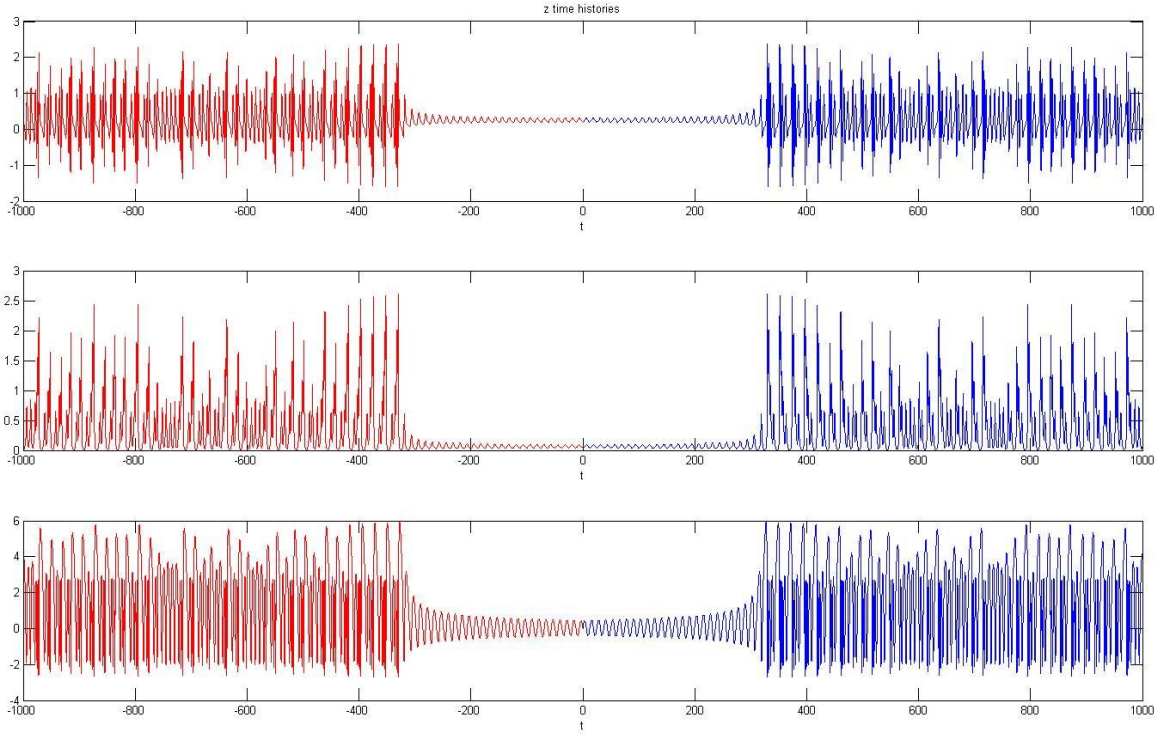

Fig.5 - 10 Time histories of parameter $z_1. z_2. z_3.$

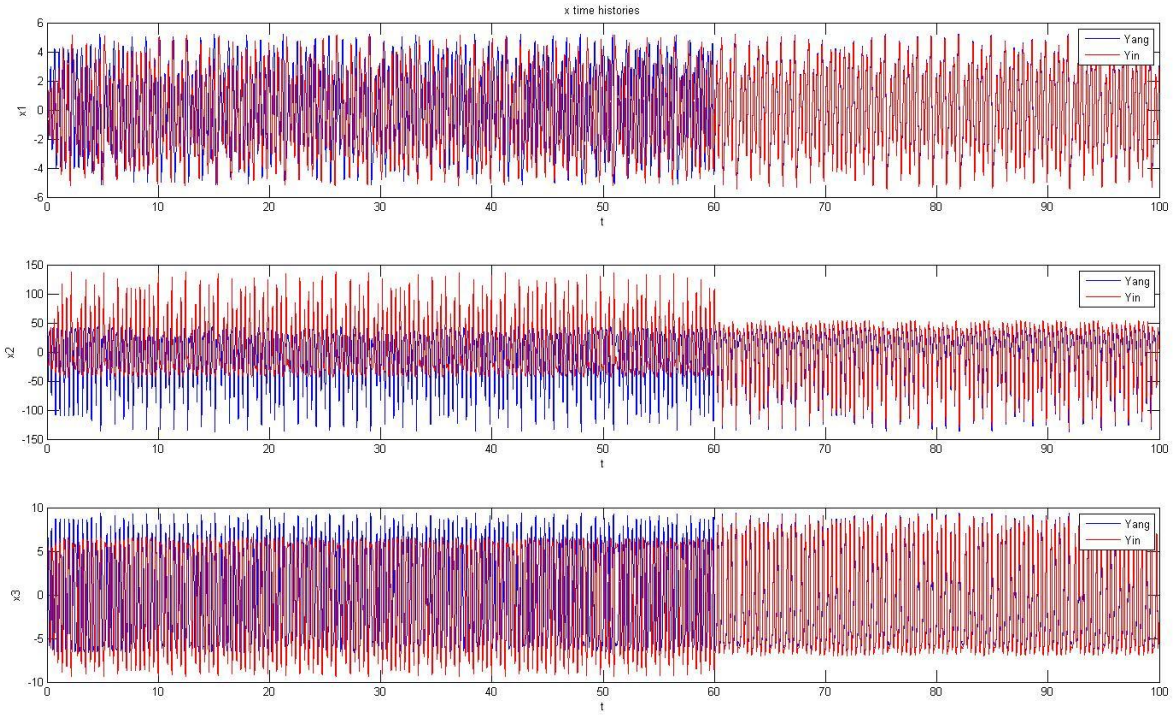

Fig.5 - 11 Time histories of parameter $x_1. x_2. x_3.$

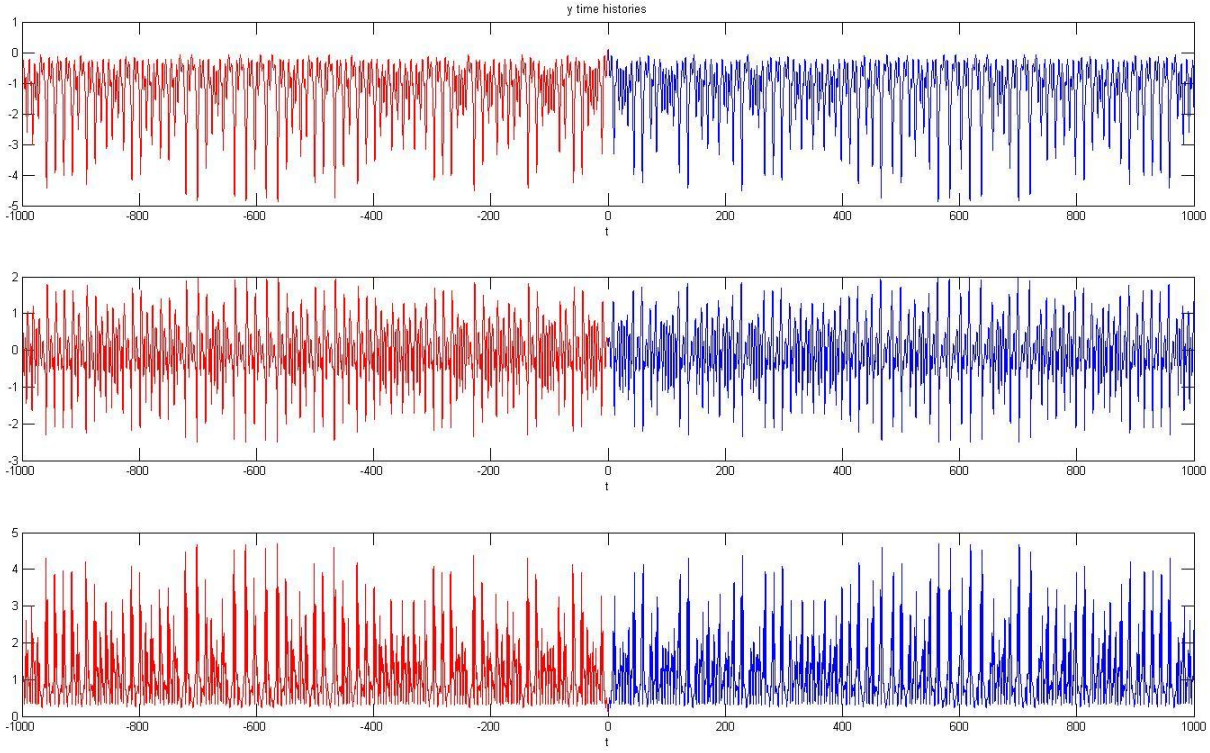

Fig.5 - 12 Time histories of parameter $y_1. y_2. y_3.$

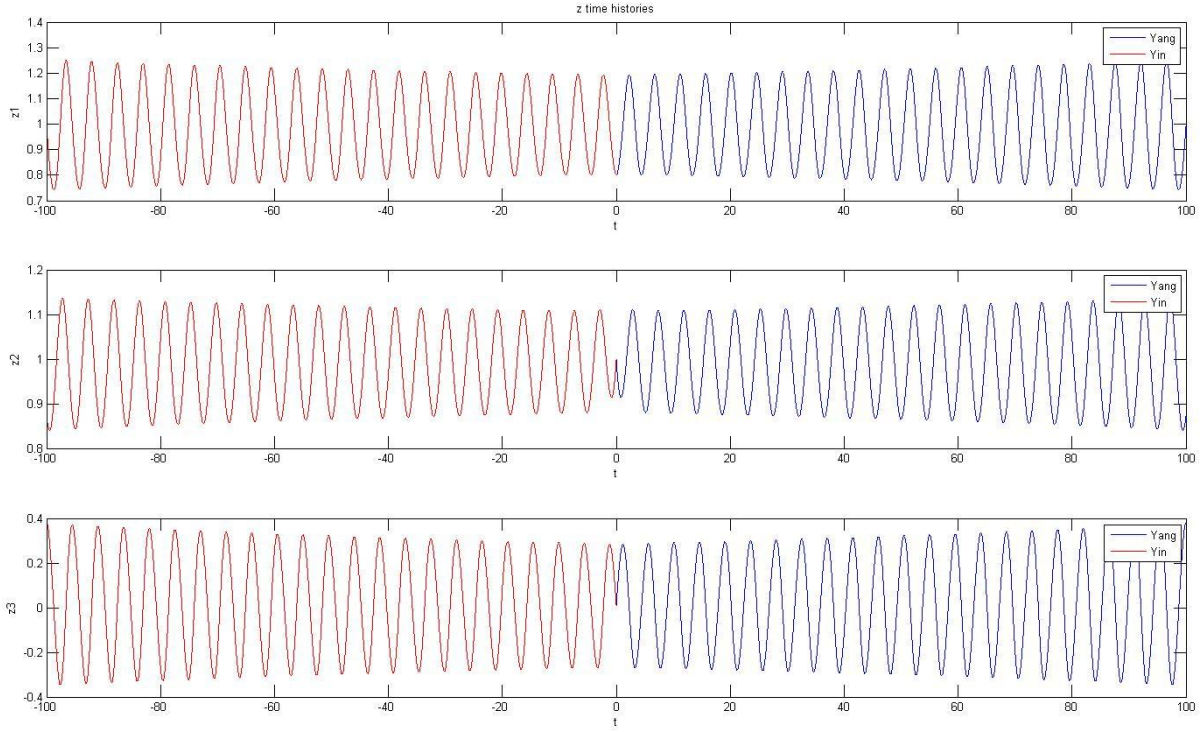

Fig.5 - 13 Time histories of parameter $z_1. z_2. z_3.$

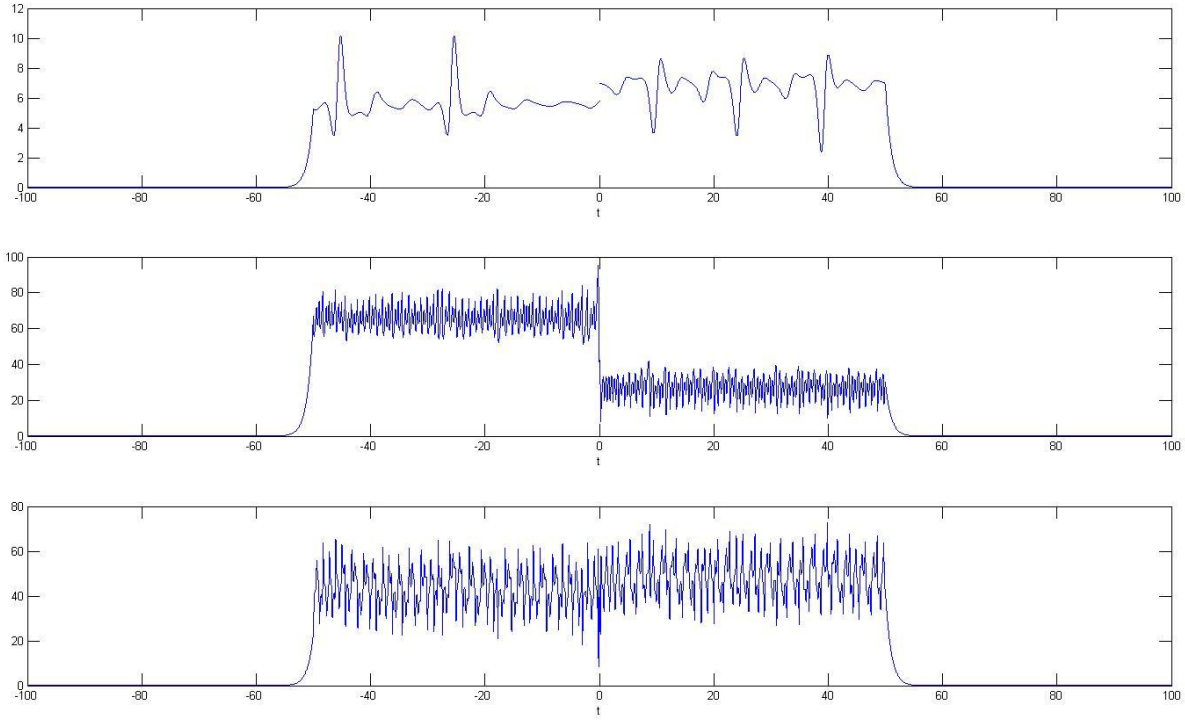

Fig.5 - 14 Time histories of error1~3 before and after control.

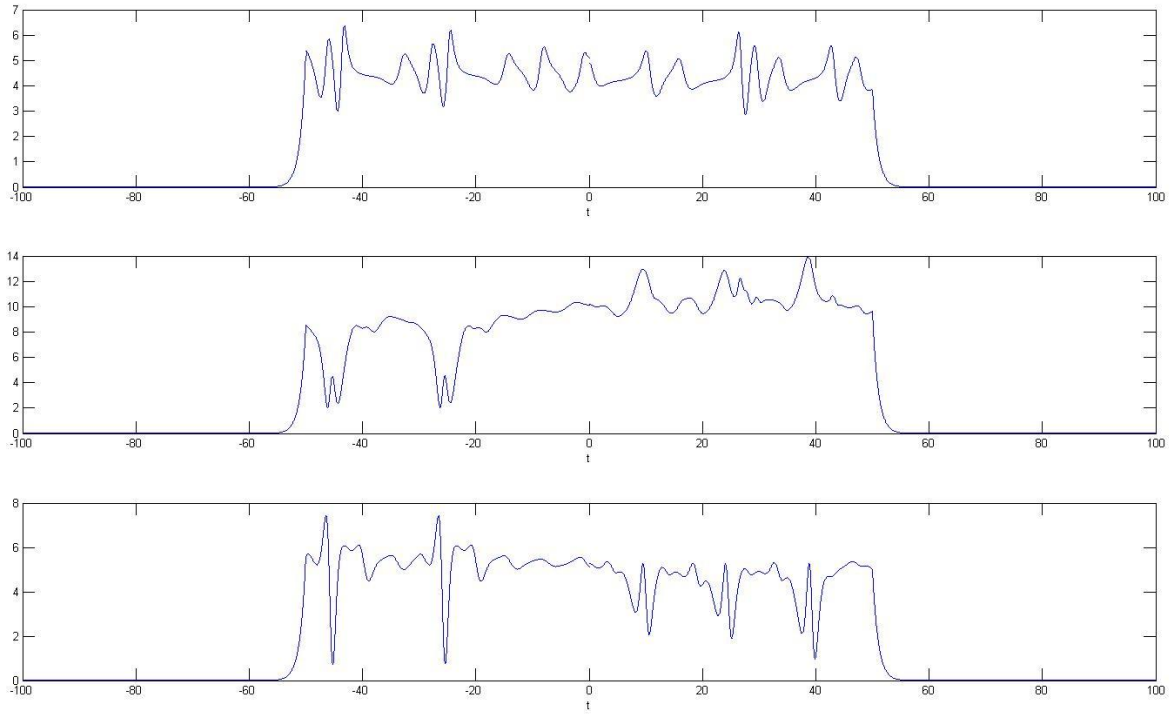

Fig.5 - 15 Time histories of error1~3 before and after control.

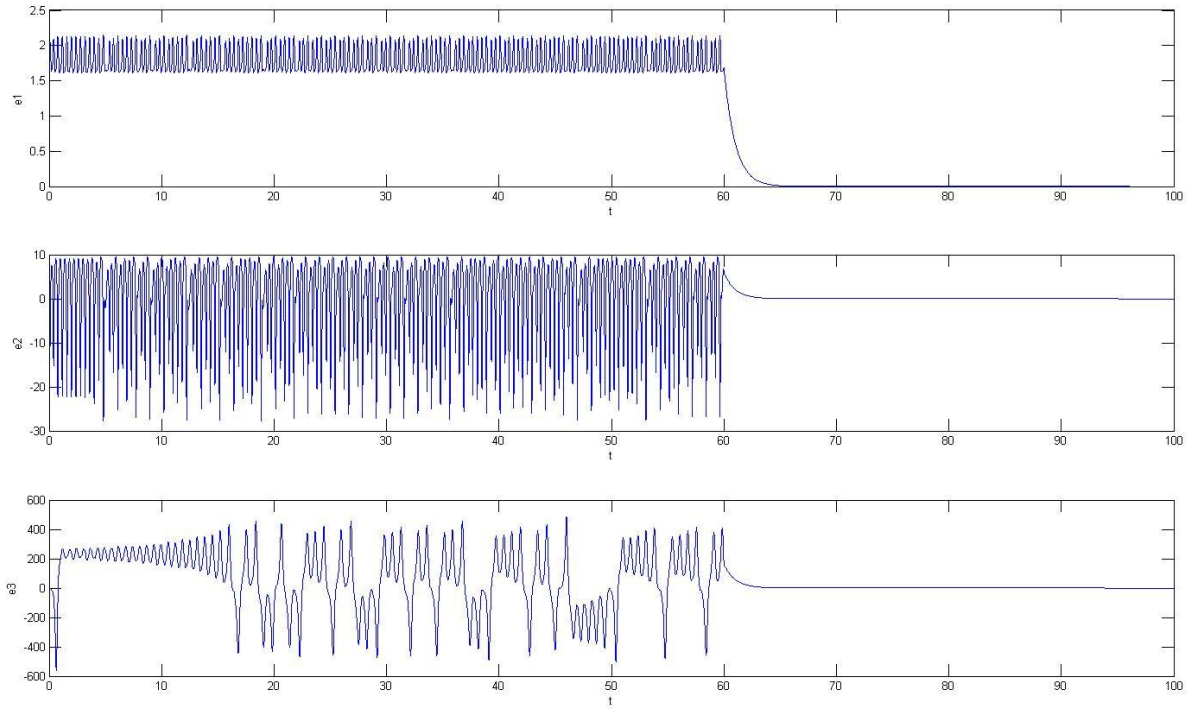

Fig.5 - 16 Time histories of error1~3 before and after control

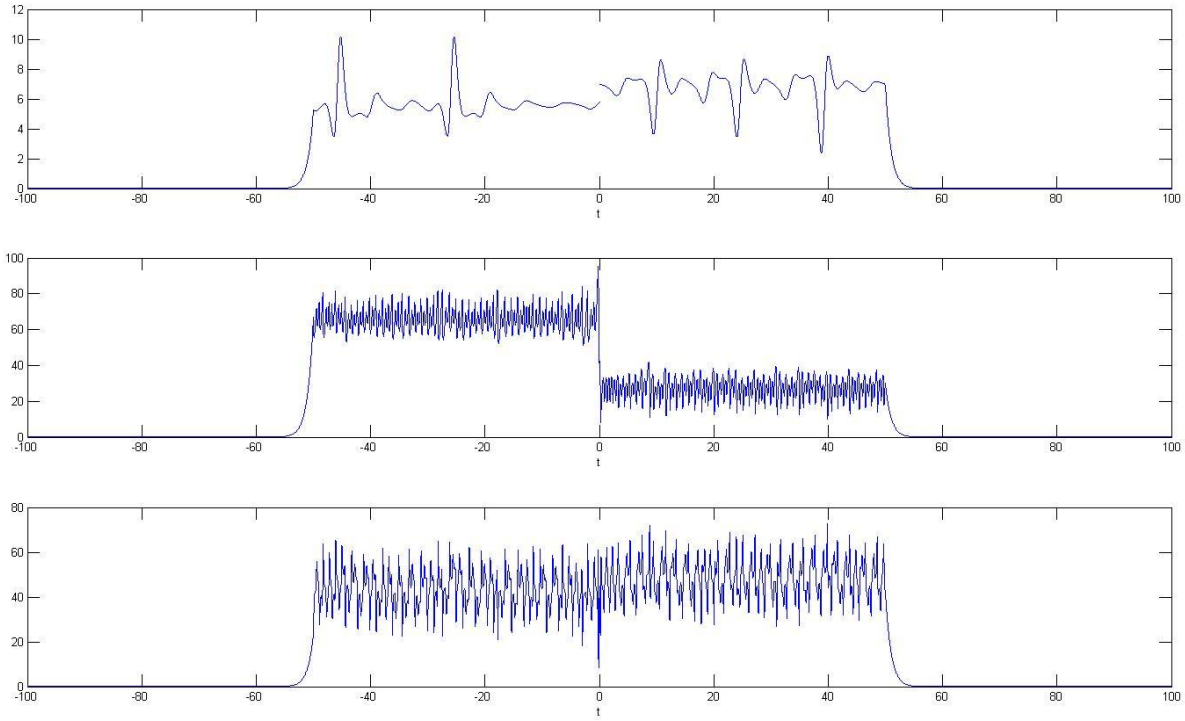

.

Fig.5 - 17 Time histories of error1~3 before and after control.

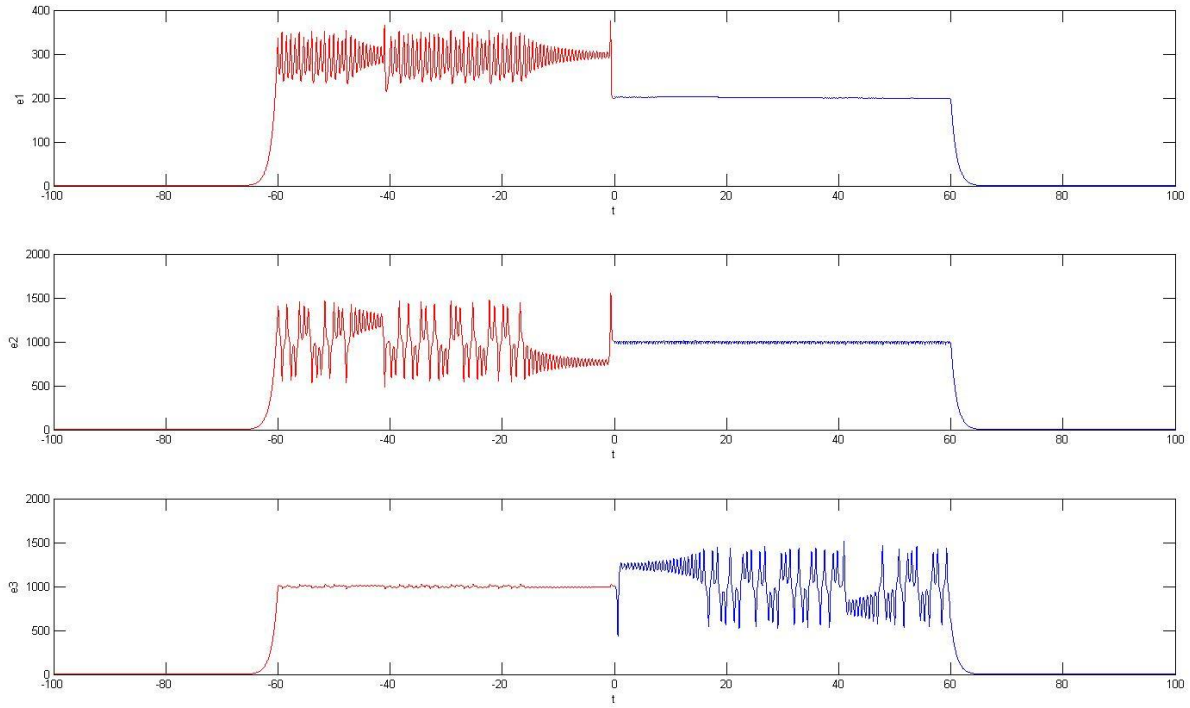

Fig.5 - 18 Time histories of error1~3 before and after control.

Reference

[1] Lacitignola D., Petrosillo I., Zurlini G., “Time-dependent regimes of a tourism-based social–ecological system period-doubling route to chaos.” Ecol.Complex.7 (2010) 44–54

[2] Huang L.-L., Feng R.-P. and Wang M., “Synchronization of chaotic systems via nonlinear control”, Phys Lett A 320(4) (2004) 271.

[3] Fuh C.C. and Tung P.C., ‘‘Controlling chaos using differential geometric method’’, Phys Rev Lett 75 (1995) 2952.

[4] Hassell M. P., Comins H. N., Mayt R. M., “Spatial structure and chaos in insect population dynamics”, Nature, Volume 353, Issue 6341(1991) 255-258.

[5] Ge Z.-M. and Cheng J.-W., ‘‘Chaos synchronization and parameter identification of three time scales brushless DC motor system’’, Chaos, Solitons and Fractals 24 (2005) 597-616.

[6] Li Guo-Hui and Zhou Shi-Ping, “An observer-based anti-synchronization”, Chaos, Solitons and Fractals 29 (2006) 495.

[7] Chen H.-K. and Sheu L.-J., “The transient ladder synchronization of chaotic systems”, Phys Lett A 207 (2006) 207.

[8] Lu J., Zhou T., G. Chen and Zhang S., “Local bifurcations of the Chen system”, Int. J.Bifurcat. Chaos 12 (2002) 2257-2270.

[9] Lorenz E.N., “Deterministic non-periodic flows”, J. Atoms.20 (1963) 130.

[10] Ge Zheng-Ming and Li Shich-Yu, “Yang and Yin parameters in the Lorenz system”, Nonlinear Dynamics 62 (2010) 105

[11] J. Lü and G.Chen, “A new chaotic attractor coined”, Int. J. Biffercation & Chaos 12 3 (2002) 659

[12] J. Lü, G.Chen and S.Zhang, “Chaos synchronization between linearly coupled chaotic system”, Chaos, Solitons and Fractals 14 4 (2002) 529

[13] Yamada, T. and Fujisaka, H. “Stability theory of synchronized motion in coupled-oscillator systems”, Progr. Theor. Phys. **70** (1983) (5) 1240–1248

[14] Pecora, LM., Carroll, TL. “Synchronization in chaotic systems”, Phys Rev Lett , 64 (2005) 821-824.

[15] Petrov V., Gaspar V., Masere J. and Showalter K., “Controlling chaos in the Belousov–Zhabotinsky reaction”, Nature 361 (1993) 240–243.

[16] Chen, SH., JH. “Synchronization of an uncertain unified chaotic system via adaptive control”, Chaos Solitons & Fractals 26 (2005) 913-920.

[17] Yu, X., Song, Y. “Chaos synchronization via controlling partial state of chaotic systems”, Int J Bifurcat Chaos 11 (2001) 1737-1741.

[18] Wang, C, Ge, SS. “Adaptive synchronization fo uncertain chaotic via backstepping design”, Chaos Solitons & Fractals 12 (2001) 1199-1206.

[19] Chua LO., Kocarev L., Eckert K. and Itoh M., “Experimental chaos synchronization in Chua’s circuit”, International Journal of Bifurcation and Chaos 2 (1992) 705–708.

[20] Elabbasy, E. M., Agiza, H. N., and El-Desoky, M. M., ‘‘Adaptive synchronization of a hyperchaotic system with uncertain parameter’’, Chaos, Solitons and Fractals, 30 (2006) 1133-1142.

[21] Garfinkel A, Spano ML, Ditto WL and Weiss JN, “Controlling cardiac chaos”, Science 257 (1992) 1230–1235.

[22] Park Ju H., ‘‘Adaptive synchronization of Rossler system with uncertain parameters’’, Chaos, Solitons and Fractals, 25 (2005) 333-338.

[23] [23] Ge Z.-M. and Yang C.-H., “Symplectic synchronization of different chaotic system”, Chaos, Solution & Fractals, 40 (2009) 2532-2543.

[24] Ge Z.-M., Yao C.-W., Chen H.-K. Stability on partial region in dynamics. Journal of Chinese Society of Mechanical Engineer 115 (1994) 140-151.

[25] Ge Z.-M. and Chen H.-K. “Three asymptotical stability theorems on partial region with applications”, Japanese Journal of Applied Physics 1998; 37:2762–2773.

[26] Ge Z.-M. Necessary and sufficient conditions for the stability of a sleeping top described by three forms of dynamic equations. Physical Review E 77 (2008) 046606.

[27] Ge Z.-M., Ho C.-Y., Li S.-Y. and Chang C.-M., “Chaos control of new Ikeda–Lorenz systems by GYC partial region stability theory”, Mathmatical Methods in the Applied Sciences, 32 (2009) 1564-1584.

[28] Lü. J. and Chen. G., “A new chaotic attractor coined”, Int. J. Biffercation & Chaos 12 3 (2002) 659

[29] Sprott J.C., “Some simple chaotic flows”, Physical Review E, 2 (1994) 5.

[30] Lorenz E.N., “Deterministic non-periodic flows”, J. Atoms.20 (1963) 130.

[31] Sprott J.C., “Some simple chaotic flows”, Physical Review E, 2 (1994) 5.

[32] Lorenz E.N., “Deterministic non-periodic flows”, J. Atoms.20 (1963) 130.